2012

Mechanisms of Shoreline Change on the Rhode Island South Coast: Past, Present, and Future

Nathan D. Vinhateiro
University of Rhode Island

MECHANISMS OF SHORELINE CHANGE ON THE RHODE ISLAND SOUTH COAST: PAST, PRESENT, AND FUTURE

BY

NATHAN D. VINHATEIRO

A DISSERTATION SUBMITTED IN PARTIAL FULFILLMENT OF THE REQUIREMENTS FOR THE DEGREE OF

DOCTOR OF PHILOSOPHY

IN

OCEANOGRAPHY

UNIVERSITY OF RHODE ISLAND

2012

ABSTRACT

The barrier-lagoon system along the Rhode Island south shore is a vital natural resource that provides critical habitat and protects the state's southern communities against storm damage. The response of this system to changes in global climate is therefore of great interest to those who live along and manage this coastline. Responsible planning and accurate assessment of coastal vulnerability will require consideration of barrier spit evolution on different time scales. Accordingly, this dissertation presents evidence from geologic and instrumental records that are used to examine how the south shore responds to changes in the extent and frequency of coastal storms, and to long-term processes such as sea level rise.

Overwash layers present in a transect of sediment cores from Quonochontaug Pond, RI are used to construct a record of major hurricane landfall spanning the last 2200 years. An annual probability for intense tropical cyclone landfall in Rhode Island was calculated to be 0.45% - a value that is notably similar to other proxy-based reconstructions throughout the western North Atlantic. The record indicates that New England has experienced changes in tropical cyclone climatology during this time, with periods of increased activity during the past ~400 years, and between 1400-2150 cal. yr BP. Similarity in the timing of overwash events between Quonochontaug Pond and sites throughout the western North Atlantic suggests that millennial-scale variability may be the result of basin-wide climatic forcings.

A long-term dataset of beach profiles is used to construct a high-resolution record of shoreline change at eight transects along the Rhode Island south shore. Shoreline positions were estimated by intersecting a local tidal datum with ~6000 coastal

profiles collected over 49 consecutive years. When compared to digital vector shorelines coincident with the survey period, the time-series of profile-derived shorelines demonstrate how sampling frequency and the choice of time-scales for analysis can bias calculated rates of shoreline change. A comparison of rate-of-change methods demonstrates that a weighted regression of vector shorelines depicts true shoreline behavior more accurately than other commonly used techniques. Annual variability resulting from changes in beach morphology in response to storms is quantified, providing the first estimates of such uncertainty for future studies of shoreline change. In addition, the offset between proxy-based, and datum-based shorelines is compared for recent years and is shown to be more than twice as large as previously estimated.

Sea level rise is predicted to be one of the largest and most sustained climate change impacts to coastal environments and populations during the next century. As a result, mitigation strategies that incorporate accelerated rates of sea level rise into coastal planning, design, and habitat restoration are increasing. In Rhode Island, estimates of sea level rise up to and exceeding 1-meter by 2100 will result in dramatic changes on the state's barrier-lagoon coastline. A range of geospatial data are already available for planning – including several high resolution elevation models – yet future trends will require sustained research to monitor sea level changes and impacts in Rhode Island. We recommend a comprehensive program of coastal monitoring that utilizes high-resolution, sequential topography, high-accuracy geodetic control, and tools to quantify relative sea level change in Rhode Island. Coastal vulnerability can

then be gauged with predictive models that integrate multiple datasets and include probabilistic estimates of shoreline response to climate change.

ACKNOWLEDGMENTS

My co-advisors, John King and Rebecca Robinson, provided exceptional opportunities as well as careful mentoring during my time in graduate school, and my foremost thanks go to them. John gave me the freedom to pursue my own research ideas, yet was always available with advice and creative suggestions when needed. Becky's thoughtful instruction and feedback were crucial to the completion of this dissertation. John and Becky taught me to think critically and always encouraged my questions. Their direction helped to make me a better scientist, and I am grateful for the expertise they so willingly shared. I also acknowledge my committee members Jon Boothroyd, Peter August, and Charley Roman for their attentive and thoughtful review of my dissertation. I learned a great deal both in and out of the classroom from each of these first-rate mentors.

Participation in the Coastal Institute IGERT Program (CIIP) was a highlight of my graduate experience, and I thank the members of the CIIP community for their collaboration and for their support, which continued long after my graduation from the program. Special thanks to Pete August, Cheryl Foster, Q. Kellogg, Judith Swift, and to my CIIP cohort (and wardrobe advisors): Carrie Byron, Kim Lellis-Dibble, and Nicole Rohr.

An assistantship with URI's Coastal Resources Center provided a valuable introduction to coastal management in Rhode Island and around the world. I thank Pam Rubinoff and Stephen Olsen for their deft guidance during my stint at the CRC. Funding is also acknowledged from the State of Rhode Island (beach survey assistantship), Rhode Island Sea Grant, the National Science Foundation (IGERT

program), U.S. Army Corps of Engineers, and the Weekapaug Foundation for Preservation.

Janet Freedman and Bryan Oakley graciously shared their expertise in coastal geology on numerous occasions. This dissertation is greatly improved as a result of our many discussions and their valuable insight. Thanks also to Galen Scott for outstanding lessons in geodesy.

A hefty thanks to my South Lab colleagues, past and present: Danielle Cares, Chris DiPerna, Carol Gibson, Chip Heil, Brad Hubeny, Jim King, Monique LaFrance, Erika Lentz, Cam Morissette, Dane Sheldon, Emily Shumchenia, Steve Smith, and Ben Vinhateiro - for help in the field and in the lab, and for their friendship and collegiality. I acknowledge and thank Rich Bell, Christian Buckingham, Mark Cantwell, Scott Graves, Matt Horn, Pat Kelly, John Merrill, and John Peck for assistance with various technical aspects of this research. Roger Larson and Rob Pockalny introduced me to of the field of marine geology and encouraged me to pursue a degree at GSO, for which I am deeply grateful.

Finally, I thank my entire family for their love and support during my years at GSO. To my parents, Dennis and June, and my in-laws, Bruce and Barbara – thank you for your unending encouragement (and unending child care). To my daughters Maia and Nina - thank you for giving me many, many reasons to smile. And to Amanda - thank you most of all - for your patience, love, and words of encouragement. Mahalo nui loa!

PREFACE

This study uses geologic and instrumental records to examine the response of Rhode Island's barrier-headland shoreline to long-term coastal processes and episodic storm impacts. This dissertation was written in manuscript format and consists of the following three manuscripts:

Chapter 1, *A late Holocene record of hurricane-induced overwash from southern Rhode Island*, uses sediment core data to reconstruct a proxy record of tropical cyclone activity from Quonochontaug Pond, a coastal lagoon fronted by a barrier beach. Overwash sand sheets observed in the sediment record are attributed to intense hurricane landfalls and are used to calculate landfall probabilities and examine millennial scale changes in hurricane climatology in southern New England.

Chapter 2, *Shoreline position and rate of change from long-term beach profile measurements: Rhode Island south shore*, presents a high-resolution record of shoreline change derived from the University's long-term (49-year) beach profile dataset. Observations from eight cross-shore transects are used to estimate shoreline change and results are compared to those calculated from historic (vector) shorelines to evaluate rate-of-change statistics for regional shoreline mapping programs.

Chapter 3, *Toward improved shoreline monitoring for southern Rhode Island*, provides a review of sea level rise predictions, describes resources at risk in Rhode Island, and summarizes the inventory of digital geospatial data available for risk assessments. Recommendations are made to establish and continuously monitor coastal evolution using high-resolution topography and to integrate multiple datasets into coastal decision-making.

TABLE OF CONTENTS

LIST OF TABLES

TABLE PAGE

LIST OF FIGURES

CHAPTER 1: A late Holocene record of hurricane-induced overwash from southern Rhode Island

A manuscript in preparation for submission to:

The Geological Society of America Bulletin

by

Nathan Vinhateiro[1], John W. King[1], Rebecca S. Robinson[1]

[1] Graduate School of Oceanography, University of Rhode Island, Narragansett, RI 02881

1.10 Abstract

Barrier-lagoon complexes, which typify much of the east coast of the U.S., offer a unique environment to examine the effects of coastal inundation due to storms and sea level rise. Here we present a sedimentary record of storm-induced overwash from Quonochontaug Pond, a back-barrier lagoon located on Rhode Island's south shore. Radiometric dating indicates that recent overwash deposits correlate with hurricane-induced storm surges measured by local tide gauges in A.D. 1954 and 1938, and with historical accounts of hurricanes in 1815 and 1635. At least 6 additional events of comparable magnitude impacted the site during the past 2200 years. We therefore calculate a probability of 0.45% for intense hurricane landfall in Rhode Island, similar to estimates from proxy-based reconstructions at a range of locations throughout the North Atlantic. The record of overwash also demonstrates that New England has experienced changes in the timing of intense hurricane landfall during the late Holocene. We observe periods of increased activity between 1635 A.D. and the present and 1400-2150 cal. yr BP. A relative lull in activity is observed between these periods, with only one deposit preserved in >1000 years. Similarity in the timing of intense tropical cyclone activity between Rhode Island and locations throughout the western North Atlantic provides further evidence that millennial-scale variability is the result of basin-wide climatic forcings.

1.20 Introduction

Tropical cyclones (hurricanes and tropical storms) represent one of the greatest hazards to life and property in the coastal zone. In the United States, hurricanes are responsible for more insured losses than any type of other natural disaster (III, 2009; Elsner and Kara, 1999) and the societal impacts have grown as coastal populations increase. Major hurricanes (wind speeds > 50 m s^{-1}) account for only 24% of landfalling tropical cyclones in the U.S., yet are responsible for the vast majority of damages (Pielke et al, 2008). Consequently, there is great interest in how climate variability influences the landfall probability and characteristics of these rare but destructive storms, especially given predictions that the incidence of major hurricanes will increase as the planet warms (Emanuel, 2005; Emanuel et al., 2008; Knutson et al., 2010).

Although major hurricane landfalls are rare in New England, they pose a substantial risk nonetheless. For example, Pielke et al. (2008) have estimated that the New England Hurricane of 1938 would rank as the 6th most costly hurricane in U.S. history if it made landfall under contemporary levels of coastal development. The probability of an event of similar magnitude is therefore of great importance for coastal policy, emergency management, and risk assessment, particularly when coupled with a rise in sea level - up to and exceeding 1 meter - during the next century (Rahmstorf, 2007; Vermeer and Rahmstorf, 2009).

A major constraint when assessing risk and vulnerability to tropical cyclones is that available data are often limited to instrumental records from the last ~160 years (Blake et al., 2011; Landsea et al., 2004). Decadal to centennial variability in

hurricane activity is difficult to observe at these scales, particularly for intense storms because the frequency of occurrence is not great enough to provide a statistically reliable sample. In New England, historical accounts of hurricanes from newspapers, diaries, and ships logs have been used to lengthen the record to the time of European settlement (Ludlum, 1963), but uncertainties in the data become more problematic as the period of observation is extended.

For this reason, many researchers are turning to geologic (proxy) evidence as a way to examine hurricane activities beyond the instrumental or historical period. Recent work has demonstrated that tropical cyclones produce a wide range of effects that can be preserved in the geologic record, including $\delta^{18}O$ anomalies in tree rings (Johnson and Young, 1992; Miller et al., 2006), offshore microfossil assemblages in coastal marsh sediments (Hippensteel and Martin, 1999; Collins et al., 1999), overwash deposits (Liu and Fearn, 1993; Donnelly et al., 2001) and oxygen isotope ratios from speleothems (Lawrence and Gedzelman, 1996; Frappier et al., 2007). Two of the most important factors to understanding hurricane risk – storm frequency and intensity – have been addressed through field and modeling studies that utilize these proxy records.

In this study, we present a record of overwash deposition from Quonochontaug Pond, RI (41.33°N, 71.74°W) - a backbarrier coastal lagoon situated on the Rhode Island south coast. Overwash processes (e.g. Leatherman, 1981) and inlet formation are important mechanisms of sediment transport in this environments and provide intermittent connection between lagoon and nearshore environments during hurricanes. This work follows an approach similar to previous reconstructions of

storm-induced overwash from North America (e.g. Liu and Fearn, 2000; Donnelly et al., 2001; Scileppi and Donnelly, 2007; Donnelly and Woodruff, 2007), which allows us to compare patterns of hurricane activity in New England with other regional studies. At Quonochontaug Pond, the local morphology, and the documented history of past coastal flooding indicate that the site has a relatively high threshold for storm-induced overwash. Constrained by radiometric ages, the sediment record from Quonochontaug Pond extends over two millennia, providing a means to examine factors that influence the occurrence and intensity of tropical cyclones on geologic time scales.

1.30 Background

1.31 Study area

The south shore of Rhode Island (Figure 1.1) is a wave-dominated, mixed energy coast (after Hayes, 1979; Nummendal and Fischer, 1978), consisting of an alternating series of sandy barrier spits and headland bluffs composed of glaciofluvial sediment and till. Eight microtidal lagoons are situated behind the spits, connected to Block Island Sound through narrow inlets. Radiocarbon dates indicate that lagoonal sedimentation began approximately 4,000–5,000 years BP, coincident with a slow-down in the rate of relative sea level rise (Oldale and O'Hara, 1980; Donnelly, 1998). Since that time, the barrier spits have migrated landward through the combined effects of sea level rise, overwash processes, and through construction of flood tidal deltas (Dillon, 1970). The transgressive nature of the coastline is revealed by the salt water peat and lagoonal deposits that underlie the present day barrier and commonly outcrop on the eroding beach face (Dillon, 1970; Boothroyd et al., 1985).

Owing to its geography in the North Atlantic and its south facing orientation, the Rhode Island coast is ideal for examining the impact of landfalling hurricanes. This part of New England is frequently affected by late-stage tropical cyclones that form at lower latitudes and approach from the south. Previous workers have demonstrated that the Rhode Island coastal lagoons are sensitive to storm-generated overwash and have the potential to preserve a record of storm deposits within backbarrier settings (e.g. Wilby et al., 1939; Boothroyd et al., 1985; Ford, 2003). In a study examining sediment cores from Succotash Marsh, a flood-tidal delta wetland, Donnelly et al. (2001) showed that at least 6 hurricanes (indicated by sand layers in marsh peat) have struck the southern coast of RI during the last 700 years. Ford (2003) identified discrete sand layers within the low energy basins of Quonochontaug and Garden ponds and attributed these deposits to hurricane-induced overwash during the last ~200 years.

The existing data on storm frequency and impacts are used here as a point of departure to extend the history of hurricane landfall in southern Rhode Island and to examine the coherence of overwash preservation from different geomorphic settings. We use a combination of archived sediments collected by Ford (2003) and new samples from Quonochontaug Pond, RI (Figure 1.1). The site is a relatively deep coastal lagoon with an average tidal range of 0.07 to 0.1 m (Boothroyd et al., 1985; CRMC, 1999). The modern barrier spit is fronted by a 3-5 m foredune and backed by a wide intertidal storm surge platform. Overwash of the barrier is the only known process that can account for presence of fine sand sheets in the lagoon's low-energy basin. The lagoon receives very little sediment in the form of direct runoff from land

or fluvial discharge, as the Charlestown moraine to the north blocks stream flow (Conover, 1961). Tidal inlets do serve as a conduit for sediment flux into and out of the coastal lagoons but tidal variability is low away from the inlet, which minimizes the influence of tidal currents for sediment transport in the deeper basins. Furthermore, current velocities generated by wind stress in the basin are less than the threshold for sand movement (20 cm s^{-1}), even when additive to tidal currents (Boothroyd et al., 1985).

1.32 Historic Rhode Island hurricanes

For the North Atlantic basin, the Atlantic hurricane database (HURDAT) maintained by the National Hurricane Center provides the most extensive and up-to-date track and wind speed data for all known tropical cyclones since 1851, including those that have made landfall in New England (Landsea et al., 2004; Blake et al., 2011). During that time, 19 hurricanes (category 1 or greater on the Saffir-Simpson scale) have passed within 100 km of the south shore, yet only 9 of these storms were considered direct strikes and only four storms (in 1869, 1938, 1944, and 1954) are classified as major hurricanes (category 3 or greater) at the time of landfall in Rhode Island (Blake et al. 2011) (Table 1.1). Long-term observations of water levels from the Newport, RI tide gauge show that two of these events (in 1954 and 1938) produced storm tide elevations (surge + astronomical tide) greater than 2.5 meters above the local sea level datum (NOAA, 2011) (Figure 1.2). Tide measurements in Newport extend only to 1930, but historical accounts of the September Gale of 1869 suggest that the surge from this storm was limited to 2 meters due to its smaller size and

landfall coincident with low tide (Ludlum, 1963; Boose et al., 2001; Donnelly et al., 2001).

In addition to the four storms listed above, at least 2 major hurricanes made landfall on the southern New England coast between the time of European settlement and the start of the modern instrumental record in 1851. One of these storms - the Great September Gale of 1815 - made landfall approximately 55 km to the west of Quonochontaug Pond, and resulted in widespread damage and extensive overwash along the south shore (Lee, 1980). At Newport, RI, a storm surge of greater than 3 m was observed (Ho, 1989; Jarvinen, 2006). A second storm - the Great Colonial Hurricane (A.D. 1635) - was a rapidly moving system that resulted in a storm tide of greater than 4 meters along the Rhode Island south shore (Vallee and Dion, 1998; Ludlum 1963). Although little exists in the way of meteorological or hydrologic data, reconstructed damage patterns based on numerical modeling (Boose et al., 2001) and storm surge simulations (Jarvinen, 2006) have estimated that the 1635 Colonial Hurricane was a major hurricane (category 3 intensity) when it made landfall in New England.

1.40 Methods

A cross-shore transect of sediment cores, between 1.1 and 2.2 meters in length, were used for this study. Cores were retrieved from Harmonic Cove, a low energy basin separated from the barrier by a deep (3-4 meter) channel. The barrier and washover platform adjacent to the transect is approximately 300 meters wide at this location. Sediment cores were collected by two separate techniques; fixed-piston push cores (~1.5 m) were used to retrieve the uppermost lagoon sediments while preserving

the sediment-water interface, and a Rossfelder vibracoring mechanism was used to collect deeper samples. Both piston cores and vibracores were recovered from a pontoon boat platform using a hydraulic winch and A-Frame. Core locations were determined using a Garmin® hand held GPS unit, which provides an approximate horizontal accuracy of 3-5 meters.

To identify overwash deposits, cores were split in the laboratory and described for sedimentary characteristics (texture, structure, and lithology). Select core halves were then run through a non-destructive GEOTEK® logging system to obtain centimeter-resolution physical property measurements including p-wave velocity, bulk density, and magnetic susceptibility (King and Peck, 2001; Zolitschka et al., 2001). Digital bitmap images of each core in red/green/blue (RGB) color scheme were also generated. Down-core logs and imagery were used to interpret lithofacies as well as to correlate between different cores.

X-ray fluorescence (XRF) provided an additional, nondestructive and high-resolution measurement, which has been used in previous studies to distinguish overwash deposits and identify pollution and land-clearance horizons based on elemental analysis of split sediment cores (e.g. Woodruff et al., 2008a; Boldt et al., 2010). The technique measures fluorescent radiation from sediments that have been excited by bombardment with high-energy X-rays or gamma rays to detect the abundances of elements that are present in the sample (Dzubay, 1977). Elemental analysis for select core halves was measured at one-centimeter intervals with an Innov-X XRF spectrometer integrated into a GEOTEK® multi-sensor core logging

system (Brown University). Anomalous samples with total XRF counts below 8000 were removed from the downcore record.

For all cores, grain size was measured at a one-centimeter interval using a Malvern Mastersizer 2000® laser diffraction particle size analyzer. The centimeter-scale sampling resolution was chosen because previous studies have shown that overwash deposits from lagoon settings can be on the scale of 1 cm or less (Liu and Fearn, 1993; Donnelly and Woodruff, 2007; Smith, 2010). Prior to analysis, the siliciclastic fraction of the sediment was isolated by treatment with 1N acetic acid, followed by a 30% H_2O_2 solution to remove any carbonate and organic material. The remaining sediment was immersed in a particle dispersant (sodium hexametaphosphate) and deflocculated in an ultrasonic bath prior to analysis. For each sample, the average of three optical measurements was used to generate a representative grain size distribution.

Loss on ignition (LOI) analysis (Dean, 1974) was also used to confirm the occurrence of sand layers, as they have much lower organic carbon content than typical lagoon mud (Liu and Fearn, 2000). One cubic centimeter samples were taken from select cores at the same interval and resolution as grain size samples. The wet weight was determined for the sediment, and the sediment was then dried in a muffle furnace at 100°C for 24 hours. After cooling to room temperature in a dessicator, the samples were reweighed to yield a dry weight. Samples were then heated at 550°C for one hour and the mass of the cooled sampled was measured to determine the percentage of combustible organic material (LOI). Percent organic carbon was calculated by multiplying the LOI value by 0.432.

A number of different methods were used to provide age control to the sediments from Quonochontaug Pond. Samples of seeds and plant fragments from core QP-25 were analyzed for radiocarbon (^{14}C) at the National Ocean Sciences Accelerated Mass Spectrometry (NOSAMS) facility at the Woods Hole Oceanographic Institution. In order to avoid reservoir corrections that would be necessary for marine aquatic material, terrestrial macrofossils were selected for ^{14}C dating (Björck and Wohlfarth, 2001). Three additional dating methods were used to provide age control for the historical period: (i) dried sediment samples from the uppermost ~50 cm of core QP-17 were analyzed for ^{137}Cs by direct gamma assay using a germanium well-type detector (Appleby et al., 1986); (ii) the rise of ragweed (*Ambrosia artemisiifolia*) pollen associated with land clearing by European colonists was identified using standard laboratory procedures (Faegri and Iversen, 1989); and (iii) pollution horizons associated with synthetic organic contaminants (polychlorinated biphenyls –PCBs, and dichlorodiphenyl tricholorethane -DDT) were identified. Ages and age uncertainties associated with fossil pollen and PCB/DDT horizons were originally presented by Ford (2003).

1.50 Results

1.51 Stratigraphy

Sediment cores from Quonochontaug Pond consist of massive silt and clay intervals that are intermittently punctuated by coarse-grained layers consisting of fine to medium sand and shell fragments. The massive silt unit is characterized by high organic carbon (TOC) values and is analogous to the back-lagoon, low-energy lithofacies described by Boothroyd et al. (1985). Coarse-grained layers interspersed

within this unit are between 2 and 10 cm in thickness and composed of a mixture of light grey, fine to medium sand and lagoonal mud (Figure 1.3). The transition between sandy layers and overlying lagoon mud is gradational, while the lower contact is often more abrupt. The coarse fractions of sand layers consist of sub-rounded quartz and feldspar grains, similar to the composition of the modern barrier (McMaster, 1960) (Figure 1.4). In cores taken from areas closer to the barrier, these layers appear as a mixture of sand and shell fragments. Down-core, the coarse-grained lithofacies are characterized by peaks in density and magnetic susceptibility, relatively high concentrations of Fe, and low TOC values (Figure 1.3). With the exception of these intermittent coarse-grained units, cores do not exhibit significant changes in color, texture, or elemental composition that indicate a change in depositional environment (facies shift) over the length of the sedimentary record.

The stratigraphy of coarse-grained deposits is similar between cores in transect (Figure 1.5). The upper ~50 cm of the sediment record is dominated by 2 to 3 relatively thick, sandy deposits that exhibit a general fining trend away from the barrier; a similar fining pattern is noted in layers that are continuous throughout the lower sections. The mineralogy of these units, the abrupt nature of contacts, and their lateral continuity fit criteria defined by a number of previous studies that describe sedimentary characteristic of backbarrier overwash deposits (Liu, 2004; Donnelly and Webb, 2004; Scileppi and Donnelly, 2007), suggesting that coarse-grained deposits are the result of sediment transport due to storm-induced coastal flooding (overwash processes). Grain-size distributions of coarse-grained units show a bimodal mixture of

two distinct sediment sources, inferred to represent a combination of re-suspended lagoonal mud and sand washed into the lagoon during storm events (Figure 1.6).

1.52 Chronology

Excellent dating of overwash deposits at Quonochontaug Pond is required for comparison to documented storm events (Figure 1.7). In core QP-17, measurements of the activity of ^{137}Cs – a bi-product of atmospheric nuclear weapons testing – show a concentration spike (indicating A.D. 1963 ± 2 years) at 14.5 cm, approximately 1.5 cm above the uppermost overwash unit. The depth of the cesium peak in QP-17 is in general agreement with estimates by Ford (2003) who calculated that the uppermost sand layer was deposited in the 1950's based on observations that 50% of the ^{137}Cs inventory was above 12 cm in core QP-27. Ford (2003) also used the occurrence of synthetic organic contaminants (PCBs and DDT) and fossil pollen in the sediment record as additional age control in core QP-25. Both PCBs and DDT are now banned but were produced in the U.S. during the decades of the 1930s through the 1970s. The background of both contaminants was found at a depth of 23 cm in QP-25, corresponding to an approximate date of A.D. 1940 (Hom et al., 1974). Analysis of fossil pollen (also by Ford, 2003) places the *Ambrosia* horizon and the corresponding decline in arboreal species at a depth of 45 cm in QP-25. In southern New England, the rise of *Ambrosia* (ragweed) is commonly associated with European colonization and related land use changes at the end of the seventeenth century (Francis and Foster, 2001). The timing of this horizon in Washington County, RI has been dated to A.D. 1700 ± 30 years based on an annually resolved varve chronology from the Pettaquamscutt River (Hubeny et al., 2008).

AMS-measured radiocarbon dates and calibrated calendar ages from five macrofossil samples recovered from core QP-25 are reported in Table 1.2 and shown in Figure 1.7. Radiocarbon ages were calibrated using the IntCal09 calibration data set (Reimer et al., 2009) and the resulting dates and 1σ ranges are reported in calendar years before present (cal. yr BP) with present being A.D. 1950 by convention. As no single value completely describes the probability distribution function of the calibrated age ranges, the median probability of calendar ages and ± 1σ age uncertainties were used to calculate sediment ages and accumulation rates. One inverted ^{14}C date was not included in the age model due to possible contamination. This sample, recovered from between 56-57 cm depth, is not compatible with other independent age constraints from QP-25. The age discrepancy is approximately 120 years outside the range of error. Re-suspension of an older macrofossil in the basin and/or sample contamination are possible explanations for the anomalously old date.

1.53 Lithostratigraphic correlations and age model

Previous workers have noted that transect-scale observations can be useful for determining favorable locations for overwash preservation (Liu and Fearn, 2000; Donnelly and Woodruff, 2007). In backbarrier lagoons, cores retrieved from areas close to the barrier are more likely to record an amalgamation of multiple overwash deposits, while areas located at the distal ends of a core transect may not provide a complete record of storm events. Given the length and continuity of the sediment record, the lateral distance from the barrier, the potential for overwash preservation, and the cross-shore trends in grain size (Figure 1.5), we selected core QP-19 to further examine the history of overwash activity from this site.

The age model for core QP-19 was constructed by tying the upper portion of the sediment record into the ^{137}Cs age model from core QP-17 and remaining age controls from core QP-25. Examination of the grain size data shows that the upper portion of QP-19 is slightly compressed when compared to other sites, possibly due to compaction of the uppermost sediments during vibracoring. Correlation between cores was accomplished by examining physical properties with depth and correlating tie points based on changes in the texture, color, and grain size of the sediment record at each site. The repetition of cm-scale facies of overwash sand, and the character of the lagoonal silt/clay intervals that bound them was particularly useful for establishing robust correlation between locations. Using the tie points shown in Figure 1.8, age controls from cores QP-17 and QP-25 were shifted to QP-19 based on a re-scaling of sample depths in Analyseries software (Paillard et al., 1996) with core QP-19 as a reference.

Curves illustrating the age-depth relationship were determined by linear interpolation between $\pm 1\sigma$ age uncertainties and are shown in Figure 1.9. The basal age of QP-19 was determined by assuming a constant sedimentation rate and extending the linear trend of the oldest age control point to the base of the core. The non-linear behavior observed in the interpolation curve is, in part, attributed to the episodic nature of storm-induced sedimentation in the basin. Overwash processes complicate the age model by instantaneously depositing large quantities of sediment, and by potentially causing erosion at the lower depositional contact. Furthermore, overwash events that occur in rapid succession may not be distinguishable if the deposits are not discrete. Proxy storm records based on overwash deposits will carry

this uncertainty and ages assigned to specific events must therefore recognize these limitations. This potential for undercounting storm-induced deposits results in minimum estimates of landfall probability.

1.54 Age estimates for recent overwash deposits

At least 10 discrete overwash layers are preserved in core QP-19 (Figure 1.3). Based on our age model, coarse-grained deposits within the upper 60 cm are coincident with four of the most intense storm-surge events recorded in southern New England during the historical period. Specifically, we find:

(i) The uppermost deposit predates the ^{137}Cs peak and is bound on the lower end by the rise of PCB and DDT contaminants above background ~2 cm below the base of the deposit. Given the ages bracketing this layer, and the fact that no major hurricanes have impacted the study area since 1954, we attribute the uppermost deposit to overwash from Hurricane Carol, a powerful category 3 storm that made landfall near the time of astronomical high tide on August 31, 1954.

(ii) The rate of sediment accumulation between the PCB/DDT horizon (ca. 1940) and the rise of Ambrosia pollen (A.D. 1700) place the event layer found between 18 and 21 cm at A.D. 1936-1937, an age compatible with the Great New England Hurricane of 1938. As was noted by Boldt et al., (2010), water levels of nearly 2 m above msl were also observed during the Great Atlantic Hurricane in September 1944 (Figure 1.2). Given that this storm occurred just six years after the 1938 hurricane, it is

possible that the deposit could represent a mixture of sand transported during both events.

(iii) The ± 1σ uncertainties for the age model indicate that the layer found at an approximate depth of 36 cm was deposited between 173-136 cal. yr BP (A.D. 1777-1814). In transect, this sand sheet is not identified in all cores, but its presence is noted in QP-19, as well as in cores located closer to the barrier. Given its age range, and the historical accounts of storm surge elevations (Ho, 1989; Jarvinen, 2006), it is probable that this deposit is the result of overwash from the Great September Gale of 1815.

(iv) Finally, the rise of Ambrosia pollen places a date of ~A.D. 1700 at a depth of 47 cm, approximately 3 cm above a relatively thick (8 cm) sand layer. Age uncertainties in this interval are larger, due to the coincidence of two closely spaced chronostratigraphic controls with a ca. 130-year age discrepancy (Figure 1.9). Nonetheless, the ± 1σ age uncertainties place this deposit between A.D. 1511 and 1650 and we therefore attribute this layer to the A.D. 1635 Colonial Hurricane.

1.60 Discussion

1.61 Overwash preservation at Quonochontaug Pond

Robust instrumental and documentary records of storm surge in southern Rhode Island offer a means to calibrate storm washovers with the events that deposit them. Age-depth relationships from QP-19 show that the timing of sandy layers deposited during the last ~400 years correlates closely with the incidence of major hurricanes (wind speeds > 50 m s^{-1}) that have impacted the Rhode Island south coast.

Tide gauge measurements (and storm surge reconstructions for hurricanes that pre-date the instrumental record) indicate that each of these events likely resulted in water levels that exceeded 2.5 m above msl at the site (Figure 1.2). In addition, the four uppermost sand layers are coincident with records of storm-induced overwash since A.D. 1600 at Succotash Marsh in East Matunuck, RI (Donnelly et al., 2001) and at Mattapoisett Marsh, MA (Boldt et al., 2010) (Figure 1.10).

Can we interpret the relationship between the sediment record and historically documented hurricanes as indication that our coring site has a high threshold for storm-induced overwash? Continuous beach profiling at eight sites along the RI south shore has recorded changes in beach volume and shoreline position since 1962 (Lacey and Peck, 1998). During this time, 19 tropical cyclones have passed within 100 km of the Quonochontaug barrier, including two hurricanes (Gloria in 1985, and Bob in 1991) that were of category 2 intensity at landfall. Beach profiles following these events show that morphological impacts at the Quonochontaug barrier were generally limited to erosion of the berm and foredune (up to 4 meters) and minor quantities of overwash. Nearly 50 $m^3 m^{-1}$ of sand was removed from the barrier following hurricane Gloria (~25% of the profile volume), yet most of this was returned to the beach within a few weeks of the storm's passage. By comparison, Wilby et al. (1939) and Nichols and Marsten (1939) documented extensive damage to the south shore barriers following the 1938 hurricane, including region-wide overwash. The surge and superimposed wave heights from this storm exceeded the height of the foredune, resulting in inundation of the entire barrier spit and incision of washover channels through the barrier core (Nichols and Marsten, 1939). An aerial survey of beaches

conducted just 3 days following the 1938 hurricane show a wide, low barrier that is nearly leveled and clear of wreckage. Numerous incised channels are noted as well as a large ebb-flowing inlet at the westernmost end of the barrier (Figure 1.11, U.S. Army Air Corps, 1938).

Transport of beach sand to locations ~500 m from the back of the modern barrier also supports the hypothesis that the deposits preserved in QP-19 represent only severe storm landfalls. A recent analysis of the morphological impacts of storms from the U.S. Atlantic and Gulf coasts indicates that only the most intense storms (category 3 and higher hurricanes on the Saffir-Simpson scale) are capable of transporting sand more than 300 m inland for long segments of coast (Morton and Sallenger, 2003). Normally, the foredune fronting the Quonochontaug barrier acts to buffer the landward impacts of surge from moderate storms, and when overwash does occur, the channel separating the surge platform from the basin impedes bedload transport of sand-sized particles in the cross-shore direction.

These observations, coupled with the timing of recent deposits, provide strong evidence that the coarse-grained deposits preserved at this site are the result of major hurricanes landfalls - events with the capacity to breach or overtop the barrier and with flow velocities capable of carrying fine sand in suspension for several hundred meters. Assuming that the sensitivity of this site has only increased during the late Holocene transgression, the record here provides a ~2200 year history of southern Rhode Island's most intense hurricanes.

1.62 Relative comparison of storm intensities

The capacity of a storm for sediment transport can also be used to assess hurricane intensities. Woodruff et al. (2008a) recently developed an advective-settling model for estimating relative flooding intensities from paleo-event deposits. In brief, the model relies on the physics of sediment transport in order to calculate the flow conditions necessary to form an observed deposit (Appendix A). The approach is ideal for laterally sorted deposits that are assumed to have travelled primarily in suspension from their source (the barrier) to the deposit. The method predicts a maximum instantaneous water level above the barrier during breaching ($<h_b>$), thus it reconstructs the cumulative effects of storm surge and maximum wave runup. Core stratigraphies (landward fining of overwash fans) and local morphology at Quonochontaug Pond suggest that this method may be a valid approach for comparison of prehistoric events at our coring site.

We first assessed the validity of the model using the 1938 hurricane deposit as a modern analogue for predicted $<h_b>$ values (Appendix A). For all cores, the maximum water levels predicted using this approach range between 4.1 and 4.5 m relative to msl, and are consistent with observations along the RI south shore of combined wave heights during the 1938 hurricane between 4.1 and 5.2 m (Tannehill, 1938; Paulsen et al., 1940). To examine how inundation magnitudes may have varied during the late Holocene we reconstructed $<h_b>$ for all 10 deposits identified in core QP-19. During this time, the cumulative effects of sea level rise and storms have likely translated the Quonochontaug barrier landward, effectively increasing the sensitivity of our core site to overwash processes. These effects are notable in the sediment

record, where the scale of overwash deposits from modern storms stands out prominently. We therefore modified the Woodruff et al. (2008a) approach with an additional variable to account for the long-term transgression of the shoreline through time (Appendix A).

The final reconstruction of flood magnitudes from Quonochontaug Pond is shown in Figure 1.12. Estimates of $<h_b>$ for prehistoric events are similar to modern storms, and range from 1.9 to 2.9 m. A comparatively large value is predicted for hurricane Carol (1954), though the relative impact of this storm may be an artifact of changes in the barrier morphology that heightened the sensitivity of the site to overwash processes. Hurricane Carol was the second category 3 storm to strike the Rhode Island south shore in relatively close succession (16 years). Morton et al. (1995) and Fenster et al. (2001) have shown that post-storm recovery for barrier spits may persist for decades, and hurricane impacts can be amplified if storm frequency exceeds the beach recovery period. Overall, the similarity of event magnitudes during the late Holocene indicates that nearly all events had a competence for sediment transport that was similar to storms from the last ~400 years, and provides further evidence that overwash deposits preserved in Quonochontaug Pond represent major hurricane landfalls.

1.63 Landfall probability in southern New England

Stratigraphic evidence of at least 10 intense hurricanes during the past 2200 years yields a landfall probability of 0.45% (return period of ~220 years) for Quonochontaug Pond, RI. This value is an order of magnitude lower than estimates based on total occurrences from instrumental records (e.g. Elsner and Kara, 1999;

Neumann, 1987) but is in general agreement with model-derived estimates, constrained using HURDAT landfall data, which predict an annual probability between 0.15% and 0.81% for wind speeds in excess of 50 m s^{-1} along the RI south coast (Murnane et al., 2000; Donnelly and Webb, 2004).

To illustrate how landfall probabilities can vary regionally depending on the period of observation and threshold for overwash at each site, storm events at Quonochontaug Pond are compared with two published records from sites in southern New England: Succotash Marsh, RI (41.38°N, 71.52°W), located 18 km to the east of our site, and Mattapoisett Marsh, MA (41.65°N, 70.79°W) (Donnelly et al., 2001; Boldt et al., 2010) (Figure 1.10). Deposits that have been calibrated to the historic record are contemporaneous at all sites, yet we find no corollary to 2 prehistoric storms that were documented at Succotash Marsh between 527-511 and 641-559 cal. yr BP. Additional cores and more robust dating of deposits in QP-19 is needed to confirm this discrepancy, although slight changes in barrier spit morphology could account for the difference between these records. Indeed, Donnelly et al. (2001) describe the formation of inlets within the backbarrier system at Succotash Marsh and note that the presence of such an inlet could alter the threshold for prehistoric overwash preservation. By contrast, the overwash history at Mattapoisett Marsh shows a relatively constant tropical cyclone activity over the past 2000 years. The record is presumed to represent storms of varying intensity (Boldt et al., 2010). As a result, nearly every storm deposit preserved at Quonochontaug Pond is coincident with a deposit at this site.

Wallace and Anderson (2010) provided evidence of similar probabilities of intense hurricane strikes throughout the Gulf of Mexico and Caribbean during the late Holocene. Extending this comparison to include proxy-based storm records from sites throughout the mid-Atlantic and New England coastlines indicates general consistency throughout the entire basin (Figure 1.13). The landfall probability at Quonochontaug Pond (0.45%) is notably similar to those estimated from storm-induced overwash along the Gulf, Caribbean, and mid-Atlantic coastlines, particularly for locations with high overwash thresholds that are assumed to reflect only intense hurricane strikes. The similarities imply that on millennial time scales, the probability of a direct strike by the most rare and energetic storms is relatively constant for individual coastal locations.

1.64 Millennial-scale variability

The cumulative frequency of overwash deposits at Quonochontaug Pond (Figure 1.14) shows periods of increased hurricane activity between 1635 A.D. and the present (~1 deposit per century) and 1400-2150 cal. yr BP (~0.7 deposits per century). A relative lull in activity is observed between these intervals, with only one deposit preserved in over 1000 years. While Woodruff et al. (2008b) have noted a potential for undercounting storm events during periods when sedimentation rates are low, this pattern is in general agreement with millennial-scale variability observed in reconstructions of intense hurricane activity along the mid-Atlantic and Gulf coasts, and in the Caribbean (Figure 1.15).

Similarity in the timing of overwash at sites in the North Atlantic has been noted by previous workers (Scileppi and Donnelly, 2007; Woodruff et al., 2008b) but

to our knowledge, this is the first study to observe this pattern in New England. At Quonochontaug Pond, the period of decreased overwash prior to the instrumental record is more protracted and we see no indication of a peak in hurricane activity around 1000 A.D. noted by Mann et al. (2009), yet a comparison of the records show remarkable similarity nonetheless (Figure 1.15).

The basin-wide decrease in activity prior to 400 cal. yr BP at first suggests that overall hurricane occurrences were lower during this interval, although this interpretation is inconsistent with findings by Boldt et al. (2010) who show a relatively constant tropical cyclone frequency in southern New England during the last 2000 years (Figure 1.10). There is also no evidence of a drop in eustatic sea level at this time that might account for wide-scale and synchronous change to individual barrier systems at coring sites throughout the North Atlantic (Kemp et al., 2011). Boldt et al (2010) proposed that collectively, these reconstructions indicate a relatively unchanging tropical cyclone frequency with variations only in the number of intense hurricane landfalls during the late Holocene. Our record from Quonochontaug Pond, RI provides additional support for this hypothesis, particularly given the proximity of the two sites in southern New England and the similar periods of observation.

The observation that millennial-scale patterns of overwash in the western North Atlantic are synchronous suggests that these changes are climatically driven. Past studies that have examined climatic influences on North Atlantic tropical cyclones consider the North Atlantic Oscillation (NAO), El Nino/Southern Oscillation (ENSO), and sea surface temperature (SST) to be the primary factors that influence

the occurrence and intensity of hurricanes on interannual time scales (Sabbatelli and Mann, 2007; and references therein).

Liu and Fearn (2000) and Elsner et al. (2000) have postulated that millennial-scale variability in overwash records from the Gulf coast can be explained by changes in the intensity of the NAO, which affects the track of storms by changing the position of the Bermuda High. The result is an anti-phase (seesaw) pattern in major hurricane activity that oscillates between the Gulf and Atlantic coastlines on long time scales. Scileppi and Donnelly (2007), noting a similarity between records in western Long Island and those from the northern Gulf coast, suggest instead that landfall patterns are related to overall storm frequency as opposed to storm track, emphasizing the need for additional records to test the competing hypotheses. The general agreement between our record from Quonochontaug Pond, and those from the Caribbean, Gulf coast, and mid-Atlantic corroborates this pattern at an additional site in the northeastern U.S. Overall, the similarity between the available records shows no obvious anti-phase relationships that would suggest a storm steering influence on landfall patterns at these time scales.

A recent synthesis of proxy-based hurricane reconstructions has attributed a period of peak hurricane activity around 1000 A.D. to the reinforcing effects of La Nina and relatively warm SSTs in the tropical North Atlantic (Mann et al., 2009). The reconstruction was supported by a statistical model of Atlantic tropical cyclone activity constrained by proxy reconstructions of past climate changes. As noted above, however, we see no evidence of increased activity at Quonochontaug Pond during the Medieval Warm Period (between A.D. 950-1250) or for that matter a decrease during

the Little Ice Age (A.D. 1700-1815) when tropical SSTs were 2-3 degrees cooler than present (Winter et al., 2000). This suggests that climate forcings other than SSTs have played a more dominant role in modulating intense hurricane landfall patterns in New England on centennial to millennial time scales.

Donnelly and Woodruff (2007) hypothesized that variability in the El Nino / Southern Oscillation and the strength of the West African monsoon have been the primary controls for North Atlantic tropical cyclone variability during the last 5,000 years. This hypothesis is consistent with observations from the instrumental record that indicate North Atlantic hurricane activity is generally suppressed during El Nino years, due to increased tropospheric vertical shear (Gray, 1984). A qualitative inspection of our record does indicate that the gap in overwash activity between ~1400 and 400 years BP at Quonochontaug Pond coincides with two intervals of more frequent, moderate to strong El Nino events identified by Donnelly and Woodruff (2007) (Moy et al., 2002). We emphasize however, that more detailed records of overwash from New England are necessary to properly examine this relationship.

1.70 Conclusions

A greater understanding of tropical cyclone variability requires studies that extend observations of hurricane activity beyond instrumental or historical periods. In this study, a transect of cores from Quonochontaug Pond, RI provides sedimentary evidence of late Holocene hurricane landfalls in southern New England. The region has been impacted by numerous events during the historical period that have been used to calibrate the sediment record. Age estimates from radiometric and fossil pollen markers suggest that the timing of recent deposits coincides with hurricane-induced

storm surge recorded by local tide gauges in 1954 and 1938, and historical accounts of major hurricane landfalls in 1815 and 1635. In addition, the record shows that at minimum, 6 prehistoric events impacted the region during the last 2200 years. These events were comparable to modern storms in their capacity for sediment transport, and estimates of relative storm intensities support the interpretation that overwash deposits at this site can be attributed to intense hurricanes landfall.

Using the National Hurricane Center's best track database (Landsea et al., 2004), the annual probability of intense hurricane activity for Washington County, RI ranges between 1.9% and 3.1% (Neumann, 1987; Elsner and Kara, 1999). By extending the period of observation over the past two millennia, we calculate a landfall probability of 0.45%, comparable to estimates from a wide range of proxy-based reconstructions throughout the western North Atlantic. We find that the relatively high tropical cyclone activity during the modern period is not unprecedented when compared to other intervals during the last 2200 years. We also observe a relative lull in activity prior to the historical period. The similarity in timing of intense hurricane landfalls between Quonochontaug Pond and sites throughout the North Atlantic basin suggests that variability observed in our record is not an artifact of changes in the tracking of storms, but instead probably due to basin-wide changes in hurricane climatology during the late Holocene. In New England, more intense hurricane activity during the last millennium is not observed during periods of warmer tropical SSTs. However, reduced activity prior to the historical record may be coincident with paleoclimate reconstructions of more frequent El-Nino conditions in

the tropical Pacific. Additional reconstructions from New England will be necessary to explore this potential correlation.

1.80 References

Appleby, P.G.; Nolan, P.J.; Gifford, D.W.; Godfrey, M.J.; Oldfield, F.; Anderson, N.J., and Battarbee, R.W., 1986. ^{210}Pb dating by low background gamma counting. *Hydrobiologia*, 141(21-27).

Björck, S., and Wohlfarth, B., 2001. ^{14}C chronostratigraphic techniques in paleolimnology. *In:* Last, W.M., and Smol, J.P. (eds.), *Tracking environmental change using lake sediments. Volume 1: Basin analysis, coring, and chronological techniques.* Dordrecht, The Netherlands: Kluwer Academic Publishers, pp. 205-245.

Blake, E.S.; Landsea, C.W., and Gibney, E.J., 2011. The deadliest, costliest, and most intense United States tropical cyclones from 1851 to 2010 (and other frequently requested hurricane facts). Miami, FL: National Hurricane Center *(NOAA Technical Memorandum NWS NHC-6)*. 47p.

Boldt, K.V.; Lane, P.; Woodruff, J.D., and Donnelly, J.P., 2010. Calibrating a sedimentary record of overwash from Southeastern New England using modeled historic hurricane surges. *Marine Geology*, 275, 127-139.

Boose, E.R.; Chamberlin, K.E., and Foster, D.R., 2001. Landscape and regional impacts of hurricanes in New England. *Ecological Monographs*, 71(1), 27-48.

Boothroyd, J.C.; Friedrich, N.E., and McGinn, S.R., 1985. Geology of microtidal coastal lagoons: Rhode Island. *Marine Geology*, 63, 35-76.

Boothroyd, J.C., and Sirkin, L., 2002. Quaternary geology and landscape development of Block Island and adjacent regions. *In:* Paton, P.; Gould, L.; August, P., and Frost, A. (eds.), *The Ecology of Block Island.* Kingston: Rhode Island Natural History Survey, pp. 13-27.

Boothroyd, J.C., and Hehre, R.E. (Cartographer). (2007). *Shoreline change maps for the south shore of Rhode Island: Rhode Island Geological Survey Map Folio 2007-2, for RI Coastal Resources Management Council, 150 maps (scale:1:2,000).*

Collins, E.S.; Scott, D.B., and Gayes, P.T., 1999. Hurricane records on the South Carolina coast: Can they be detected in the sediment record? *Quaternary International*, 56(1), 15-26.

Conover, R.J., 1961. A study of Charlestown and Green Hill ponds, Rhode Island. *Ecology*, 42, 119-140.

CRMC (Coastal Resources Management Council), 1999. RI Salt Pond Region: Special Area Management Plan. CRMC. 150 pp.

Dean, W.E., 1974. Determination of carbonate and organic matter in calcareous sediments and sedimentary rocks by loss on ignition: Comparison with other methods. *Journal of Sedimentary Petrology*, 44(1), 242-248.

Dillon, W.P., 1970. Submergence effects on a Rhode Island barrier and lagoon and inferences on migration of barriers. *Journal of Geology*, 78, 94-106.

Donnelly, J.P., 1998. Evidence of late Holocene post-glacial isostatic adjustment in coastal wetland deposits of eastern North America. *GeoResearch Forum*, 3-4, 393-400.

Donnelly, J.P., and Webb III, T., 2004. Back-barrier sedimentary records of intense hurricane landfalls in the northeastern United States. *In*: Murnane, R.J., and Liu, K. (eds.), *Hurricanes and Typhoons: Past, present, and future*. New York, NY: Columbia University Press, pp. 58-95.

Donnelly, J.P.; Bryant, S.S.; Butler, J.; Dowling, J.; Fan, L.; Hausmann, N.; Newby, P.; Shuman, B.; Stern, J.; Westover, K., and Webb III, T., 2001. 700 yr sedimentary record of intense hurricane landfalls in southern New England. *GSA Bulletin*, 113(6), 714-727.

Donnelly, J.P., and Woodruff, J.D., 2007. Intense hurricane activity over the past 5,000 years controlled by El Nino and the West African monsoon. *Nature*, 447, 465-468.

Dzubay, T.G. (Ed.). (1977). *X-ray flourescence analysis of environmental samples*. Ann Arbor, MI: Ann Arbor Science Publishers.

Elsner, J.B., and Kara, A.B., 1999. *Hurricanes of the North Atlantic*. New York, NY: Oxford University Press, 488p.

Elsner, J.B.; Liu, K., and Kocher, B., 2000. Spatial variations in major U.S. hurricane activity: statistics and a physical mechanism. *Journal of Climate*, 13, 2293-2305.

Emanuel, K.A., 2005. Increasing destructiveness of tropical cyclones over the past 30 years. *Nature*, 436, 686-688.

Emanuel, K.A.; Sundararajan, R., and Williams, J., 2008. Hurricanes and global warming: results from downscaling IPCC AR4 simulations. *Bulletin of the American Meteorological Society*, 89, 347-367.

Faegri, K., and Iversen, J., 1989. *Textbook of pollen analysis*. New York, NY: John Wiley and Sons, Ltd., 237p.

Fenster, M.S.; Dolan, R., and Morton, R.A., 2001. Coastal storms and shoreline change: signal or noise? *Journal of Coastal Research*, 17(3), 714-720.

Ford, K.H. (2003). *Assessment of the Rhode Island coastal lagoon ecosystem.* Ph.D.

Dissertation, University of Rhode Island, Kingston, R.I.

Francis, D.R., and Foster, D.R., 2001. Response of small New England ponds to historic land use. *The Holocene*, 11(3), 301-312.

Frappier, A.B.; Sahagian, D.; Carpenter, S.J.; Gonzalez, L.A., and Frappier, B.R., 2007. Stalagmite stable isotope record of recent tropical cyclone events. *Geology*, 35(2), 111-114.

Godfrey, P.J., and Godfrey, M.M., 1973. Comparison of ecological and geomorphic interactions between altered and unaltered barrier island systems in North Carolina. *In:* Coates, D.R. (ed.), *Coastal Geomorphology*. Binghamton, NY: State University of New York, pp. 239-258.

Gray, W.M., 1984. Atlantic seasonal hurricane frequency. Part I: El Nino and 30 mb quasi-biennial oscillation influences. *Monthly Weather Review*, 112, 1649-1668.

Hapke, C.J.; Himmelstoss, E.A.; Kratzmann, M.G.; List, J.H., and Thieler, E.R., 2010. National assessment of shoreline change: historical shoreline change along the New England and Mid-Atlantic coasts. US Geological Survey *(USGS Open File Report No. 2010-1118)*. 57p.

Hayes, M.O., 1979. Barrier island morphology as a function of tidal and wave regime. *In:* Davis, R.A. (ed.), *Geology of Holocene Barrier Island Systems*. Berlin: Springer-Verlag, pp. 233-304.

Hippensteel, S.P., and Martin, R.E., 1999. Foraminifera as an indicator of overwash deposits, barrier Island sediment supply, and barrier Island evolution: Folly Island, South Carolina. *Palaeogeography, Palaeoclimatology, Palaeoecology*, 149(1-4), 115-125.

Ho, F.P., 1989. Extreme hurricanes in the nineteenth century. NOAA *(NOAA Technical Memorandum NWS HYDRO 43A)*. 134p.

Hom, W.; Risebrough, R.W.; Soutar, A., and Young, D.R., 1974. Deposition of DDE and polychlorinated biphenyls in dated sediments of the Santa Barbara Basin. *Science*, 184, 1197-1199.

Hubeny, J.B.; King, J.W., and Cantwell, M., 2008. Anthropogenic influences on estuarine sedimentation and ecology: examples from the varved sediments of the Pettaquamscutt River Estuary, Rhode Island. *Journal of Paleolimnology*, 41, 297-314.

III (Insurance Information Institute). http://www.iii.org/facts_statistics/catastrophes-us.html: accessed on 6 July 2011.

IPCC, 2007. Summary for Policymakers. *In:* Solomon, S.; Qin, D.; Manning, M.; Chen, Z.; Marquis, M.; Averyt, K.B.; Tignor, M., and Miller, H.L. (eds.), *Climate*

Change 2007: The Physical Science Basis. Contribution of Working Group I to the Fourth Assessment Report of the Intergovernmental Panel on Climate Change. Geneva, Switzerland: UNEP, pp. 1-18.

Jarvinen, B.R., 2006. Storm tides in twelve tropical cyclones (including four intense New England hurricanes). Miami, FL: NOAA National Hurricane Center. 99p.

Johnson, S.R., and Young, D.R., 1992. Variation in tree ring width in relation to storm activity for mid-Atlantic Barrier Island populations of Pinus taeda. *Journal of Coastal Research*, 8, 99-104.

Kemp, A.C.; Horton, B.P.; Donnelly, J.P.; Mann, M.E.; Vermeer, M., and Rahmstorf, S., 2011. Climate related sea-level variations over the past two millennia. Proceedings of the National Academy of Sciences, 108(27), 11017-11022.

King, J.W., and Peck, J.A., 2001. Use of paleomagnetism in studies of lake sediments. *In:* Last, W.M., and Smol, J.P. (eds.), *Tracking environmental change using lake sediments. Volume 1: Basin analysis, coring, and chronological techniques*. Dordrecht, The Netherlands: Kluwer Academic Publishers, pp.

Knutson, T.R.; McBride, J.L.; Chan, J.; Emanuel, K.; Holland, G.; Landsea, C.; Held, I.; Kossin, J.P.; Srivastava, A.K., and Sugi, M., 2010. Tropical cyclones and climate change. *Nature Geosciences*, 3, 157-163.

Lacey, E.M., and Peck, J.A., 1998. Long-term beach profile variations along the south shore of Rhode Island, USA. *Journal of Coastal Research*, 14(4), 1255-1264.

Landsea, C.W.; Anderson, C.; Charles, N.; Clark, G.; Dunion, J.; Fernandez-Partagas, J.; Hungerford, P.; Neumann, C., and Zimmer, M., 2004. The Atlantic hurricane database reanalysis project: documentation for 1851-1910 alterations and additions to the HURDAT database. *In:* Murnane, R.J., and Liu, K. (eds.), *Hurricanes and typhoons: past, present, and future*. New York: Columbia University Press, pp. 177-221.

Lawrence, J.R., and Gedzelman, S.D., 1996. Low stable isotope ratios of tropical cyclone rains. *Geophysical Research Letters, v. 23, p. 527-530*, 23, 527-530.

Leatherman, S.P. (Ed.). (1981). *Overwash Processes*. Stroudsburg, PA: Hutchinson Ross Publishing Company.

Lee, V., 1980. An elusive compromise: Rhode Island coastal ponds and their people. Narragansett, RI: University of Rhode Island Coastal Resources Center *(Marine Technical Report 73)*. 82p.

Liu, K., and Fearn, M.L., 1993. Lake-sediment record of late Holocene hurricane activities from coastal Alabama. *Geology*, 21, 793-796.

Liu, K., and Fearn, M.L., 2000. Reconstruction of prehistoric landfall frequencies of

catastrophic hurricanes in northwestern Florida from lake sediment records. *Quaternary Research*, 54, 238-245.

Liu, K., 2004. Paleotempestology: principles, methods and examples from Gulf Coast lake sediments. *In:* Murnane, R.J., and Liu, K. (eds.), *Hurricanes and typhoons: past, present, and future*. New York, NY: Columbia University Press, pp. 13-57.

Ludlum, D., 1963. *Early American Hurricanes 1492-1870*. Boston: American Meteorological Society, 198p.

McMaster, R.L., 1960. Sediments of Narragansett Bay system and Rhode Island Sound. *Journal of Sedimentary Petrology*, 30(2), 249-274.

Miller, D.L.; Mora, C.I.; Grissino-Mayer, H.D.; Mock, C.J.; Uhle, M.E., and Sharp, Z., 2006. Tree-ring isotope records of tropical cyclone activity. *Proceedings of the National Academy of Sciences*, 103(39), 14294-14297.

Morton, R.A.; Gibeaut, J.C., and Paine, J.G., 1995. Meso-scale transfer of sand during and after storms: implications for prediction of shoreline movement. *Marine Geology*, 126, 161-179.

Morton, R.A., and Sallenger Jr., A.H., 2003. Morphological impacts of extreme storms on sandy beaches and barriers. *Journal of Coastal Research*, 19(3), 560-573.

Moy, C.M.; Seltzer, G.O.; Rodbell, D.T., and Anderson, D.M., 2002. Variability of El Nino/Southern Oscillation activity at millennial timescales during the Holocene epoch. Nature, 420, 162-165.

Murnane, R.J.; Barton, C.; Collins, E.; Donnelly, J.; Elsner, J.; Emanuel, K.; Ginis, I.; Howard, S.; Landsea, C.; Liu, K.; Malmquist, D.; Mckay, M.; Michaels, A.; Nelson, N.; O'Brien, J.; Scott, D., and Webb Iii, T., 2000. Model estimates hurricane wind speed probabilities. *Eos, Transactions AGU*, 81(38), 433-438.

Neumann, C.J., 1987. The National Hurricane Center Risk Analysis Program (HURISK). Coral Gables, FL: National Hurricane Center *(NOAA Technical Memorandum NWS NHC 38)*. 56p.

Newcomer, D. (1991). *Effect of future sea level rise on barrier migration and headland erosion along the southern coast of Rhode Island.* University of Rhode Island, Kingston, RI.

Nichols, R.L., and Marston, A.F., 1939. Shoreline changes in Rhode Island produced by Hurricane of September 21, 1938. *Bulletin of the Geological Society of America*, 50, 1357-1370.

NOAA (National Oceanic and Atmospheric Administration). (2011). *NOAA tides and currents, mean sea level trend 8452660 Newport, Rhode Island.* Retrieved July

14, 2011, from
http://tidesandcurrents.noaa.gov/sltrends/sltrends_station.shtml?stnid=8452660

Nummendal, D., and Fischer, I., 1978. Process-response models for depositional shoreline: the German and Georgia bights. *In: 16th Conference on Coastal Engineering*. New York: American Society of Civil Engineering, pp. 1212-1231.

Oldale, R.N., and O'Hara, C.J., 1980. New radiocarbon dates from the inner Continental Shelf off southeastern Massachusetts and a local sea-level-rise curve for the past 12,000 yr. *Geology*, 8(2), 102-106.

Paillard, D.; Labeyrie, L., and Yiou, P., 1996. Macintosh program performs time-series analysis. *Eos Trans. AGU*, 77, 379.

Paulsen, C.G.; Bigwood, B.L.; Harrington, A.W.; Hartwell, O.W., and Kinnison, H.B., 1940. Hurricane floods of September 1938. Washington, DC: U.S. Department of the Interior, Geologic Survey *(No. Water-Supply Paper 867)*.

Pielke Jr, R.A.; Gratz, J.; Landsea, C.W.; Collings, D.; Saunders, M.A., and Musulin, R., 2008. Normalized hurricane damage in the United States: 1900-2005. *Natural Hazards Review*, 9(1), 29-42.

Rahmstorf, S., 2007. A semi-empirical approach to projecting future sea-level rise. *Science*, 315, 368-370.

Redfield, A.C., and Miller, A.R., 1957. Water levels accompanying Atlantic Coast hurricanes. *Meteorological Monographs*, 2, 1-22.

Reimer, P.J.; Baillie, M.G.L.; Bard, E.; Bayliss, A.; Beck, J.W.; Blackwell, P.G.; Bronk Ramsey, C.; Buck, C.E.; Burr, G.S.; Edwards, R.L.; Friedrich, M.; Grootes, P.M.; Guilderson, T.P.; Hajdas, I.; Heaton, T.J.; Hogg, A.G.; Hughen, K.A.; Kaiser, K.F.; Kromer, B.; McCormac, F.G.; Manning, S.W.; Reimer, R.W.; Richards, D.A.; Southon, J.R.; Talamo, S.; Turney, C.S.M.; Van Der Plicht, J., and Weyhenmeyer, C.E., 2009. IntCal09 and Marine09 radiocarbon age calibration curves, 0-50,000 years cal BP. *Radiocarbon*, 51(4), 1111-1150.

Sabbatelli, T.A., and Mann, M.E., 2007. The influence of climate state variables on Atlantic tropical cyclone occurrence rates. *Journal of Geophysical Research*, 112, D17114.

Scileppi, E., and Donnelly, J.P., 2007. Sedimentary evidence of hurricane strikes in western Long Island, New York. *Geochemistry Geophysics Geosystems*, 8(6).

Scott, D.B.; Collins, E.S.; Gayes, P.T., and Wright, E., 2003. Records of prehistoric hurricanes on the South Carolina coast based on micropaleontological and sedimentological evidence, with comparison to other Atlantic Coast records. *Geological Society of America Bulletin*, 115(9), 1027-1039.

Simpson, R.H., and Riehl, H., 1981. The hurricane and its impact. Baton Rouge, LA, USA: Louisiana State University.

Smith, S.G. (2010). *A sedimentary record of intense storms and environmental change from a coastal freshwater lake in Rehoboth Beach, Delaware.* MS thesis, University of Rhode Island, Narragansett, RI.

Tannehill, I.R., 1938. Hurricane of September 16 to 22, 1938. *Monthly Weather Review*, 66, 286-288.

U.S. Army Air Corps, 1938. Aerial survey of Connecticut 1938 Hurricane damage photograph. Connecticut State Library, State Archives *(Aerial Photo Section No. 118).*

Vallee, D.R., and Dion, M.R., 1998. Southern New England tropical storms and hurricanes: A ninety-seven year summary 1900-1996 including several early American hurricanes. Silver Spring, MD: National Weather Service. 134p.

Vermeer, M., and Rahmstorf, S., 2009. Global sea level linked to global temperature. *Proceedings of the National Academy of Sciences*, 106(51), 21527-21532.

Wallace, D.J., and Anderson, J.B., 2010. Evidence of similar probability of intense hurricane strikes for the Gulf of Mexico over the late Holocene. *Geology*, 38(6), 511-514.

Webster, P.J.; Holland, G.J.; Curry, J.A., and Chang, H.-R., 2005. Changes in tropical cyclone number, duration, and intensity in a warming environment. *Science*, 309, 1844-1846.

Wilby, F.B.; Young, G.R.; Cunningham, C.H.; Liieber Jr., A.C.; Hale, R.K.; Saville, T., and O'Brien, M.P., 1939. Inspection of beaches in path of the hurricane of September 21, 1938. *Shore and Beach*, 7, 43-47.

Winter, A.; Ishioroshi, H.; Watanabe, T.; Oba, T., and Christy, J., 2000. Caribbean sea surface temperatures: Two-to-three degrees cooler than present during the Little Ice Age. *Geophysical Research Letters*, 27(3365-3368).

Woodruff, J.D.; Donnelly, J.P.; Mohrig, D., and Geyer, W.R., 2008a. Reconstructing relative flooding intensities responsible for hurricane-induced deposits from Laguna Playa Grande, Vieques, Puerto Rico. *Geology*, 36(5), 391-394.

Woodruff, J.D.; Donnelly, J.P.; Emanuel, K., and Lane, P., 2008b. Assessing sedimentary records of paleohurricane activity using modeled hurricane climatology. *Geochemistry Geophysics Geosystems*, 9(9).

Zolitschka, B.; Mingram, J.; Van Der Gaast, S.; Jansen, J.H.F., and Naumann, R., 2001. Sediment logging techniques. *In:* Last, W.M., and Smol, J.P. (eds.), *Tracking environmental change using lake sediments: Volume 1: Basin analysis,*

coring, and chronological techniques. Dordrecht, The Netherlands: Kluwer Academic Publishers, pp. 137-153.

Table 1.1 Historical hurricanes from the HURDAT database classified as direct strikes to Rhode Island according to the criteria of Jarrell et al. (1992). Data from Blake et al. (2011).

Year	Month	Storm name	Saffir-Simpson category at landfall in RI	Highest Saffir-Simpson category	Central pressure (mb)	Max wind (kt)
1858	Sept.	-	1	1	976	80
1869	Sept.	September Gale of 1869	3	3	963	100
1894	Oct.	-	1	3	955	105
1896	Sept.	-	1	1	985	70
1938	Sept.	The Great New England Hurricane	3	3	946	-
1944	Sept.	The Great Atlantic Hurricane	3	3	947	-
1954	Aug.	Carol	3	3	960	-
1960	Sept.	Donna	2	4	930	-
1991	Aug.	Bob	2	2	962	90

Table 1.2 Quonochontaug Pond radiocarbon results. *denotes sample omitted from age model as it is older than would be expected based on other age control points in the series.

NOSAMS lab number	Core	Sample depth (cm)	^{14}C age (yr BP)	1σ calendar age (cal yr BP)	Relative area under distribution	$\delta^{13}C$ (‰)	Sample material
OS-44815	QP-25	46-47	295 ± 50	297-333 350-436	0.298083 0.701917	-28.67	seed/plant
*OS-44774	QP-25	56-57	730 ± 25	667-683	1	-18.15	seed/plant
OS-44509	QP-25	66-67	675 ± 30	567-584 648-670	0.379689 0.620311	-28.98	seed/plant
OS-44775	QP-25	101-102	1810 ± 35	1708-1744 1752-1812	0.39078 0.60922	-20.02	seed/plant
OS-44813	QP-25	109-110	1930 ± 60	1817-1949	0.98756	-21.13	seed/plant

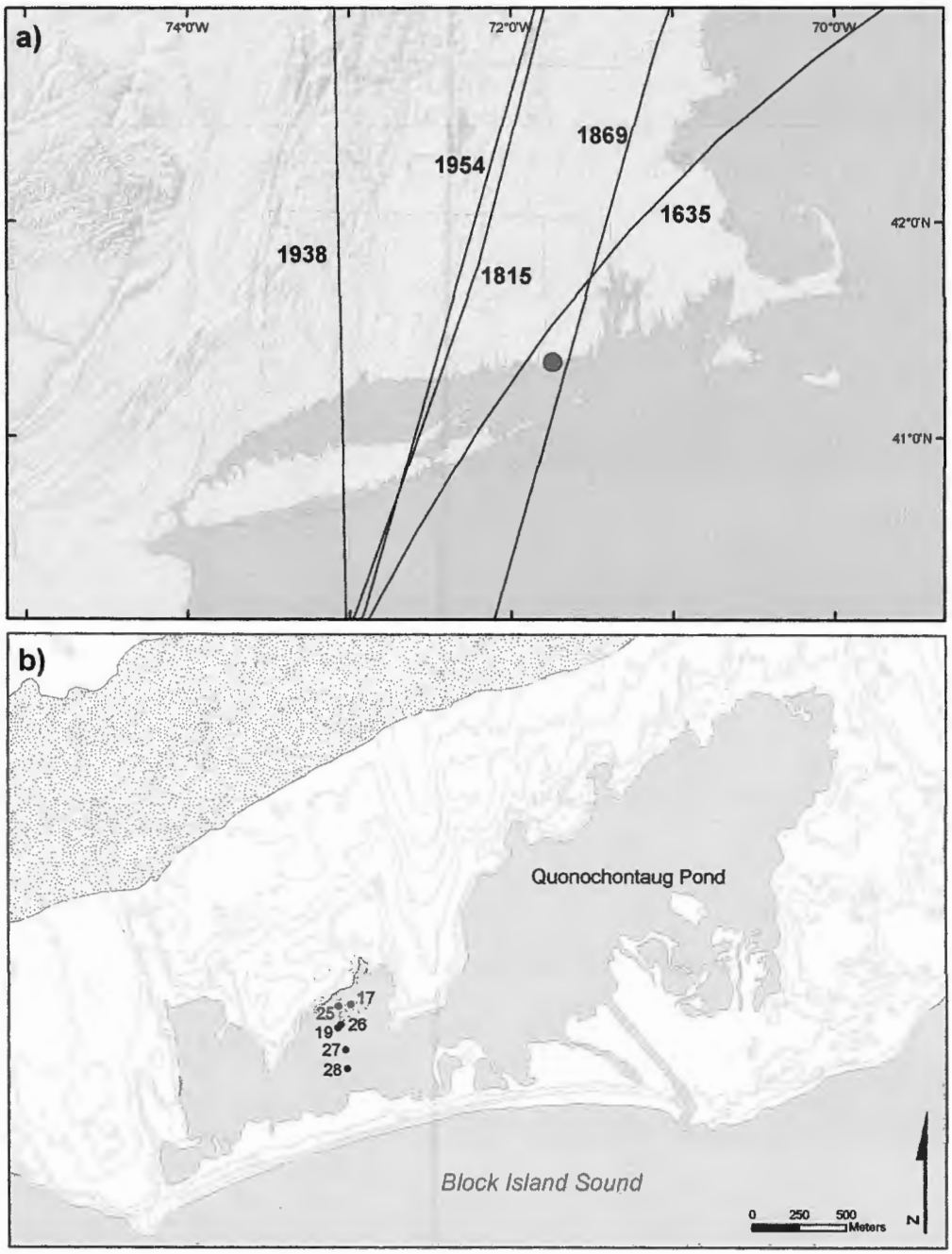

Figure 1.1 Quonochontaug Pond site map and core transect location. a) Map of southern New England; the location of Quonochontaug Pond is noted with a red circle. Tracks of intense hurricanes discussed in the text are from Knapp et al. (2010) and Jarvinen (2006). b) Map of Quonochontaug Pond showing core locations. Shaded pattern indicates the location of the Charlestown moraine. Contour interval = 5 m

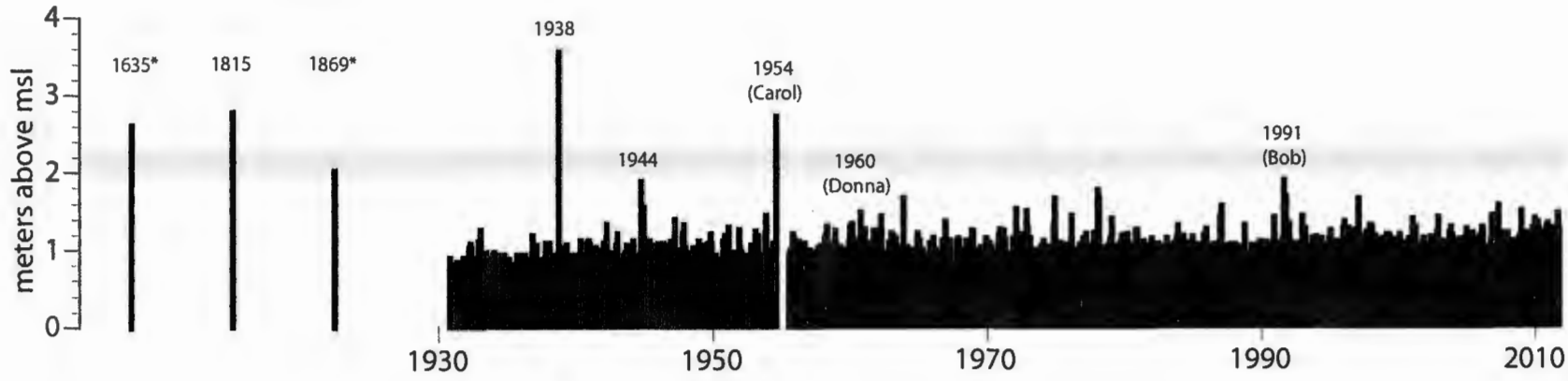

Figure 1.2 Maximum monthly water levels (m relative to contemporary msl) from Newport, RI (NOAA, 2011). Sea, Lake and Overland Surges from Hurricanes (SLOSH) simulations for storms that predate the tide gauge record in 1635 and 1815 are from Jarvinen (2006), and historical accounts of the1869 storm surge are from Ludlum (1963). * denotes water levels relative to astronomical tide (no tidal correction). Grey shading indicates range of modeled elevations for the barrier following a 100-year flooding event (FEMA, 2010).

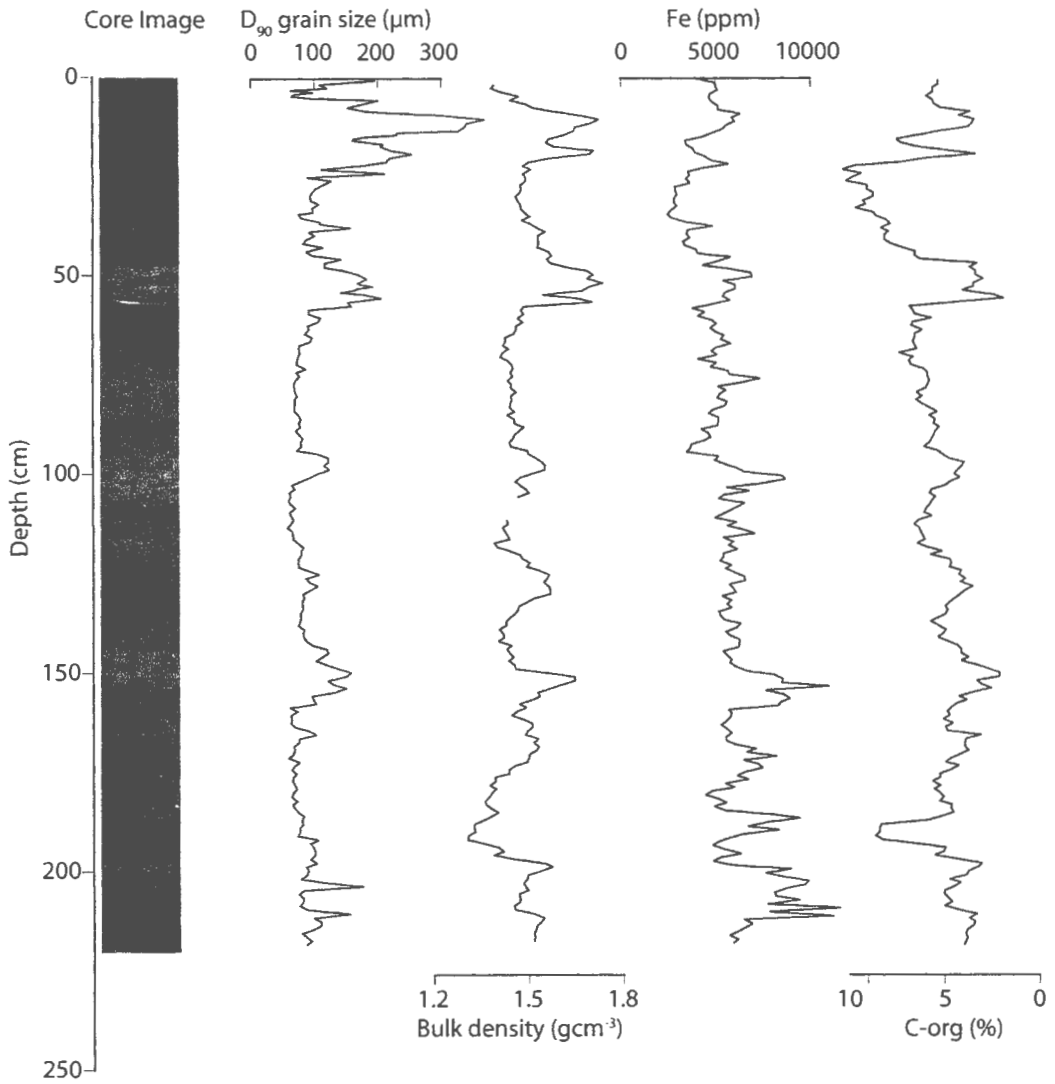

Figure 1.3 Sedimentological data from core QP-19. D_{90} grain size is the particle size below which 90% of the sample lies. Peaks in grain size correlate with dense layers with high iron (Fe) content and low organic carbon. Grey shading indicates coarse-grained layers interpreted as overwash deposits.

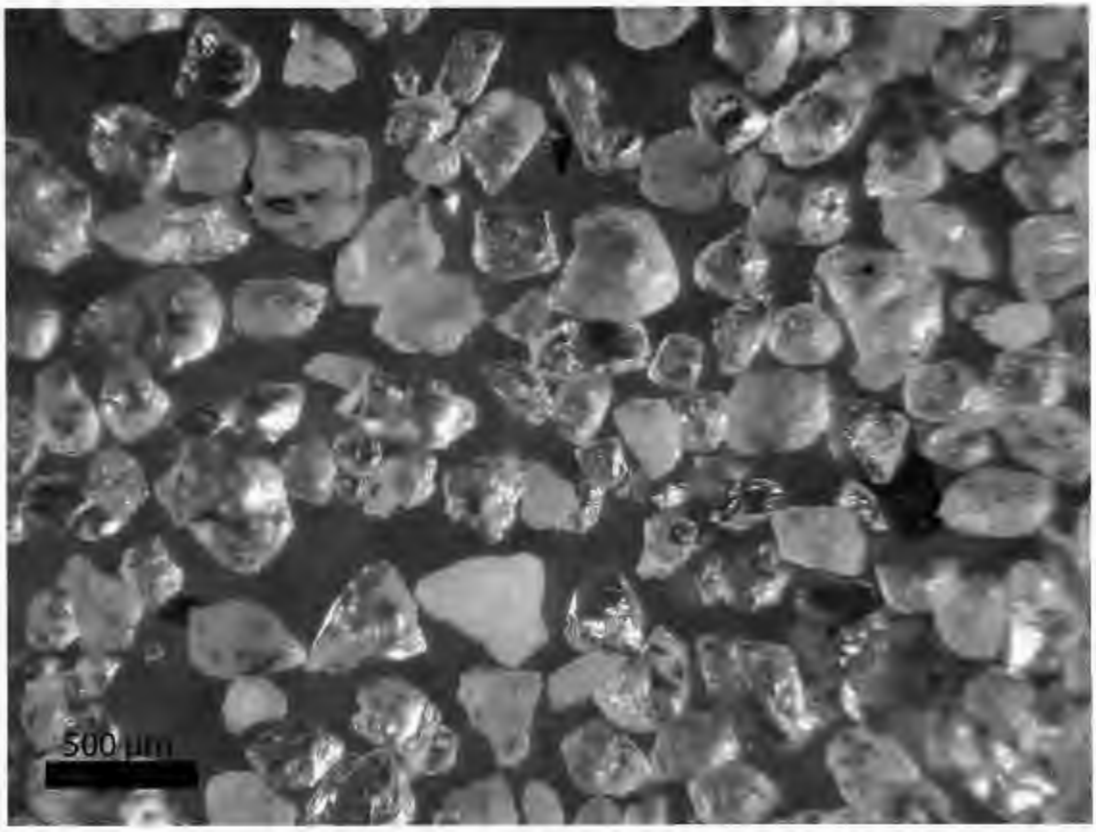

Figure 1.4 Photomicrograph of coarse fraction from overwash deposit. Note the sub-rounded quartz and feldspar grains. Sample is from approximately 37.5 cm depth in core QP-27.

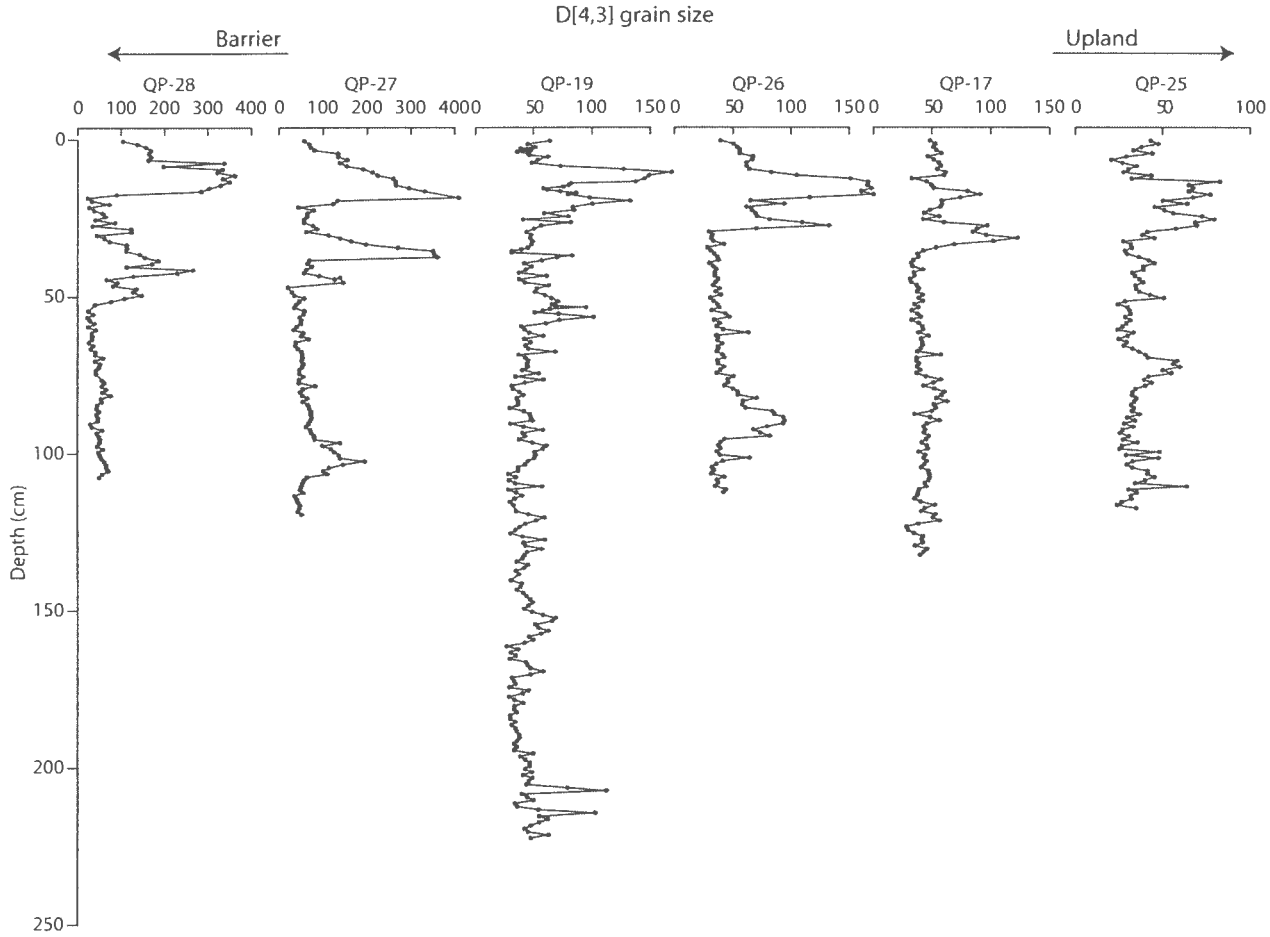

Figure 1.5 Lateral trends in storm-induced deposits illustrated by mean grain size data (μm). D[4,3] is the volume mean diameter, derived from the size distribution. Note the change in scale for more distal portions of the transect.

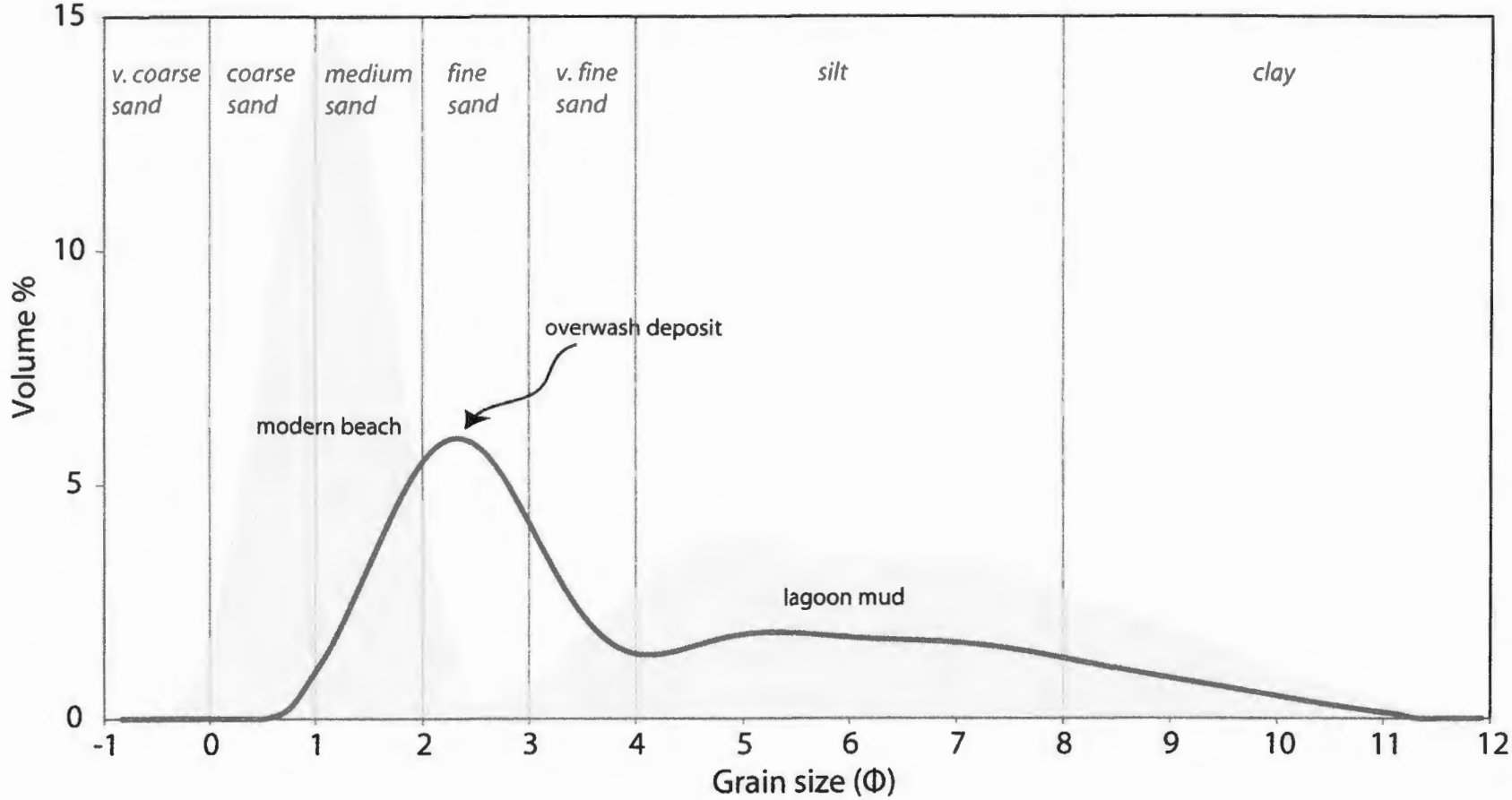

Figure 1.6 Representative grain size distributions for samples from the modern barrier and lagoon, and from an overwash deposit at 10 cm depth in core QP-19 (mid-transect).

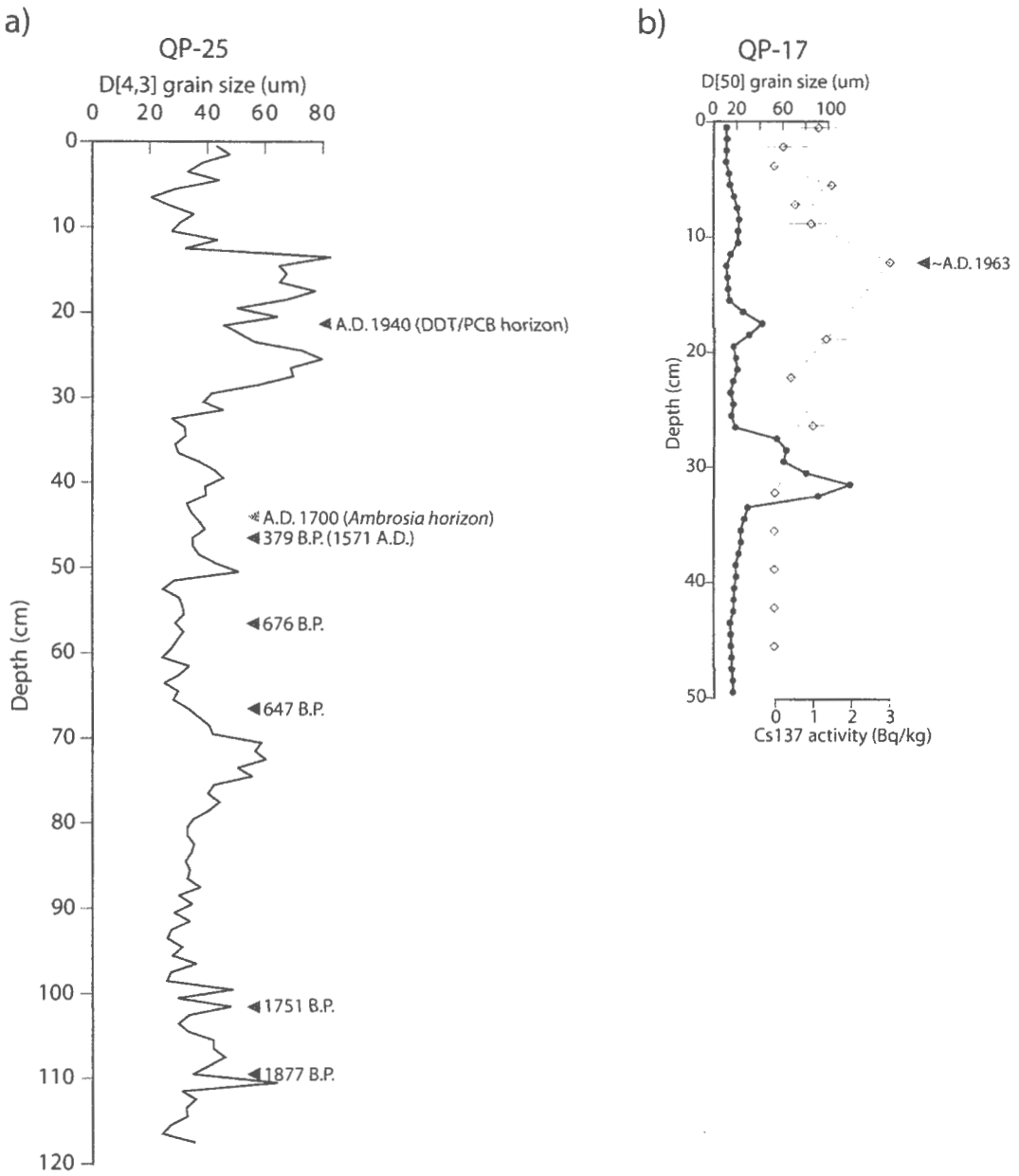

Figure 1.7 Chronostratigraphic age markers for QP-25 and QP-17. Black arrows show AMS-radiocarbon dates calibrated to calendar ages before 1950. Blue and green arrows show the position of PCB/DDT and fossil pollen horizons respectively, as reported by Ford (2003). The spike in ^{137}Cs activity at 14.5 cm in core QP-17 (red arrow) corresponds to a peak in atmospheric nuclear weapons testing in A.D. 1963.

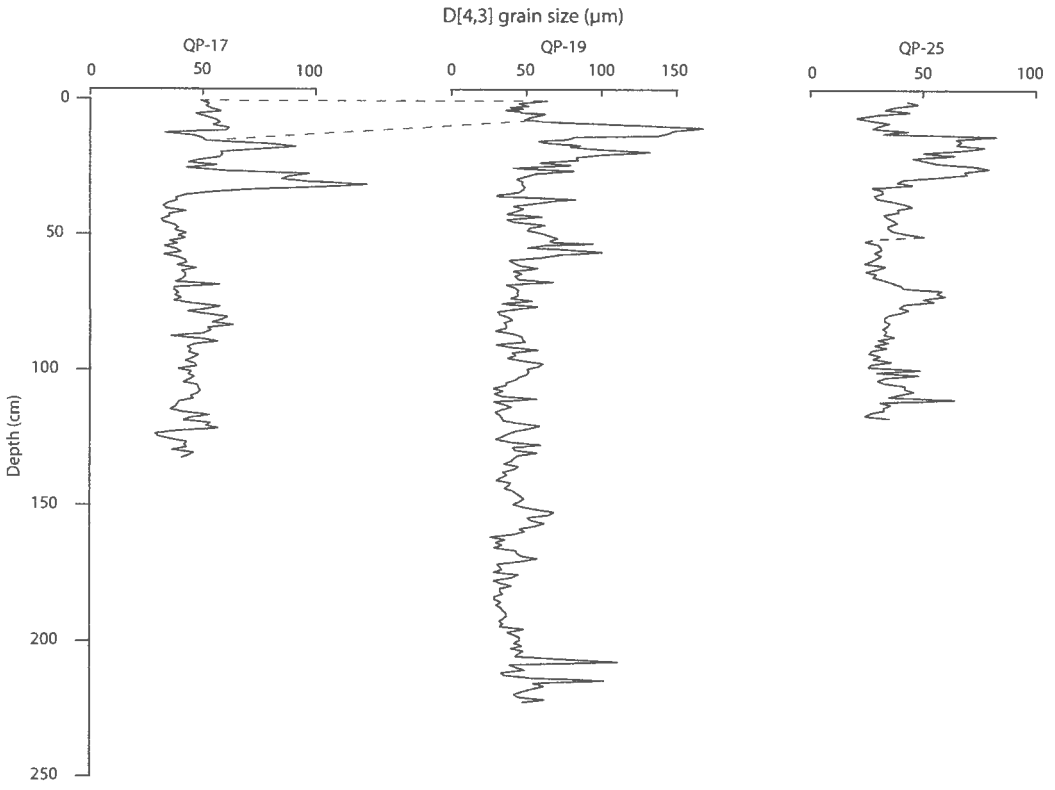

Figure 1.8 Mean grain size data for cores QP-17, QP-19, and QP-25. Tie lines indicate distinct features in the data used to correlate between cores.

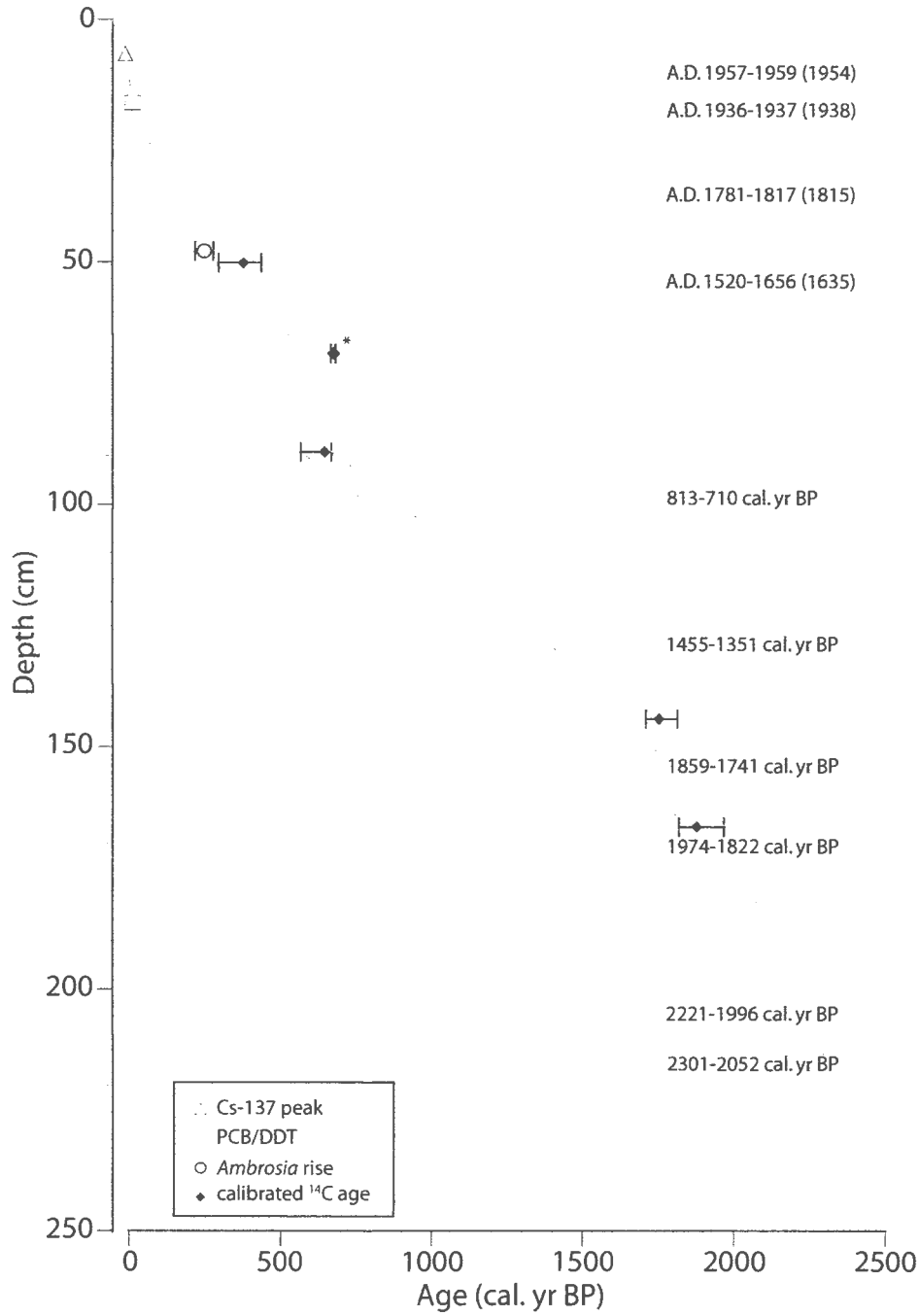

Figure 1.9 Age-depth relationship for core QP-19 based on correlations from dated cores. Error bars for calibrated ^{14}C dates represent ± 1σ age uncertainties (Table 1.2). One ^{14}C date at 56-57 cm (marked by *) was not included in the age model. The position of the A.D. 1963 ^{137}Cs peak, A.D. 1940 PCB/DDT pollution increase, and the rise in Ambrosia pollen (indicating A.D. 1700) are also noted. Shading denotes position and approximate thickness of overwash deposits identified in QP-19. Ages in parenthesis indicate dates of historic hurricanes.

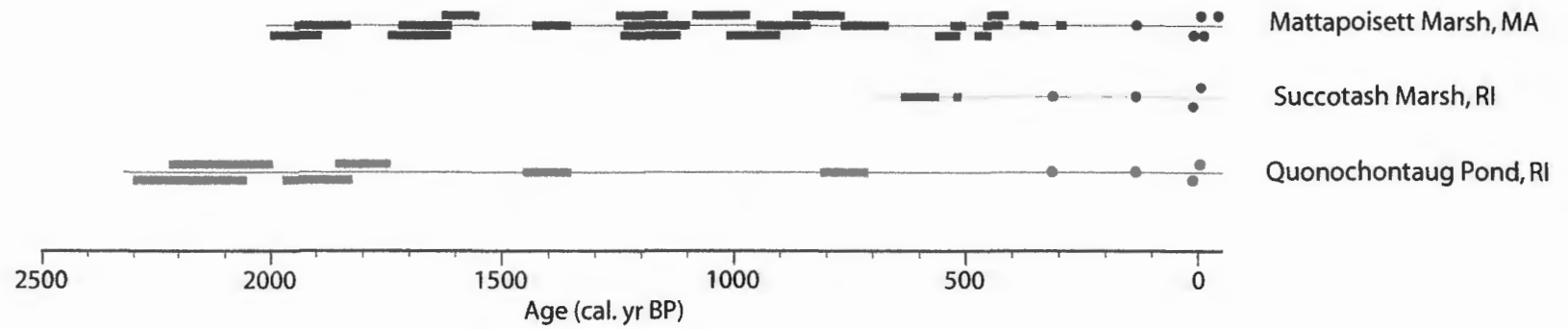

Figure 1.10 Timing of overwash deposits at Quonochontaug Pond compared to records from East Matunuck, RI (Donnelly et al., 2001) and Mattapoisett, MA (Boldt, et al., 2010). Circles indicate historical hurricanes (after Mann et al., 2009).

Figure 1.11 Oblique aerial photograph of extensive damage caused by the 1938 New England Hurricane, Quonochontaug barrier, RI. September 24, 1938 (United States Army Air Corps aerial photo section no. 118).

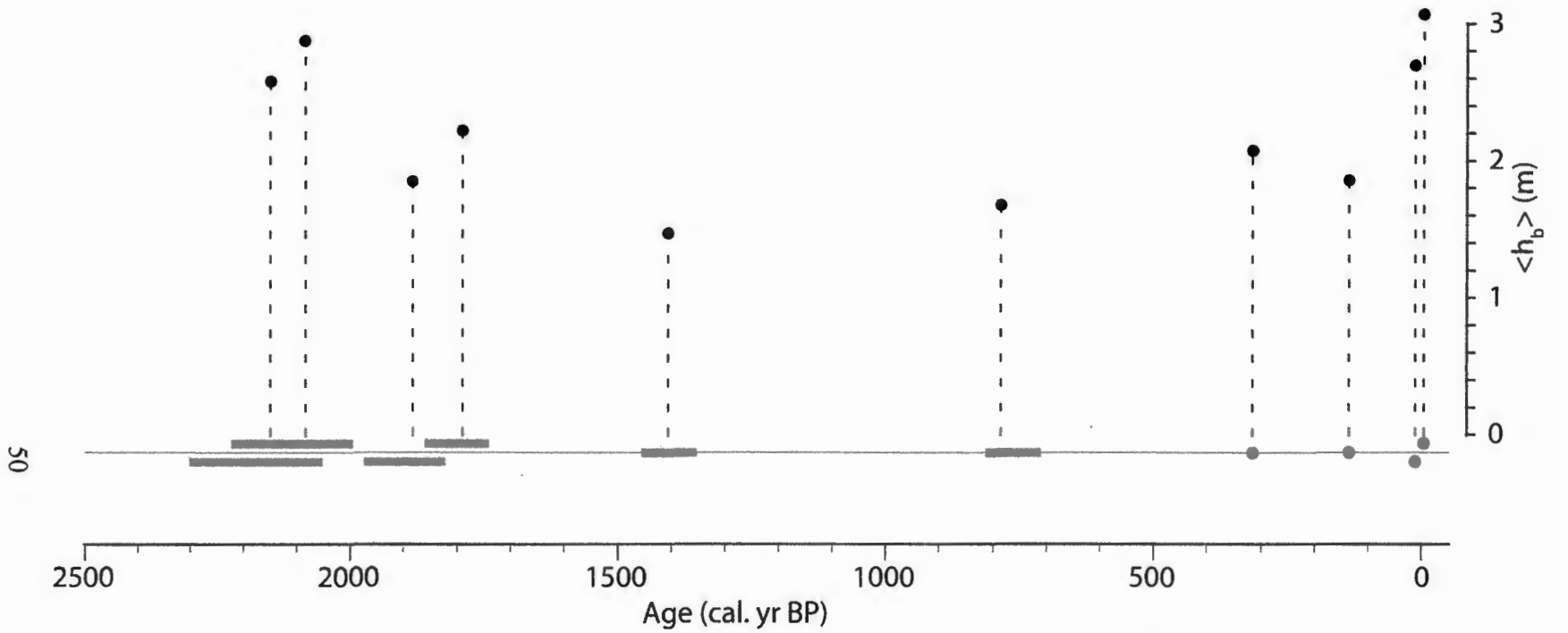

Figure 1.12 Estimates of <h_b> for prehistoric overwash events at Quonochontaug Pond, RI.

Figure 1.13 Comparison of landfall probability estimates from late Holocene records of overwash in the western North Atlantic (after Wallace and Anderson, 2010).

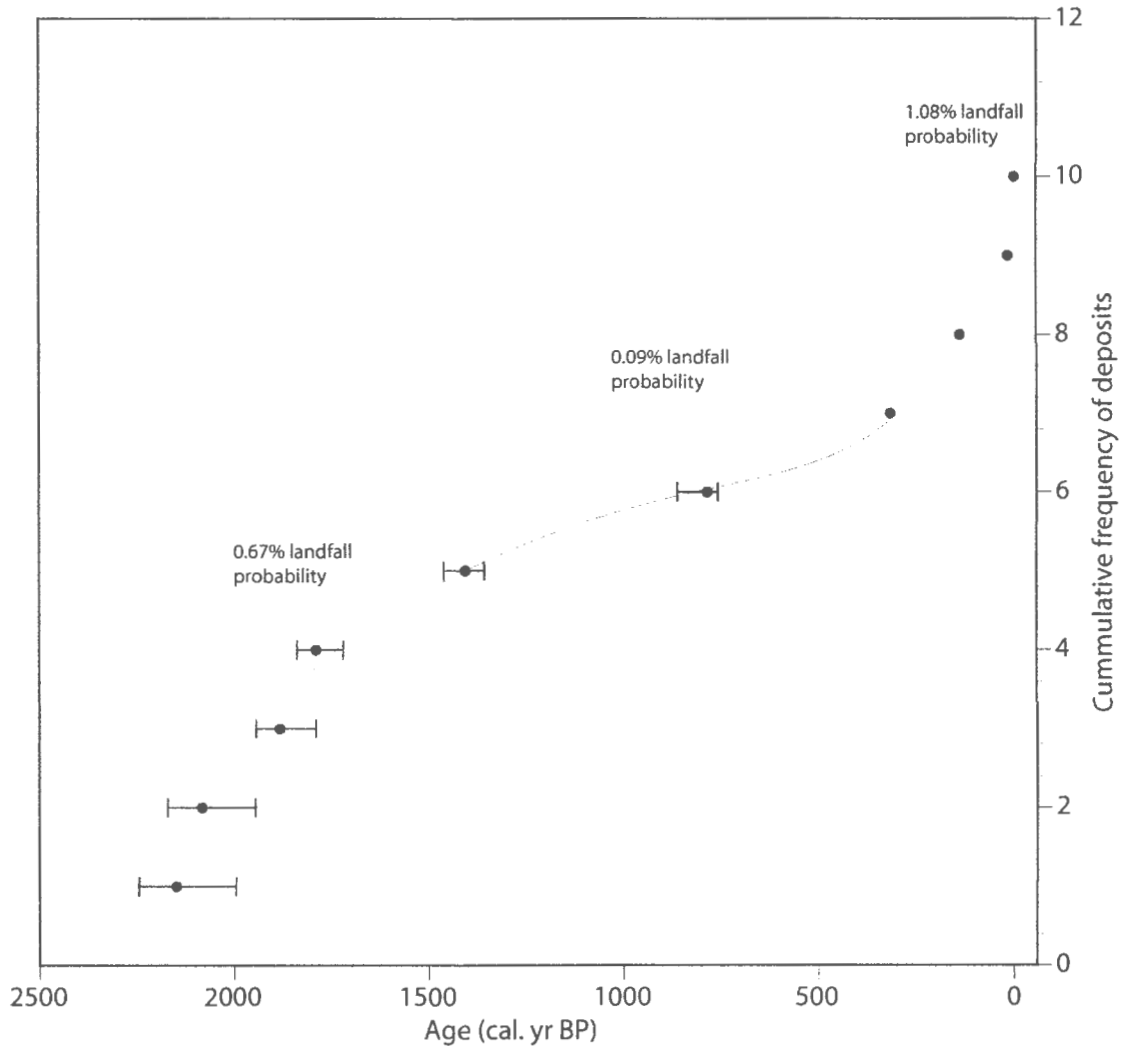

Figure 1.14 Cumulative frequency of overwash deposits at Quonochontaug Pond since ~2200 cal. yr BP. Error bars indicate maximum and minimum 1σ uncertainties of deposit ages. Periods of enhanced hurricane activity noted by grey shading.

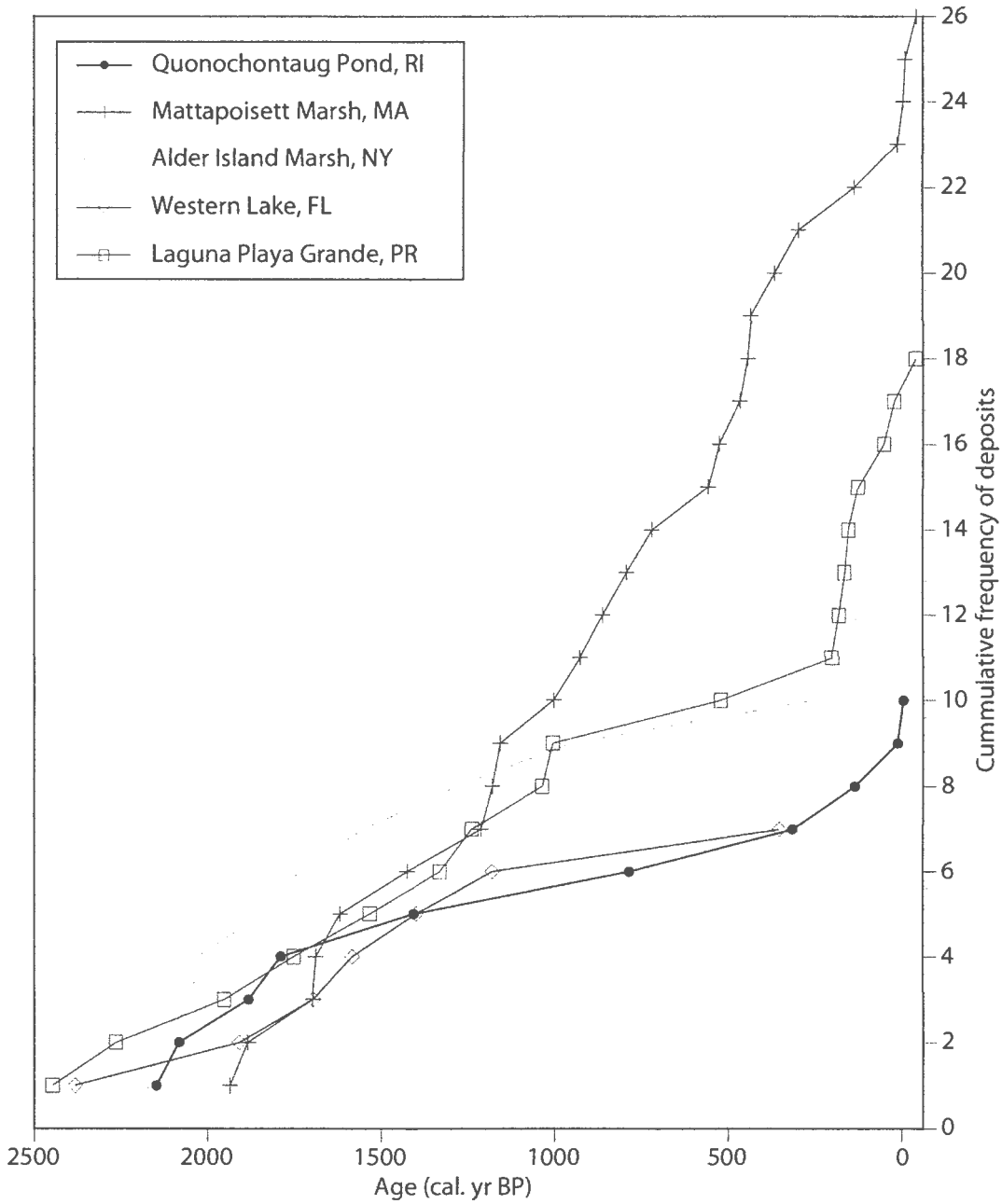

Figure 1.15 Similarity in the timing of overwash deposition from North Atlantic records. Cumulative frequency of overwash deposits from Quonochontaug Pond, RI, compared to Mattapoisett Marsh, MA (Boldt et al., 2010), Alder Island Marsh, NY (Scileppi and Donnelly, 2007), Western Lake, FL (Liu and Fearn, 2000), and Laguna Playa Grande, PR (Donnelly and Woodruff, 2007). Note the period of decreased activity between ~400 and ~1000 cal. yr BP that is synchronous among records thought to reflect intense hurricane landfalls.

CHAPTER 2: Shoreline position and rate of change from long-term beach profile measurements: Rhode Island south shore

A manuscript in preparation for submission to:

Journal of Coastal Research

by

Nathan Vinhateiro[1], Emily A. Himmelstoss[2], John W. King[1], Rebecca S. Robinson[1]

[1] Graduate School of Oceanography, University of Rhode Island, Narragansett, RI 02881

[2]U.S. Geological Survey, Coastal and Marine Geology Program, 384 Woods Hole Road, Woods Hole, MA 02543

2.10 Abstract

Data sets that quantify long-term coastal change are fundamental to understanding processes that shape the coast and anticipating impacts from storms and sea level rise. Here we present a long-term, high-resolution record of shoreline change from Rhode Island's south-facing, sandy barrier coastline. The shoreline time-series are based on bi-weekly beach profiles, collected at eight transects between 1962 and the present. We use an objective and repeatable method to estimate shoreline positions by intersecting a local tidal datum with each coastal profile. Regression of the time-series data yield rates-of-change that range from +0.27 m yr^{-1} at Charlestown Breachway to -0.93 m yr^{-1} at Green Hill beach, but notably, survey measurements highlight how sampling frequency and analysis time-scales can bias the calculated rates-of-change. To evaluate shoreline change methods and illustrate variability produced by short-term changes in beach morphology, the time-series are compared to historical (vector) shorelines derived from maps, charts, and aerial photography coincident with the survey period. At 7 of the 8 transects, weighted regression of vector shorelines more closely depicts true shoreline behavior when compared to normal linear regression and end-point methods. Annual variability resulting from changes in beach morphology is observed at all sites and is attributed to seasonal changes in the frequency of coastal storms. The offset between proxy-based, and datum-based shorelines is also compared for recent years and is shown to be more than twice as large as previously estimated. Variability in this offset indicates that a proxy-datum correction is more appropriately applied to datum–based shorelines.

2.20 Introduction

The purpose of most shoreline change studies is to identify areas prone to erosion, forecast future shoreline positions and provide simple, science-based information for policy makers. The rate of shoreline change is one of the most commonly used metrics in coastal zone management, yet the extent to which these statistics reflect actual variations in shoreline positions is highly dependent on the method used to calculate rates, the accuracy of the source data, and the scale of observations needed to establish change trends (Dolan, Fenster, and Holme, 1991; Genz et al., 2007; Hapke et al., 2010). Because management decisions are commonly made on regional scales, current research has focused on shoreline change mapping, whereby historical shoreline positions derived from charts, aerial photography, and coastal elevation data such as lidar are compared to determine erosion rates (*e.g.* USGS National Assessment of Shoreline Change Project; NOAA-NOS National Shoreline; NOAA-NGS Vector Shoreline Project). Map-based assessments utilize vector shorelines to estimate shoreline change over broad spatial and temporal scales, but they are often limited in sampling frequency (regression statistics are commonly based on 10 or fewer points). In addition, proxy-based shorelines that are digitized from map data are subject to interpretation error (Moore, Ruggiero, and List, 2006) and can vary dramatically in response to meteorological or seasonal forcings (Smith and Zarillo, 1990). While lidar data provide an accurate and objective measure of shoreline position over similar spatial scales (Stockdon et al., 2002), lidar-derived shorelines are limited to a relatively small number of surveys collected during the last two decades.

In contrast, weekly to monthly beach profiling provides extremely detailed information about short-term morphological changes (Larson and Kraus, 1994; Lee et al., 1995; Morton, Gibeaut, and Paine, 1995). Yet the scale and nature of profile data often preclude their use in studies of shoreline change because beach surveying programs are typically too short to identify long-term trends (Clarke and Eliot, 1983; Eliot and Clarke, 1989) and observations are limited to the location of cross-shore transects. To effectively manage the coastline, it is necessary to not only identify areas that are prone to the highest rates of change, but to understand the processes that drive shoreline change and the time scales at which they operate. This objective requires the ability to quantify both long-term trends and short-term variability of the shoreline.

In this paper, we use a simple technique to derive shoreline positions from cross-shore beach profiles. We have used the method to construct time-series of datum-based shoreline positions using survey data from the University of Rhode Island (URI) Graduate School of Oceanography (GSO) long-term beach monitoring program. The resulting dataset provides an accurate, highly resolved, and long-term history of shoreline behavior along the south-facing Rhode Island coastline, which is used to investigate patterns and scales of shoreline change. Comparisons of annualized rates of change from this high-resolution data to rates derived from map-based estimates of shoreline position are made to evaluate the latter technique. The results demonstrate how a priori knowledge concerning the timescales and amplitudes of coastal change can be used to improve methods of shoreline change analysis and inform management decisions on regional scales.

2.30 Regional setting

The south shore of Rhode Island is a microtidal, wave-dominated, mainland-segmented, barrier coastline (Fitzgerald and Van Heteren, 1999; Hayes, 1979). The 33-km stretch between Point Judith and Napatree Point, RI (Figure 2.1), is comprised of a series of barrier spits that extend between till and glaciofluvial headlands. A string of shallow, shore-parallel, coastal lagoons are situated behind the barriers. This barrier-lagoon configuration formed as a result of onlap over glaciofluvial and glaciolacustrine sediment during the late Holocene (Boothroyd, Friedrich, and McGinn, 1985; Boothroyd and Sirkin, 2002), when rising sea levels caused waves to reach and erode outwash deposits, producing a supply of sediment to the longshore transport system. Since that time, the barrier spits have migrated landward primarily by overwash processes and through construction of flood tidal deltas (Dillon, 1970).

Shoreline mapping has indicated that this coastline is transgressive, and erosional on multi-decadal time scales (Boothroyd and Hehre, 2007; Hapke et al., 2010). Because no major rivers introduce sediment to the south shore, source material for the beaches is limited to Pleistocene-aged sediment from eroding headland bluffs, erosion of the barrier core and foredune zone, and erosion of the transgressed proglacial landscape on the shoreface (Graves, 1990). The addition of limited quantities of sediment from beach nourishment projects has occurred periodically since the 1950s, primarily through emplacement of materials dredged from the coastal lagoons and inlets (Friedrich, 1982; Oakley, Alvarez, and Boothroyd, 2007).

Beach sediment is deposited and modified by the action of waves, tidal currents, and storm-induced processes. Onshore transport of sediment is primarily due

to southwesterly, fair-weather winds that produce a combined upwelling-wave orbital induced onshore flow (Oakley et al., 2009). Alongshore sediment transport is predominantly to the east as indicated by records of dredging within the Harbor of Refuge (Boothroyd, Friedrich, and McGinn, 1985) and by patterns of sand accretion along the western jetty at the Harbor of Refuge (Friedrich, 1982). Mean tidal range at Newport, RI is 1.06 m, and while tidal currents are not sufficient to transport sand-sized sediment in the nearshore (Graves, 1990) the flood and ebb currents that result from the relative water level differences between the ocean and coastal lagoons are capable of transporting sand through tidal inlets (Boothroyd, Friedrich, and McGinn, 1985; CRMC, 1999).

Extratropical and tropical storms play a significant role in the cross-shore transport of sediment along the Rhode Island south shore. In addition to increased flow through inlets, elevated water levels associated with landfalling storms give rise to downwelling currents that can result in offshore transport of sediment (Oakley et al., 2009). During severe storms, overwash processes are responsible for cutting temporary storm-surge channels through the barriers and depositing washover fans and storm-surge platforms on the back of the barrier. Evidence from sediment cores (Donnelly et al., 2001; Ford, 2003) has demonstrated that overwash events are often intense enough to transport coarse-grained beach sand hundreds of meters into the adjacent lagoons and salt marshes.

Relative sea level rise in Rhode Island is 2.58 millimeters/year, based on monthly mean sea level between 1930-2010 at Newport, RI (NOAA, 2011). Radiometrically dated basal salt-marsh peat samples from nearby Connecticut suggest

this rate has undergone a three-fold increase during the latter half of the 19th century (Donnelly et al., 2004). The consequences of accelerated sea level rise become apparent during storm events, when waves gain access to increasingly higher elevations.

2.40 Background

2.41 The GSO long-term beach profile program

For nearly 50 years, the Graduate School of Oceanography (GSO) at URI has maintained a monitoring program to regularly measure and quantify morphological changes to the state's barrier spits. Cross-shore elevations are measured biweekly (monthly during summer months) at eight survey transects along Rhode Island's south shore (Figure 2.1). Survey data have been collected at Weekapaug (wkg), East (est-1), Green Hill (grh), and Moonstone (mst) barrier beaches since 1962. Additional transects at Misquamicut (mis), East (est-2), and Charlestown (cha-bw, cha-tb) barriers were established in the mid-1970s. The GSO beach profile program was initiated by Dr. Robert McMaster and since its inception, graduate student assistants have collected the data and compiled reports that summarize the annual changes in the morphology of south shore beaches. To our knowledge, the dataset represents the world's longest continuous record of beach profiling along a sandy barrier coastline

2.42 Previous studies

Complementing the GSO beach profiling program are transects initiated by the URI Geosciences department in the late 1970s (Boothroyd et al., 1986; Boothroyd et al., 1988). Collectively, records from the two programs have been utilized in a number

of studies that have examined patterns in beach shape and volume in response to seasonal and storm-induced coastal processes. Rosenberg (1985) used five years of profile measurements at Charlestown Beach to document that south shore beaches recover rapidly from large storm events, with post-storm recovery usually completed within 4-7 days by onshore migration and welding of swash bars to the beachface. Gibeaut (1986) examined records from 10 south shore beaches and used eigenfunction analysis to define modes of variance ("beach functions") according to the geomorphic areas that were affected. His work showed that volume time series were positively correlated with changes in the shoreface-berm function and attributed a strong 10-11 year cycle and a secondary 5-yr cycle in the volume time series to onshore sediment movement, and longshore transport respectively. Graves (1991) dissected individual beach profiles to determine the role of the active beach in the volume time series. His analysis revealed distinct seasonal and annually repeated patterns of beach growth and depletion and he attributed previously identified multi-year signals to growth and depletion of the inactive backshore and dune component reservoirs. Lacey and Peck (1998) used spectral analysis to identify peaks in the profile-volume power spectra at periods between 1.5 and 5 years at four of the profile sites. A phase shift between adjacent sites was attributed to eastward sediment transport from longshore currents.

Our study offers an opportunity to add to the results of previous work by examining trends in shoreline behavior on multi-decadal time scales. To date, the GSO profile data set has been used to investigate changes in the time-series records of beach shape and beach volume, yet the dataset has not been used to assess long-term shoreline change. By doing so, we aim to improve traditional methods by quantifying

measurement uncertainties and comparing statistical methods for calculating shoreline rates-of-change.

2.43 Shoreline definition

The shoreline is a time-dependent boundary and quantifying shoreline change, therefore, requires the use of shoreline indicators to ensure that observed changes are not simply the result of inconsistencies in the measurement technique. On sandy beaches, the high water line (HWL), wet-dry line, or last high tide swash are the most commonly used indicators for shoreline mapping due to the fact that they can be easily identified both in the field, and on aerial imagery (Boak and Turner, 2005; Crowell, Leatherman, and Buckley, 1991). The HWL is defined as the landward extent of the last high tide and is commonly identified on photographs as a tonal change between wet and dry beach (Dolan and Hayden, 1983; Moore, Ruggiero, and List, 2006; Pajak and Leatherman, 2002). While their use is widespread, visual indicators like the HWL can sometimes appear gradational on aerial photographs, or may not be visible at all (Byrnes, McBride, and Hiland, 1991; Crowell, Leatherman, and Buckley, 1991), requiring interpretation by the investigator. Because the HWL is also influenced by the wave and tidal conditions at the time of measurement, the errors associated with HWL shorelines can amount to tens of meters in the horizontal direction (Pajak and Leatherman, 2002; Smith and Zarillo, 1990; Thieler and Danforth, 1994).

In contrast, datum-based shorelines, such as mean high water (MHW) or mean sea level, correspond to a specific elevation at the land-water interface and are defined by the tidal constituents at a particular coastal location. While they require no visual interpretation, datum-based shorelines can only be derived from elevation-based

datasets. Water levels can be raised or lowered to intersect the coastal topography at any particular tidal datum, thereby removing the effects of waves and runup that are inherent to visual shoreline indicators (Moore, Ruggiero, and List, 2006).

2.50 Methods

2.51 Beach profile measurements

The GSO beach profiles are measured by a two-person team using a transit level and stadia rod. Measurements are referenced to a back stake or other permanent feature of known elevation (R_0), which is positioned at a fixed location landward of the foredune crest. R_0 elevations have been surveyed to NAVD88 using a Trimble R8 real-time kinematic global positioning system (RTK GPS) with a temporary benchmark created using a National Geodetic Survey (NGS) On-line User Positioning Service (OPUS) solution (NGS OPUS solution: 48611070.09o 000026774). The positional accuracy of RTK GPS survey points is within 1-2 cm in both the vertical and horizontal dimension.

At each profile station, the transit is positioned and leveled on the foredune, and surveying begins with a back sighting to R_0. After the back sighting has been completed, a second reading is taken to record the height of the transit. Sightings are then recorded at points of noticeable inflection perpendicular to the shoreline and extending to the water line (Figure 2.2a). While surveys are planned to coincide with low tide in order to maximize beach exposure, the time required to visit all profile sites during a single low tide period precludes other types of field measurements. Specifically, the upper shoreface is not surveyed, and only qualitative descriptions of

wave and meteorological conditions, grain size transitions, and beach features are made.

For the purpose of this study, archived profile measurements were updated to a common geodetic reference. Prior adjustments to reference stakes due to storm damage or deterioration documented in field notes and annual reports were used to amend past data. Shifts in positional location of R_0 were calculated based on the measured ground distance offset and azimuth of the profile transect while changes in the elevation of R_0 were simply added / subtracted from previous elevations (Table 2.1).

2.52 Shoreline extraction from beach profiles

Shoreline position is estimated based on the intersection of each profile with the plane of mean high water at Newport, RI (MHW = 0.475 m NAVD88). Transit sightings, along with the instrument height and reference stake elevations were used to construct cross-shore profiles for each survey date. Depending on tides, wave action, and the complexity of beach morphology at a given site, there are typically between 8 and 15 transit sightings collected during each beach survey. Once created, the cross-shore location of any elevation contour can be interpolated along the profile. For this study, the position of MHW was estimated from the slope given by the two points that bracket the MHW elevation (Figure 2.2b). Because surveying is timed to coordinate with low tide, the MHW contour is typically captured in the process of surveying the beach. On occasions when surveying did not capture the MHW elevation, the last two points from the profile were used to extrapolate the slope from the final point to the MHW elevation. Outliers in the shoreline record resulting from extrapolation of flat or

upward sloping foreshore morphology have been corrected using the beach slope of the previous survey date to extrapolate a shoreline position. These occasions account for less than 1 percent of the total survey data at each site. The rate of shoreline change was analyzed at each transect site with standard linear regression methods using Statistical Analysis System (SAS) software version 9.2.

2.53 Comparison with proxy-based shoreline data

We compare our record of MHW shorelines with a standard and repeatable method of shoreline change analysis used operationally by the U.S. Geological Survey (USGS). The Digital Shoreline Analysis System (DSAS) is an ArcGIS extension that makes use of historical (vector) shorelines, digitized from maps, charts, and aerial imagery to determine rates of change (Thieler et al., 2009). For this analysis, eight DSAS transects were cast from a shore-parallel baseline at the location and along the azimuth of the GSO beach profiles (Figure 2.3). The intersections of DSAS transects with the historical shorelines define intercept points, which are used to calculate rates of shoreline change along each transect. Shoreline change was estimated using end-point rate (EPR), linear regression (LRR), and weighted linear regression (WLR) methods in DSAS for historical shorelines that were either coincident with, or close to beach profile measurements (Table 2.2). Vector shorelines are available back to 1872 for southern Rhode Island (Himmelstoss et al., 2010), however only shorelines between 1954 and 2006 were selected for this comparison due to the overall length of the beach survey record. This dataset includes shorelines compiled from NOAA T-sheets, air photos, and lidar elevations.

2.60 Results

Considerable spatial and temporal variability is observed in the time-series of shoreline positions from the eight beach profile transects (Figure 2.4). The record includes measurements from the start of surveying through December 2010. Long-term trends at the south shore barriers are as likely to be accretional as they are to be erosional and regression of MHW positions yields shoreline change rates between +0.27 m yr^{-1} at Charlestown Breachway (cha-bw) and -0.93 m yr^{-1} at Green Hill beach (grh). Long-term rates of change are relatively flat at Misquamicut (mis), Weekapaug (wkg), and Charlestown Town beach (cha-tb), accounting for less than ± 0.15 m yr^{-1} of position change. The R-squared values that correspond to the best-fit lines are indicative of the overall variability of shoreline positions and the robustness of the data used in the regression; the slope of all regression lines was significantly different from zero ($p<0.001$ for every site).

An annual signal of shoreline advance and retreat is present at all sites and is in-phase at all barriers except for wkg. In general, shorelines migrate seaward during summer months and retreat landward during winter months. Quasi-periodic behavior is also apparent on longer time scales, and can be observed in decadal-scale oscillations of shoreline position above and below the best-fit regression lines.

Because R_0 stakes are located at varying distances from the foredune crest at each of the respective beaches, absolute distance cannot be compared between profile sites; however, trends and relative changes between sites can be compared. Overall, beaches east of the stabilized inlet at Charlestown, RI exhibit greater variance than those to the west. Shoreline positions at mis and wkg show the least variance at all

sites, but 5-10 year long patterns of erosion/accretion appear to be out-of-phase between the transects. Similarly, the two profiles on East Beach, (est-1 and est-2), are 2 km apart on the same barrier spit (Figure 2.1) but also display opposite shoreline change trends on decadal and longer scales. The rapid patterns of accretion at cha-bw are presumed to be a product of the history of dredging and deposition at the stabilized inlet immediately to the west. Similar multi-year patterns are observed at cha-tb (1 km to the east) although the changes at this site have lower amplitudes. The two sites with the highest rates of long-term change (grh and mst) lie at the eastern end of the littoral cell. Both transects show a steady decline in shoreline position since surveying began in 1962. Large, rapid decreases in shoreline position at all sites reflect erosion during major coastal storms (for example the "Patriot's Day" storm, April 2007).

A Pearson test for correlation was conducted to examine similarities in the record of long-term shoreline positions between each transect. A correlation matrix was constructed using SAS software (version 9.2) to measure the strength of the linear relationship between any two shoreline records. Positive association exists between shorelines at est-1 and cha-tb ($r=0.66$), est-2 and grh ($r=0.58$), est-2 and mst ($r=0.54$), and grh and mst ($r=0.79$). On the short term, the scale and amplitude of shoreline change is quite variable between all sites. The two most similar in terms of the absolute value of variance are wkg and cha-tb and they are significantly different using a t test of means and a pairwise t test.

2.70 Discussion

Consideration of different shoreline indicators, rate-of-change statistics, and a distinction between processes that influence long-term change and short-term

variability is fundamental to coastal zone management. Here, using examples from the Rhode Island south shore, we demonstrate ways in which high-frequency observations from beach profiles can be used to predict trends in shoreline behavior, establish criteria for methods and scales of analysis, and provide a process-based framework to inform regional shoreline assessment programs. Overall, our results add to a growing literature (Eliot and Clark, 1989: Ruggiero, Kaminsky and Gelfenbaum, 2002; Smith and Zarillo, 1990) demonstrating the importance of beach profile data for coastal management, and for research devoted to shoreline change.

2.71 Quantifying shoreline change

Because datum-based measurements are numerous, accurate, and require minimal interpretation, the rate-of-change values derived from beach profiles are likely to represent actual long-term shoreline behavior, despite high frequency noise. As a consequence, they offer an opportunity to compare rate-of-change statistics using a dense dataset to those calculated using the limited number of vector shorelines that can be derived from map-based data. As an example, the family of regression lines in Figure 2.5 compares results of the different regression models at (a) est-1 and (b) grh profile sites to the time-series of MHW shoreline positions. The effect of sampling resolution on the record of shoreline change becomes apparent when compared at these scales and demonstrates how different signals become indistinguishable (aliased) when sampled infrequently. It also emphasizes that applying linear models to shoreline behavior can, at best, only approximate an average rate of change.

The US Geological Survey has established long-term and short-term shoreline change rates for the New England and Mid-Atlantic coast using LRR and EPR

methods respectively (Hapke et al., 2010). Our analysis, however, suggests that the WLR method more consistently depicts behavior of the shoreline on a wave-dominated coastline. With the WLR technique, more reliable data are given greater emphasis in determining the best fit line by a weighting factor – defined as a function of the variance in the uncertainty of the measurement (Genz et al., 2007; Himmelstoss, 2009). When historical shoreline uncertainties can be quantified, Rhode Island beaches (with the exception of grh) follow trends predicted by weighted regressions more closely than other methods (Table 2.3). Genz et al., (2007) came to a similar conclusion that weighting methods were superior to other methods using forecasted shorelines and synthetic time series data.

The EPR statistic appears to be the least accurate method for predicting rates of change on these time scales. This observation is notable as the EPR is the most commonly used method of shoreline change analysis (Dolan, Fenster and Holme, 1991). It has been used by the USGS to calculate short-term erosion rates and is the method used in Rhode Island for setback requirements (Boothroyd and Hehre, 2007; CRMC, 2010).

2.72 Shoreline position uncertainty

Uncertainty associated with historical HWLs is important to quantify as it provides a way to gauge the reliability of rate-of-change estimates and predictions of future shoreline positions. HWL shorelines are subject to measurement uncertainty from: (i) mapping methods (accuracy of source maps and photos, georeferencing errors, shoreline digitizing); (ii) identification of the shoreline indicator (interpretation error); and (iii) short-term variability of true shoreline positions (Anders and Byrnes,

1991; Crowell, Leatherman, and Buckley, 1991; Moore, 2000). Average uncertainties of New England and Mid-Atlantic shorelines derived from T-sheets, aerial photos, and lidar surveys were estimated by Hapke et al. (2010) and are summarized in Table 2.4.

Variations as a result of changes in either the wave or tidal climate at the time of shoreline delineation are included in Table 2.4 as part of the high water level uncertainty estimate (Ruggiero and List, 2009) but missing from this assessment are changes in shoreline position due to short-term variations in beach morphology that result from either cyclical (seasonal and longer) behavior, or from storm activity. Because high-frequency, site-specific data are necessary to evaluate change at this scale, the profile-derived shorelines provide a means to estimate this source of variability and include it as part of the overall shoreline position uncertainty for the Rhode Island south shore.

The position of MHW naturally fluctuates throughout the year and in response to storms, as can be seen in the deviations between actual shoreline positions and the best-fit regression lines (Figure 2.4). On Rhode Island's barrier spits, MHW typically migrates over a 10-20 meter swath of beach annually, and has changed by up to 35 meters following a single event. An annual cycle was previously observed in the power spectra of beach volume data (Graves, 1991; Lacey and Peck, 1998) where observations of high profile volume during summer months and low volume during winter months was in phase at all profile sites. We observe a similar trend in the shoreline record, which is again illustrated using examples from two sites (Figure 2.6). Mean shoreline position varies by approximately 4.8 meters at grh during this annual cycle and by 7.3 meters at est-1. At both sites, 1σ error bars indicate that variability of

beach measurements is slightly lower in summer months suggesting shoreline positions are more consistent. To quantify this variability as a function of annual changes we averaged the standard deviation of shoreline positions from the annual mean for all years of profile data (Table 2.3). In doing so, we provide a best estimate of annual shoreline position uncertainty, presumably due to seasonal changes in the frequency and intensity of storms.

Smith and Zarillo (1991) first demonstrated that changes in shoreline position at seasonal scales could account for one of the greatest sources of error in calculations of long-term shoreline change. Along the RI south shore these values are large - approximately 5 to 75 times the annualized rates of shoreline change (Table 2.3). Averaging all sites results in an overall uncertainty due to seasonal variations of 4.4 meters, approximately equal to the uncertainty due water level variations (Table 2.4). Including this source increases total shoreline uncertainty by only ~7% for pre-1950 T-sheet surveys, but by approximately 28% for later years when the use of air photos had reduced overall interpretation error.

2.73 Analysis time scales

There are no simple criteria to distinguish long-term trends from short-term variations in shoreline position (Dolan, Fenster, and Holme, 1991) and the distinction can be somewhat arbitrary when samples are clustered together (as in recent decades). Furthermore, the use of linear models to quantify shoreline change ignores any periodic component that may be present in the record, and in doing so, may overlook the influence of processes that contribute to non-linear shoreline behavior (Figure 2.5; Fenster and Dolan, 1994). As a result, the definition of shoreline change is often a

function of the purpose of the investigation and/or the availability of data as opposed to the processes driving coastal change (Crowell, Leatherman, and Buckley, 1993).

Due to the lack of site specific, long time-series observations at most coastal sites, few studies have been able to offer insight into this problem. Eliot and Clark (1989) used monthly profile measurements from Scarborough Beach (Western Australia) and Warilla Beach (New South Wales) to show that a minimum of 10 years of shoreline data was needed to identify true long-term trends. Morton, Gibeaut & Paine (1995) demonstrated how coastal storms control short-term (<10 yr) behavior of shorelines, due to their ability to rapidly redistribute beach sediment.

The record from southern Rhode Island also demonstrates that natural beaches undergo variability at a number of different time scales that are typically not captured by conventional shoreline mapping techniques. Annual deviations in shoreline positions (Table 2.3) are an order of magnitude larger than the calculated rate at all sites, meaning that, at minimum, several decades of observation are necessary to separate normal fluctuations from any long-term trend. In addition to annual variability, quasi-periodic oscillations on a 5-10 year scale are present at many sites (Figure 2.3; Figure 2.7). Studies of beach volume along the RI south shore have attributed variability at these scales to onshore sediment movement (Gibeaut, 1986), growth and depletion of the dune and backshore reservoir (Graves, 1991), variations in regional climate and sea level (Lacey and Peck, 1998), and storm activity (O'Connor, 2002). While the precise cause of this variability is beyond the scope of this paper, these observations nonetheless demonstrate that natural processes contribute to non-

linear shoreline behavior on decadal (and longer) time scales and can have strong influence on rate of change statistics and the choice of analysis time scales.

2.74 Shoreline indicators

For more than a century, the HWL has been the most commonly used shoreline indicator because it can be easily identified in the field and on aerial imagery. Increasingly, elevation-based data derived from lidar or GPS surveys are becoming available to study shoreline change. The advantage of such data is that accurate and objective, datum-based shorelines can be obtained with minimal user interpretation and without the effects of waves and runup (Stockdon et al., 2002). For HWL and MHW shorelines collected simultaneously, or within a few days of each other, studies have shown that the visually identified HWL is nearly always offset on the beach profile relative to MHW (Morton et al., 2004; Morton and Speed, 1998; Pajak and Leatherman, 2002; Ruggiero, Kaminsky, and Gelfenbaum, 2003). The offset (referred to as the proxy-datum bias) acts primarily in one direction, with the HWL consistently landward of the MHW position. Quantifying the proxy-datum bias at individual coastal locations is critical, as shoreline change analyses are increasingly making use of both types of data.

Ruggiero and List (2009) proposed a methodology to estimate the horizontal offset between proxy-based and datum-based shorelines as a function of tide level (Z_T), offshore wave conditions (H_o -deep water significant wave height, L_o - deepwater wave length), and beach morphology (tan β-foreshore beach slope).

Equation (2.1) $\text{Bias} = (X_{HWL} - X_{MHW}) =$

$$\frac{\left[Z_T + 1.1\left(0.35\tan\beta(H_oL_o)^{(1/2)} + \frac{\left[H_oL_o(0.563\tan\beta^2 + 0.004\right]^{1/2}}{2}\right)\right] - Z_{MHW}}{\tan\beta}$$

The technique was used by Hapke et al. (2010) to estimate the proxy-datum bias at 1-km averaged blocks along the New England and Mid-Atlantic coastline. Because detailed measurements of wave and beach characteristics are generally not available for historical HWL shorelines, these parameters were estimated using long-term averages from U.S Army Corps of Engineers wave hindcast studies, NDBC buoy records, and lidar data. These estimates of the proxy-datum bias (and associated uncertainty) at each of the GSO beach profile sites are listed in Table 2.5.

Our record of MHW shorelines provides an empirical dataset from which we can compare the actual and estimated offset for vector shorelines that were coincident with, or within a few weeks of beach profile dates. Absolute horizontal and vertical differences between MHW position (beach profile surveys) and the visually identified HWL (aerial photo and t-sheet surveys) were calculated for 35 historical shorelines (Table 2.5). When averaged alongshore, the mean offset between MHW and HWL positions is 9.18 meters, comparable to the range of proxy-datum bias values calculated from long-term wave and tidal data. Yet the bias also shows considerable variability both spatially (between sites) and temporally when compared with the estimates of Hapke et al. (2010).

The HWL and MHW shorelines are compared here with an assumption that observed offsets are entirely a function of shoreline definition (i.e. not related to erosion or accretion between survey dates). A similar assumption is made when applying a proxy-datum correction based on hindcast, and spatially averaged datasets. However, the occurrence of negative offsets (meaning that the HWL is seaward of MHW) at three of our sites (Table 2.5) indicates that this assumption is problematic and that rapid changes in beach morphology are, in fact, responsible for some of this variability. Observed change in beach slope add further support to this reasoning. Figure 2.8 shows a time-series of foreshore beach slopes derived from profile data at grh. The time-series confirms that beach slope changes considerably between measurements and around the long-term mean, and suggests that changes in morphology may account for a much larger portion of uncertainty in the proxy-datum bias than previously assumed.

Ruggiero and List (2009) applied the proxy-datum bias to HWL shorelines, but pointed out that it is just as possible to apply an equal but opposite correction to MHW shorelines. In principle, it may seem more suitable to use the bias to shift historical HWL estimates seaward, because those shorelines are known to be less accurate (Boak and Turner, 2005) and because future shorelines are more likely to be datum-based. However, the short-term variability in coastal morphology shown here suggests that it is more accurate to adjust MHW measurements by offsetting them landward, particularly for coastal lidar. Not only is the foreshore slope simultaneously collected during lidar surveys, but the low positional uncertainty surrounding lidar shorelines result in better estimates of the horizontal bias.

2.75 Implications for coastal policy

The offset between HWL and MHW shorelines and the natural variability of shoreline positions are important considerations for current efforts to manage the coast. Several U.S. states (including Rhode Island) rely on the position of MHW to distinguish between privately held coastal property and public trust lands. While a visual shoreline proxy such as the "wrack line" or last high tide swash is commonly interpreted as this boundary, the Rhode Island Supreme Court ruled in 1982 that the property line actually occurs at "*the line that is formed by the intersection of the tidal plane of mean high tide with the shore*" (State v. Ibbison, 1982).

Figure 2.9 shows a comparison of HWL and MHW shoreline positions collected simultaneously from beach profile surveying between November 23, 2010 and August 25, 2011 (91 individual profiles). The location of the HWL is not routinely collected as part of the GSO beach profiling procedure so long-term records of this offset are not available for the lifetime of the program, however, for this analysis, the HWL was identified in the field by the tonal contrast between wet intertidal beach and dry supratidal sand, and is assumed to represent the landward extent of the last high tide swash (LHTS). Because R_0 stakes are situated at varying distances from the foredune crest, we limit this discussion to the measured offset between MHW and HWL shorelines; the absolute distance to the shoreline proxies are not compared between profile sites.

Both types of shoreline indicators follow patterns resulting from erosion and accretion, although there is considerably more variability in the position of the HWL over time when compared to MHW, suggesting the latter may be a more consistent

measure of shoreline movement. As expected, the HWL is consistently found landward of MHW at all profile sites. The mean offset is 18.5 meters, which is comparable to the long-term average between MHW and the LHTS of 19.91 meters measured at Charlestown Beach, RI by Freedman and Higgins (2003). Notably, these values are more than twice as large as the proxy-datum bias calculated by Hapke et al. (2010) for south shore beaches (Table 2.5).

When compared alongshore the offset is spatially variable, with mean values ranging from 13.9 m at grh to 22.6 m at wkg. The scale of the MHW-HWL offset reinforces previous findings (Freedman and Higgins, 2003; Morton and Speed, 1998) that have concluded that MHW is not an appropriate measure for determining property boundaries on wave-dominated coastlines. The variability observed in records of shoreline change derived from survey data indicates that this boundary fluctuates appreciably on daily, seasonal, and annual time-scales. The unidirectional nature of the offset also means that shoreline access guaranteed by the RI State Constitution (Article1, Section 17) is probably limited to periods of low tide or wave set down.

2.80 Conclusions

The economic and societal impacts of coastal erosion provide ample justification for studies that aim to understand and forecast shoreline behavior. Monitoring the position of the shoreline using map-based data has proven to be a useful and straightforward method for estimating shoreline change on regional scales. However, if historical shorelines are to be used to formulate coastal policies, the natural variability of shoreline indicators must be considered. In this paper, we have used a simple technique to estimate shoreline positions from cross-shore beach profile

measurements. A time-series of bi-weekly, datum-based shoreline positions was derived for eight beach transects along the southern Rhode Island coast. The record demonstrates that natural beaches undergo variability at a number of different time scales that are typically not captured by conventional shoreline mapping techniques. Comparing high-resolution, datum-based measurements with shoreline mapping methods, we have demonstrated that:

(i) Survey measurements can be useful to validate rate-of-change estimates for regional shoreline change, but also highlight that applying a linear model to shoreline data can only approximate shoreline behavior.

(ii) Sample resolution and analysis time-scales can strongly bias the calculated rate of shoreline change.

(iii) On wave-dominated coastlines, shoreline positions naturally fluctuate throughout the year, and in response to storms; the scale of these fluctuations is an order of magnitude larger than annualized rates of change.

(iv) The offset between MHW and HWL shorelines is large for wave-dominated shorelines and the effect of combining different shoreline indicators into a single shoreline change analysis is considerable. Short term (days to weeks) variations observed at transect scale suggest that the proxy-datum bias is more appropriately applied to datum-based shorelines than to historical HWL shorelines.

(v) Tidal datums such as MHW are not an appropriate measure for determining property boundaries on wave-dominated coastlines.

2.90 References

Anders, F.J., & Byrnes, M.R. (1991). Accuracy of shoreline change rates as determined from maps and aerial photographs. *Shore and Beach, 59*, 17-26.

Boak, E.H., & Turner, I.L. (2005). Shoreline definition and detection: A review. *Journal of Coastal Research, 21*(4), 688-703.

Boothroyd, J.C., Friedrich, N.E., & McGinn, S.R. (1985). Geology of microtidal coastal lagoons: Rhode Island. *Marine Geology, 63*, 35-76.

Boothroyd, J.C., Gibeaut, J.C., Dacey, M.F., & Rosenberg, M.J. (1986). *Geological aspects of shoreline management: A summary for southern Rhode Island* (Sea Grant Technical Report No. 6-SRG). Kingston, RI: University of Rhode Island.

Boothroyd, J.C., Galagan, C.W., & Graves, S.M. (1988). *Advance and retreat of the southern Rhode Island Shoreline, 1939-1985: including 1985 berm volume* (Sea Grant Technical Report No. 7-SRG). Kingston, RI: University of Rhode Island.

Boothroyd, J.C., & Sirkin, L. (2002). Quaternary geology and landscape development of Block Island and adjacent regions. In P. Paton, L. Gould, P. August & A. Frost (Eds.), *The Ecology of Block Island* (pp. 13-27). Kingston: Rhode Island Natural History Survey.

Boothroyd, J.C., & Hehre, R.E. (Cartographer). (2007). *Shoreline change maps for the south shore of Rhode Island: Rhode Island Geological Survey Map Folio 2007-2, for RI Coastal Resources Management Council, 150 maps (scale:1:2,000).*

Byrnes, M.R., Mcbride, R.A., & Hiland, M.W. (1991). *Accuracy standards and development of a national shoreline change database.* Paper presented at the Coastal Sediments '91, Seattle, WA.

Clarke, D.J., & Eliot, I.G. (1983). Mean sea-level and beach-width variation at Scarborough, Western Australia. *Marine Geology, 51*(3-4), 251-267.

CRMC (Coastal Resources Management Council). (1999). *RI Salt Pond Region: Special Area Management Plan*: CRMC.

CRMC (Coastal Resources Management Council). Update Dec, 2010. The State of Rhode Island Coastal Resources Management Program CRMC, 222pp.

Crowell, M., Leatherman, S.P., & Buckley, M.K. (1991). Historical shoreline change: error analysis and mapping accuracy. *Journal of Coastal Research, 7*(3), 839-852.

Crowell, M., Leatherman, S.P., & Buckley, M.K. (1993). Shoreline change rate analysis: Long term versus short term data. *Shore and Beach, 61*(2), 13-20.

Dillon, W.P. (1970). Submergence effects on a Rhode Island barrier and lagoon and inferences on migration of barriers. *Journal of Geology, 78*, 94-106.

Dolan, R., & Hayden, B. (1983). Patterns and prediction of shoreline change. In P.D. Komar (Ed.), *Handbook of Coastal Processes and Erosion* (pp. 123-149). Boca Raton, Florida: CRC Press.

Dolan, R., Fenster, M.S., & Holme, S.J. (1991). Temporal analysis of shoreline recession and accretion. *Journal of Coastal Research, 7*(3), 723-744.

Donnelly, J.P., Bryant, S.S., Butler, J., Dowling, J., Fan, L., Hausmann, N., Newby, P., Shuman, B., Stern, J., Westover, K., & Webb Iii, T. (2001). 700 yr sedimentary record of intense hurricane landfalls in southern New England. *GSA Bulletin, 113*(6), 714-727.

Donnelly, J.P., Cleary, P., Newby, P., & Ettinger, R. (2004). Coupling instrumental and geologic records of sea-level change: Evidence from southern New England of an increase in the rate of sea-level rise in the late 19th century. *Geophysical Research Letters, 31*, L05203-L05206.

Eliot, I.G., & Clarke, D.J. (1989). Temporal and spatial bias in the estimation of shoreline rate-of-change statistics from beach survey information. *Coastal Management, 17*(2), 129-156.

Fenster, M.S., & Dolan, R. (1994). Large-scale reversals in shoreline trends along the U.S. mid-Atlantic coast. *Geology, 22*, 543-546.

Fitzgerald, D.M., & Van Heteren, S. (1999). Classification of paraglacial barrier systems: coastal New England, USA. *Sedimentology, 46*, 1083-1108.

Ford, K.H. (2003). *Assessment of the Rhode Island coastal lagoon ecosystem.* Ph.D. Dissertation, University of Rhode Island, Kingston, R.I.

Freedman, J., & Higgins, M. (2003). *What do you mean by mean high tide? The public trust doctrine in Rhode Island.* Paper presented at the 13th Biennial Coastal Zone Conference, Baltimore, MD.

Friedrich, N.E. (1982). *Depositional environments and sediment transport patterns, Point Judith - Potter Pond complex, Rhode Island.* MS thesis, University of Rhode Island, Kingston.

Genz, A.S., Fletcher, C.H., Dunn, R.A., Frazer, L.N., & Rooney, J.J. (2007). The predictive accuracy of shoreline change rate methods and alongshore beach variations on Maui, Hawaii. *Journal of Coastal Research, 23*(1), 87-105.

Gibeaut, J.C. (1986). *Beach sedimentation cycles (1962-1985) along a microtidal wave-dominated coast: South shore of Rhode Island.* MS thesis, University of Rhode Island, Kingston.

Graves, S.M. (1990). *Morphotomology of Rhode Island barrier shores: A method of distinguishing beach from dune/barrier component histories within a 29 year record of shore zone profile data, with special reference to the role of the beach as a buffer and modulator of erosional coastline retreat.* MS thesis, University of Rhode Island, Kingston.

Hapke, C.J., Himmelstoss, E.A., Kratzmann, M.G., List, J.H., & Thieler, E.R. (2010). *National assessment of shoreline change: Historical shoreline change along the New England and Mid-Atlantic coasts* (USGS Open File Report No. 2010-1118): US Geological Survey.

Hayes, M.O. (1979). Barrier island morphology as a function of tidal and wave regime. In R.A. Davis (Ed.), *Geology of Holocene Barrier Island Systems* (pp. 233-304). Berlin: Springer-Verlag.

Himmelstoss, E.A., Kratzmann, M., Hapke, C.J., Thieler, E.R., & List, J. (2010). *The national assessment of shoreline change - A GIS compilation of vector shorelines and associated shoreline change data for the New England and Mid-Atlantic coasts* (U.S. Geological Survey Open-File Report No. 2010-1119): USGS.

Lacey, E.M., & Peck, J.A. (1998). Long-term beach profile variations along the south shore of Rhode Island, USA. *Journal of Coastal Research, 14*(4), 1255-1264.

Larson, M., & Kraus, N.C. (1994). Temporal and spatial scales of beach profile change, Duck, North Carolina. *Marine Geology, 117*(1-4), 75-94.

Lee, G., Nicholls, R.J., Birkemeier, W.A., & Leatherman, S.P. (1995). A conceptual fairweather-storm model of beach nearshore profile evolution at Duck, North Carolina, USA. *Journal of Coastal Research, 11*(4), 1157-1166.

Moore, L.J. (2000). Shoreline mapping techniques. *Journal of Coastal Research, 16*(1), 111-124.

Moore, L.J., Ruggiero, P., & List, J.H. (2006). Comparing mean high water and high water line shorelines: Should proxy-datum offsets be incorporated into shoreline change analysis? *Journal of Coastal Research, 22*(4), 894-905.

Morton, R.A., Gibeaut, J.C., & Paine, J.G. (1995). Meso-scale transfer of sand during and after storms: implications for prediction of shoreline movement. *Marine Geology, 126*, 161-179.

Morton, R.A., & Speed, F.M. (1998). Evaluation of shorelines and legal boundaries controlled by water levels on sandy beaches. *Journal of Coastal Research,*

14(4), 1373-1384.

Morton, R.A., Miller, T.L., & Moore, L.J. (2004). *National assessment of shoreline change: art 1, historical shoreline changes and associated coastal land loss along the U.S. Gulf of Mexico* (USGS Open File Report No. 2004-1043): US Geological Survey.

NOAA (National Oceanic and Atmospheric Administration). (2011). *NOAA tides and currents, mean sea level trend 8452660 Newport, Rhode Island.* Retrieved July 14, 2011, from http://tidesandcurrents.noaa.gov/sltrends/sltrends_station.shtml?stnid=8452660

O'Connor, S. (2002). *Storm impact on shoreline change: South shore, Rhode Island.* MS thesis, University of Rhode Island, Kingston.

Oakley, B.A., Alvarez, J.D., & Boothroyd, J.C. (2007). *Benthic geologic habitats of the Matunuck-Green Hill shoreface, Rhode Island.* Paper presented at the 42 Annual Meeting of the Geological Society of America (Northeastern Section), Durham, New Hampshire.

Oakley, B.A., Alvarez, J.D., Brenner, H., Dowling, M., Klinger, J., Zitello, M., & Boothroyd, J.C. (2009). *Depositional environments and sediment transport on a microtidal, wave dominated shoreface.* Paper presented at the Coastal Zone '09, Boston, MA.

Pajack, M.J., & Leatherman, S.P. (2002). The high water line as shoreline indicator. *Journal of Coastal Research, 18*(2), 329-337.

Rosenberg, M.J. (1985). *Temporal variability of beach profiles, Charlestown beach, Rhode Island.* MS thesis, University of Rhode Island, Kingston.

Ruggiero, P., Kaminsky, G.M., & Gelfenbaum, G. (2003). Linking proxy-based and datum-based shorelines on high-energy coastlines: Implications for shoreline change analyses. *Journal of Coastal Research, SI-38*, 57-82.

Ruggiero, P., & List, J.H. (2009). Improving accuracy and statistical reliability of shoreline position and change rate estimates. *Journal of Coastal Research, 25*(5), 1069-1081.

Smith, G.L., & Zarillo, G.A. (1990). Calculating long-term shoreline recession rates using aerial photographic and beach profiling techniques. *Journal of Coastal Research, 6*(1), 111-120.

State v. James Ibbison III et al. 728 (Supreme Court of Rhode Island 1982).

Stockdon, H.F., Sallenger, A.H., Jr., List, J.H., & Holman, R.A. (2002). Estimation of shoreline position and change using airborne topographic lidar data. *Journal of Coastal Research, 18*(3), 502-513.

Thieler, E.R., & Danforth, W.W. (1994). Historical shoreline mapping (1): Improving techniques and reducing positioning errors. *Journal of Coastal Research, 10*(3), 549-563.

Thieler, E.R., Himmelstoss, E.A., Zichichi, J.L., & Ergul, A. (2009). *Digital Shoreline Analysis System (DSAS) version 4.0ÑAn ArcGIS extension for calculating shoreline change* (USGS Open-File Report No. 2008-1278): U.S. Geological Survey.

Table 2.1 Changes in the location of R_0 at each beach profile site determined from archived field notes and annual reports.

Profile site	*Date*	*RISPF Easting*	*RISPF Northing*	*R0 elevation (m NAVD88)*	*R0 elevation (m above MLLW)*
MIS	07/26/77	251547.43	89116.42	4.629	5.253
	09/18/02	251542.50	89142.20	4.219	4.843
WKG	12/19/62	261528.77	89815.20	3.527	4.151
	12/07/72	261528.29	89816.62	3.527	4.151
	12/18/08	261528.29	89816.62	3.630	4.254
EST-1	12/19/62	277202.96	95268.14	3.206	3.830
	07/14/78	277195.31	95284.65	3.456	4.080
	10/10/85	277188.42	95299.54	2.956	3.580
EST-2	08/20/76	284679.39	97998.41	2.669	3.293
	11/05/76	284690.31	97976.82	4.330	4.954
	10/10/85	284682.91	97991.46	3.960	4.584
	01/06/93	284662.82	98031.19	3.960	4.584
	11/07/03	281551.16	96910.06	2.641	3.265
	09/26/04	284662.82	98031.19	3.960	4.584
CHA-BW	01/21/77	290479.69	99836.31	2.471	3.095
CHA-TB	11/20/75	293417.45	101216.57	3.975	4.599
	09/04/80	293417.45	101216.57	4.310	4.934
GRH	12/19/62	298717.17	102312.01	2.988	3.612
	09/28/72	298717.11	102314.01	2.988	3.612
	12/07/92	298716.38	102340.00	2.458	3.082
	04/30/99	298716.70	102328.52	2.778	3.402
	12/27/00	298716.38	102340.00	2.458	3.082
	04/17/07	298702.58	102361.89	2.458	3.082
	12/18/08	298702.58	102361.89	2.587	3.211
	07/26/10	298702.58	102361.89	2.899	3.523
	08/29/11	298704.55	102376.68	2.648	3.272
MST	12/19/62	307140.07	104537.99	3.356	3.980
	07/14/78	307140.07	104537.99	3.539	4.163
	12/19/79	307140.07	104537.99	3.965	4.589
	08/05/80	307140.07	104537.99	4.011	4.635
	08/21/80	307140.07	104537.99	3.539	4.163
	09/04/80	307140.07	104537.99	3.965	4.589
	12/07/92	307131.35	104563.54	3.345	3.969
	11/11/10	307281.12	104573.00	3.426	4.050

Table 2.2 Digital vector shorelines and uncertainties used for DSAS calculations.

Survey Date	*Shoreline type*	*Source*	*Uncertainty (m)*
04/01/54	t-sheet	NOAA	10.8
04/22/54	t-sheet	NOAA	10.8
09/02/63	air photo	RI Geological Survey/URI	5.1
09/07/63	air photo	RI Geological Survey/URI	5.1
10/15/63	air photo	RI Geological Survey/URI	5.1
04/11/75	air photo	RI Geological Survey/URI	3.2
04/14/75	air photo	RI Geological Survey/URI	3.2
03/11/85	air photo	RI Geological Survey/URI	3.2
03/22/85	air photo	RI Geological Survey/URI	3.2
03/27/85	air photo	RI Geological Survey/URI	3.2
03/29/85	air photo	RI Geological Survey/URI	3.2
09/25/00	Lidar	USGS	2.3
04/08/04	air photo	RI Geological Survey/URI	3.2
04/10/06	air photo	RI Geological Survey/URI	3.2

Table 2.3 Annualized shoreline change rates (m yr^{-1}) for proxy[1] and datum-based[2] shoreline time series at each beach profile transect. End-point rate (EPR), linear regression rate (LRR), and weighted linear regression (WLR) of vector shorelines were calculated using DSAS v. 4.2. Bold text indicates methods whose results most closely compare with regression of MHW shoreline positions. Annual variability is expressed as the average of the standard deviation of shoreline positions from the annual mean. Note that the variability of MHW shorelines is an order of magnitude larger than annualized rates of change.

	EPR[1]	*LRR*[1]	*WLR*[1]	*LRR of MHW shorelines*[2]	*Annual variability of MHW (m)*
mis	-0.36	-0.27	**-0.10**	-0.11	3.18
wkg	-0.62	-0.53	**-0.28**	-0.04	3.09
est-1	-0.46	-0.29	**0.31**	0.18	5.53
est-2	-1.13	-0.91	**-0.47**	-0.36	4.50
cha-bw	-0.49	-0.48	**-0.28**	0.27	7.51
cha-tb	-0.88	-0.57	**-0.23**	0.14	4.17
grh	-1.14	**-0.98**	-0.62	-0.93	4.20
mst	-1.20	-1.07	**-0.76**	-0.64	3.08

Table 2.4 Average uncertainties (in meters) for New England and Mid-Atlantic HWL shorelines as estimated by Hapke et al. (2010). Total shoreline position uncertainty is computed by summing of the individual terms in quadrature.

Shoreline position uncertainties	*T-sheets (1800-1950s)*	*T-sheets (1960-1980s)*	*Air photos (1970-2000s)*	*Lidar (1997-2000)*
Georeferencing	4	4	-	-
Digitizing	1	1	1	-
T-sheet survey	10	3	-	-
Air photo	-	-	3	-
HWL uncertainty	4.5	4.5	4.5	-
Lidar uncertainty	-	-	-	2.3
Total uncertainty	**11.7**	**6.8**	**5.5**	**2.3**

Table 2.5 Absolute horizontal and vertical differences between HWL and MHW shorelines at profile sites compared to proxy-datum values estimated by Hapke et al. (2010).

	Survey Date		*Vertical offset (m)*	*Horizontal offset (m)*	*Proxy-datum bias ± uncertainty (m)*
Location	*HWL*	*MHW*			
mis	03/22/85	03/20/85	0.43	5.63	8.38 ± 3.96
	03/29/85	03/20/85	0.28	3.68	
	04/08/04	04/09/04	1.78	7.35	
wkg	10/15/63	10/12/63	-0.37	-3.84	8.40 ± 3.94
	04/14/75	03/10/75	1.39	13.29	
	03/22/85	03/20/85	1.77	13.29	
	03/29/85	03/20/85	1.64	11.67	
	04/08/04	04/09/04	1.17	14.13	
est-1	04/14/75	03/10/75	0.31	18.34	7.93 ± 3.69
	03/11/85	03/06/85	0.53	7.00	
	03/29/85	03/20/85	0.72	6.06	
	04/08/04	04/09/04	1.93	10.06	
	04/10/06	04/15/06	2.00	21.13	
est-2	03/11/85	03/06/85	-0.52	-2.50	8.26 ± 3.86
	03/29/85	04/17/85	0.03	7.59	
	04/08/04	03/13/04	1.90	6.22	
	04/10/06	04/15/06	2.91	17.52	
cha-bw	03/11/85	03/06/85	0.99	17.65	8.22 ± 3.84
	03/29/85	03/20/85	0.76	9.94	
	04/08/04	04/09/04	0.94	9.78	
	04/10/06	04/15/06	0.52	4.91	
cha-tb	03/11/85	03/06/85	0.30	6.52	8.45 ± 3.98
	03/29/85	03/20/85	0.32	3.51	
	04/08/04	04/09/04	1.14	12.65	
	04/10/06	04/15/06	1.02	21.74	
grh	04/14/75	03/10/75	0.72	13.94	8.83 ± 4.16
	03/11/85	03/06/85	-0.26	-7.00	
	03/29/85	03/20/85	0.02	-0.22	
	04/08/04	04/09/04	0.76	5.38	
	04/10/06	04/15/06	0.60	1.02	
mst	04/11/75	03/10/75	0.57	6.02	8.60 ± 4.05
	03/27/85	03/20/85	0.57	10.71	
	03/29/85	03/20/85	1.38	24.68	
	04/08/04	04/09/04	1.29	6.36	
	04/10/06	04/15/06	1.51	16.92	

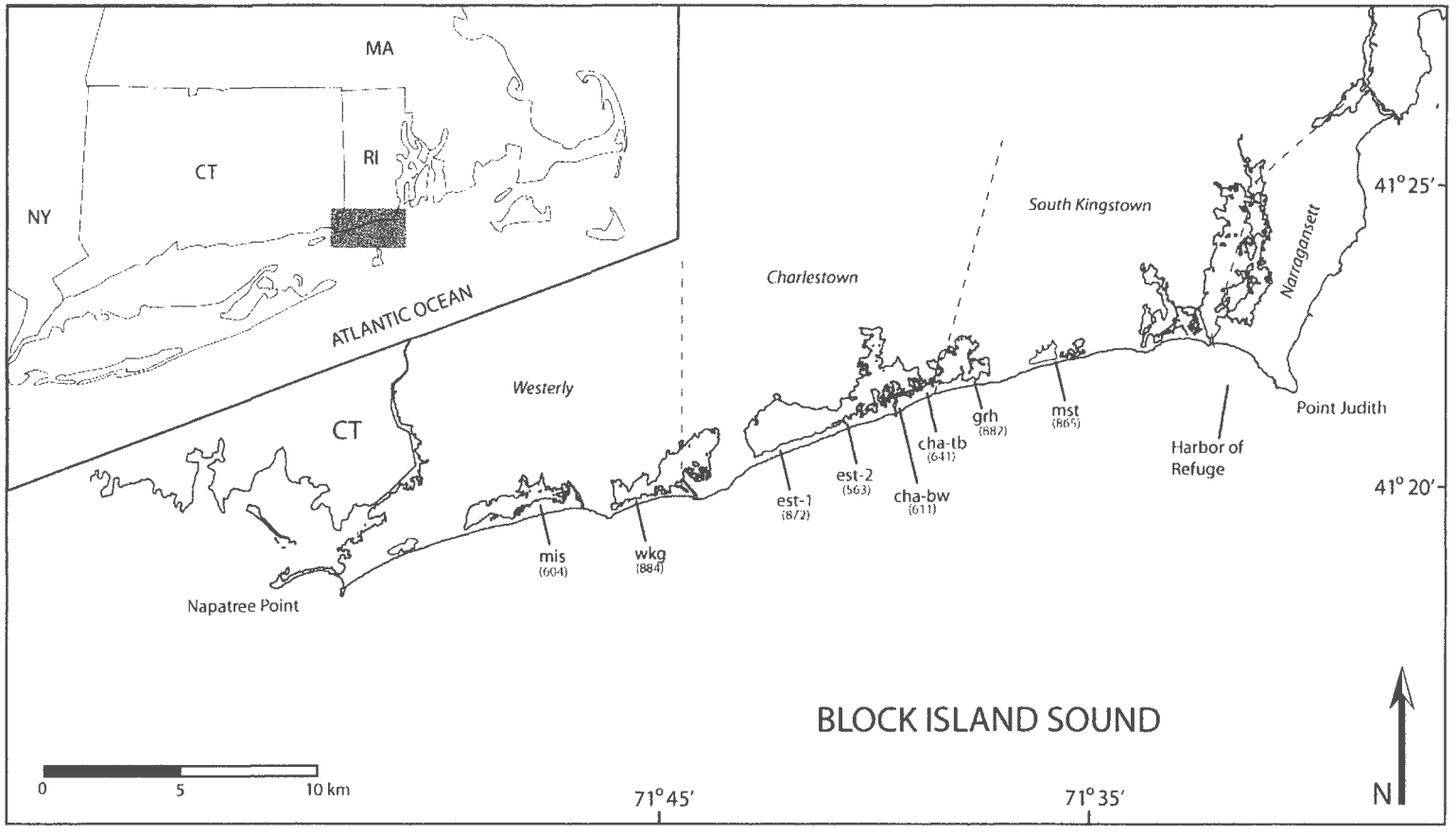

Figure 2.1 Beach profile stations along Rhode Island's barrier-headland coastline. Profile stations located on barrier beaches are abbreviated as follows: Misquamicut (mis), Weekapaug (wkg), East Beach (est-1, est-2), Charlestown Breachway (cha-bw), Charlestown Town Beach (cha-tb), Green Hill Beach (grh), Moonstone Beach (mst). The total number of beach profile surveys from each site is noted in parentheses.

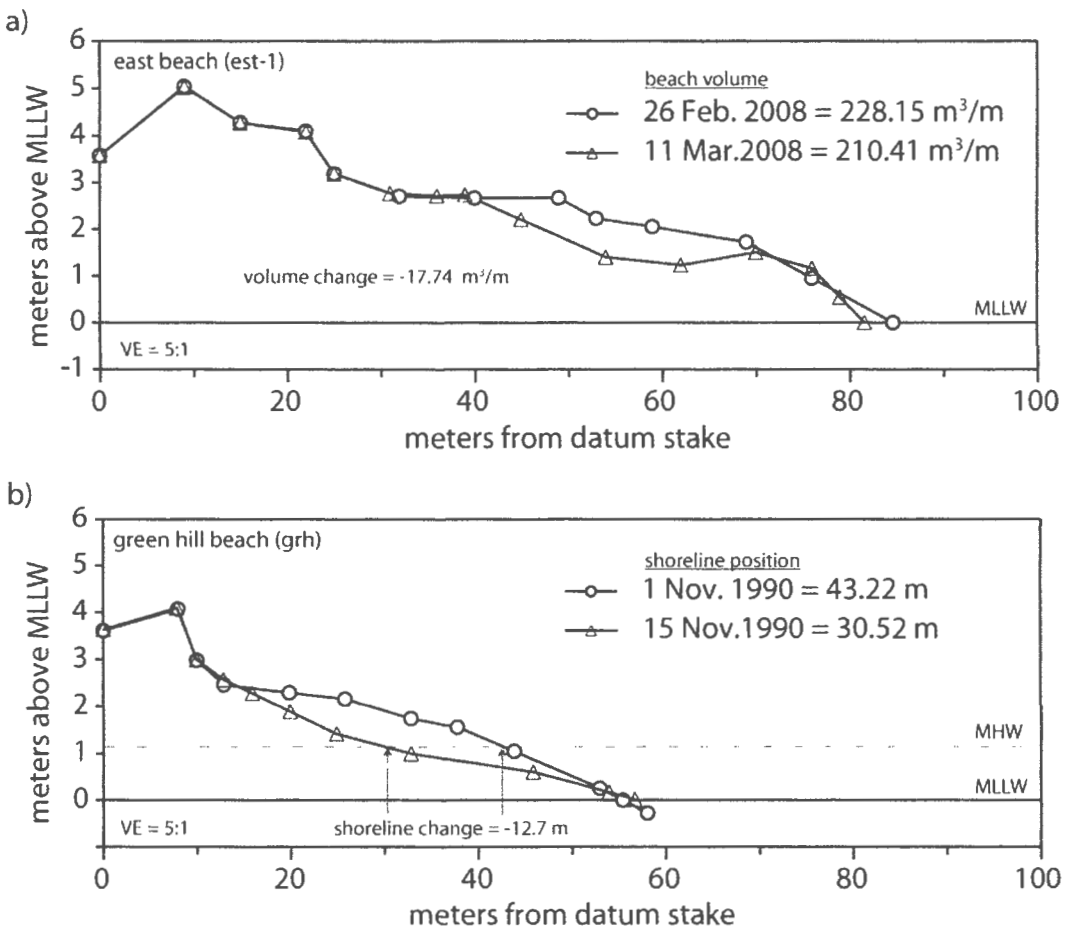

Figure 2.2 Representative beach profiles and sample calculations. Consecutive profiles are overlain to indicate (a) volume changes that occurred between February 26 and March 11, 2008 at site est-1 (East Beach) and (b) retreat of MHW shoreline position between November 1 and November 15, 1990 at Green Hill Beach (grh).

Figure 2.3 DSAS transect at est-1 and historical vector shorelines. Intercept points are used by DSAS to calculate rates of shoreline change by measuring the differences in the distance to each historical shoreline position from the baseline along each transect. The red shoreline (survey date 9/25/2000) is a lidar-derived MHW shoreline.

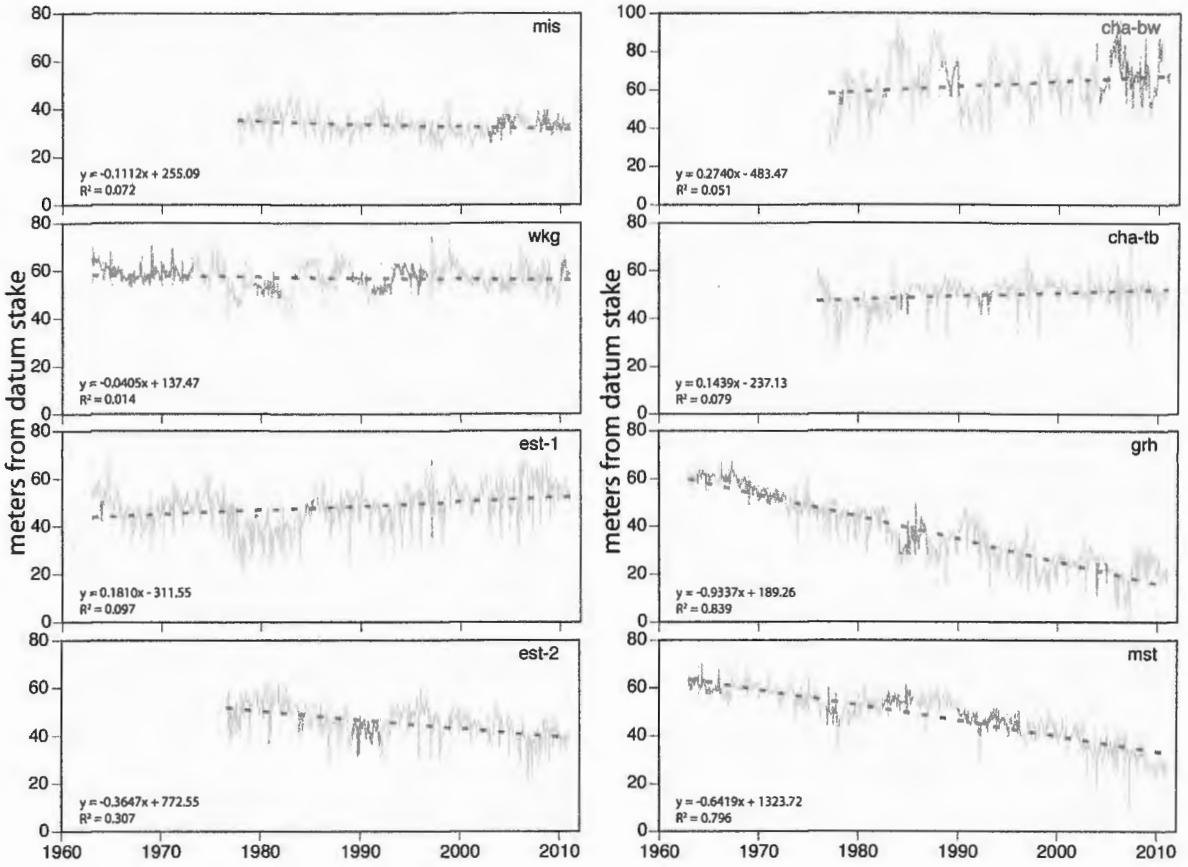

Figure 2.4 Time-series of MHW shoreline positions from RI south shore beach profile sites. Each data point represents the position of the MHW contour relative to a reference datum stake (R_0). The average time between surveys is 20 days. Vertical lines show yearly divisions. Rate-of-change estimates are indicated by the slope of the best-fit regression (dashed) line. The slope for all regression lines was significantly different from zero at the $p<0.001$ level.

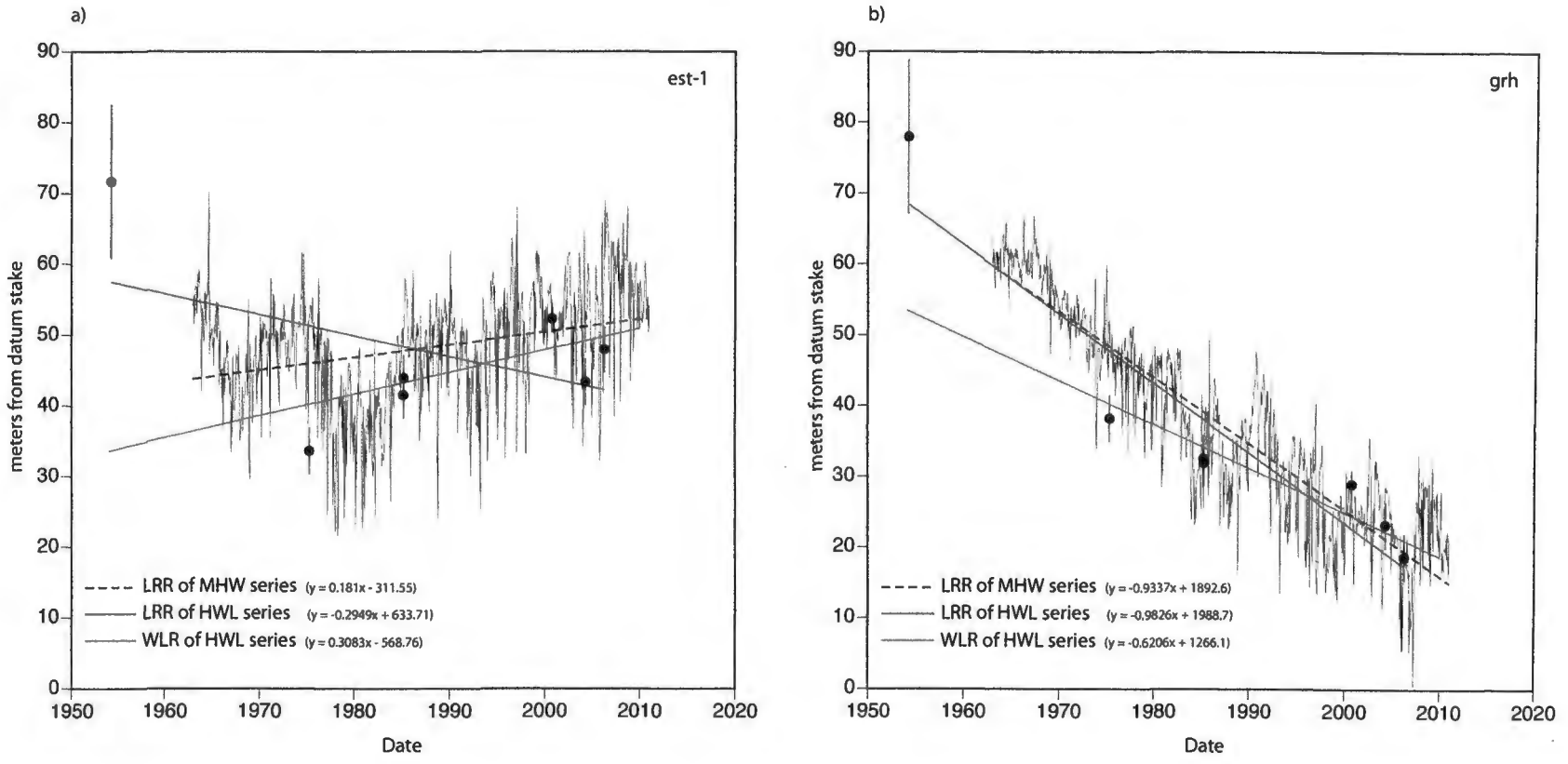

Figure 2.5 Regression statistics for the profile-derived MHW shoreline record compared with those derived from vector shorelines between 1954 and 2006 at est-1 and grh profile sites. Linear regression of the profile-derived record is shown as a dashed line. Circles represent vector shorelines. LRR (red line) and WLR (blue line) regression statistics were calculated using DSAS v.4.2. The HWL positions included in the vector shorelines have been corrected for the proxy-datum bias within DSAS. Error bars indicate the estimated positional uncertainty for each vector shoreline (Himmelstoss et al., 2010).

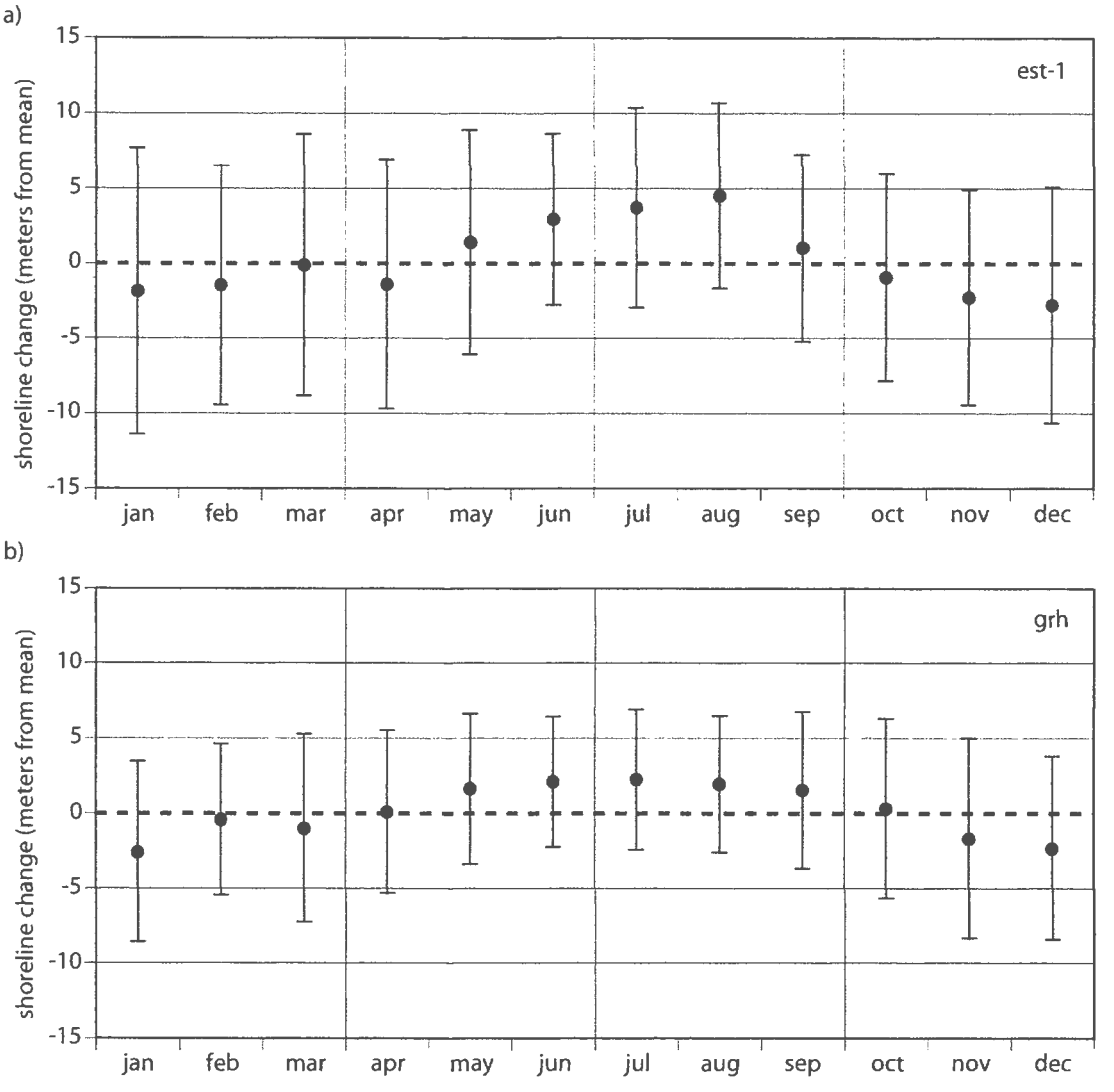

Figure 2.6 Average monthly shoreline positions from (a) est-1 and (b) grh profile sites showing shoreline maximum during summer months and minimum in winter months. Error bars show ± 1 standard deviation. Prior to averaging, the time series data were detrended by subtracting the best-fit line from each measurement.

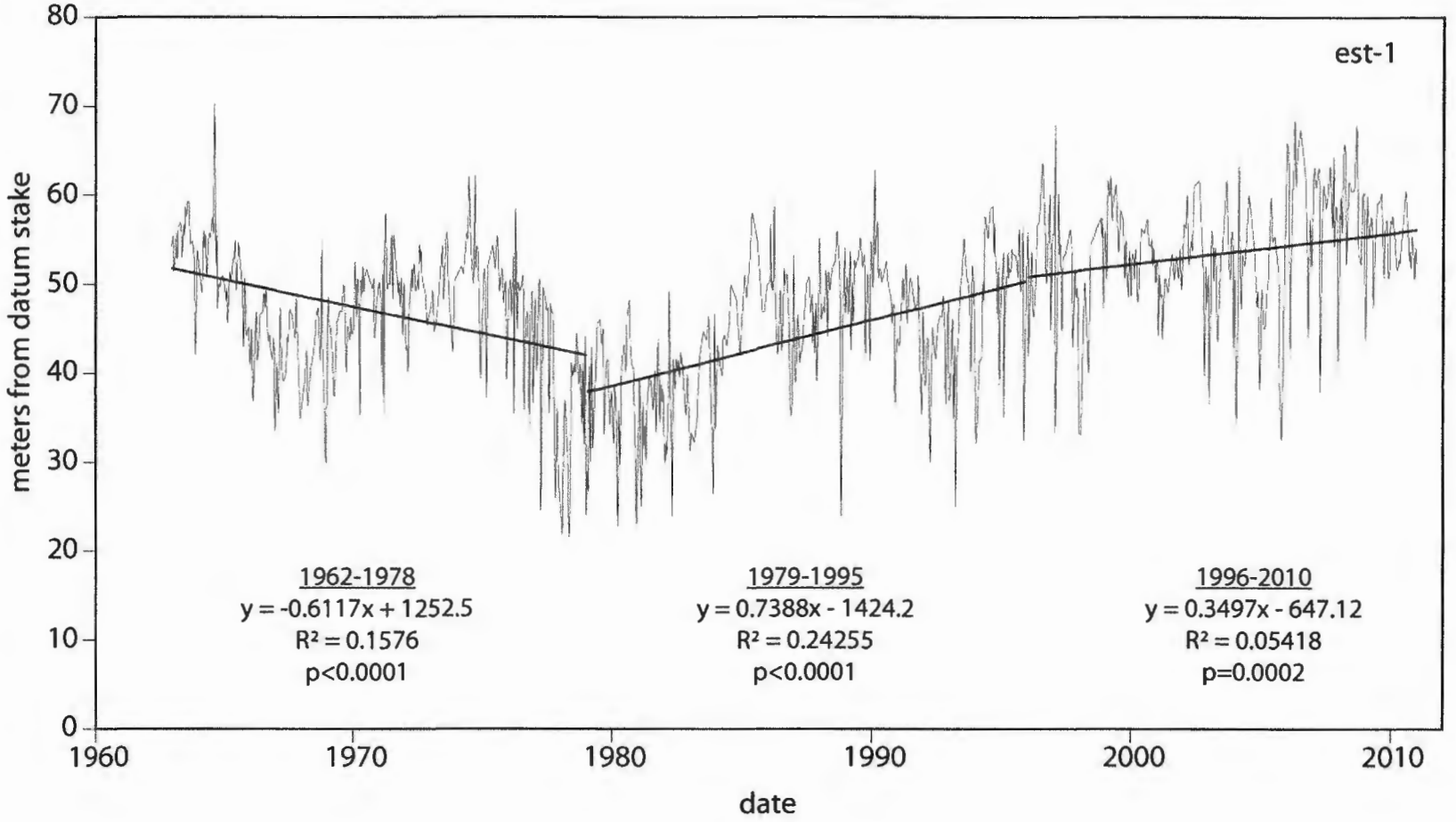

Figure 2.7 Rates of shoreline change at est-1 calculated by LRR at three different short-term intervals. Decadal scale oscillations in shoreline time-series strongly influence the rate of change statistic at these scales.

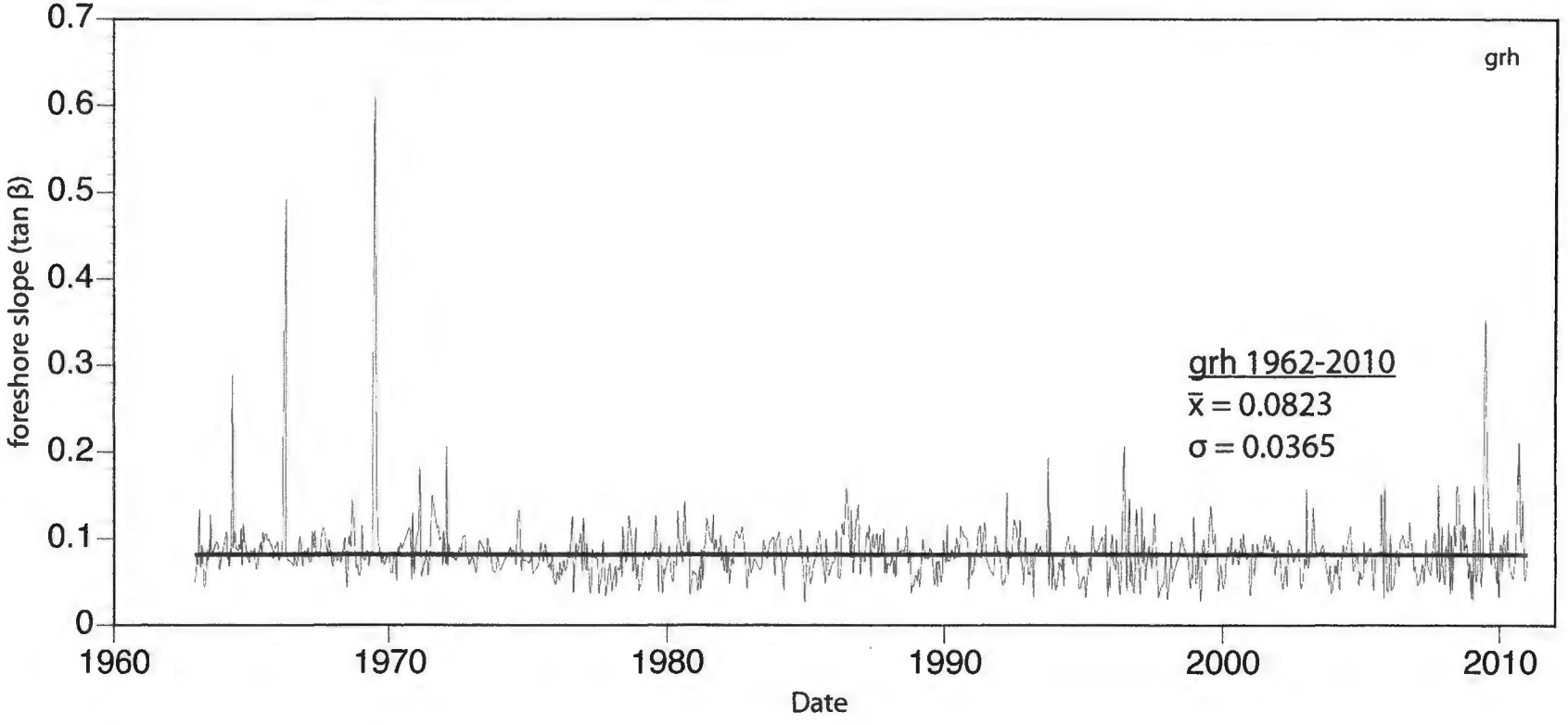

Figure 2.8 Time series of foreshore beach slope derived from survey measurements at grh. Slope is calculated from the best-fit line between mean low water and mean high water on the coastal profile.

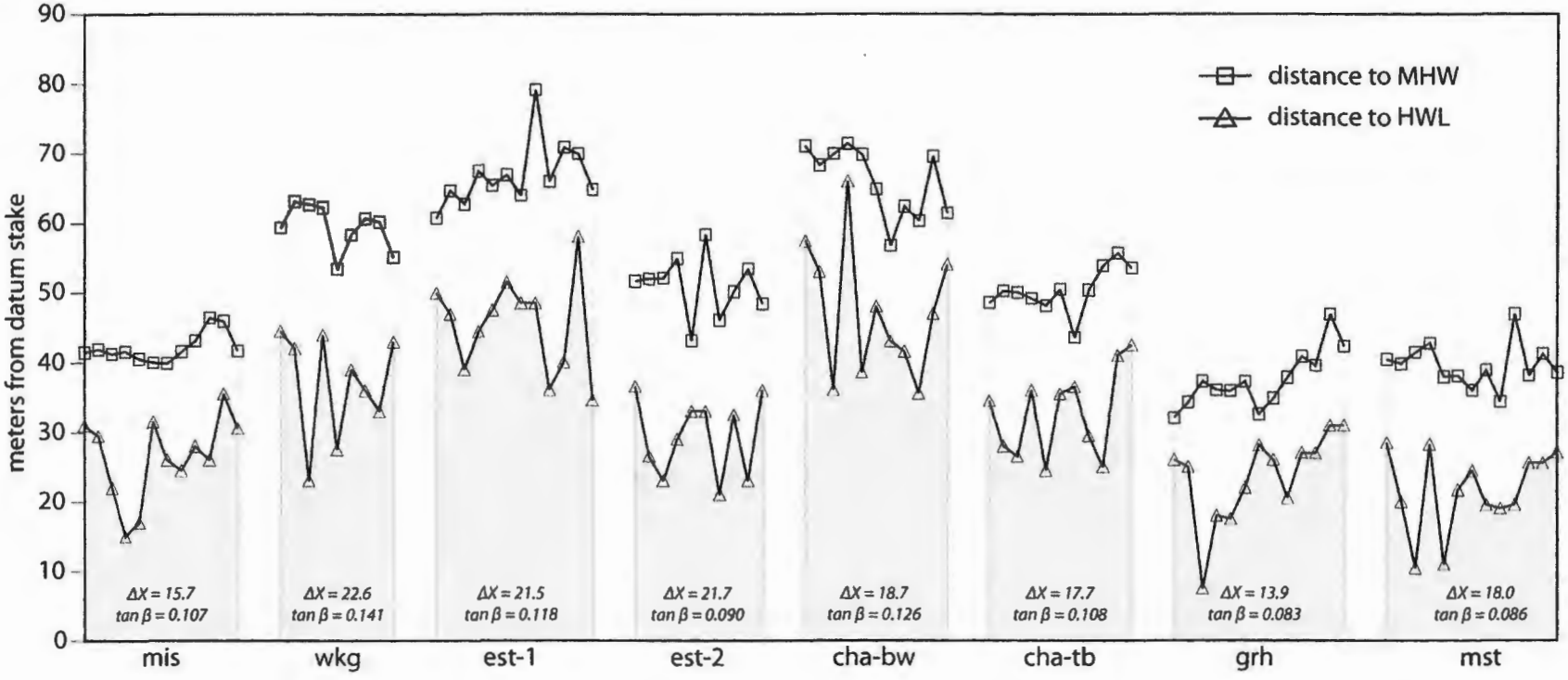

Figure 2.9 Offset between MHW and HWL shorelines from beach profile surveys between November 23, 2010 and August 25, 2011. ΔX = average offset; *tan* β = average foreshore beach slope. When averaged from all sites, the offset for south shore beaches is 18.5 meters.

CHAPTER 3: Toward improved shoreline monitoring for southern Rhode Island

by

Nathan Vinhateiro[1], John W. King[1], and Rebecca S. Robinson[1]

[1]Graduate School of Oceanography, University of Rhode Island, Narragansett, RI 02881

3.10 Abstract

Sea level rise during the 21st century is expected to have wide-ranging impacts on coastal ecosystems and coastal development. Accordingly, the Rhode Island Coastal Resources Management Council (CRMC) has adopted a policy that integrates climate change and sea level rise scenarios into its long-range planning and regulatory operations. Decisions based on this policy will require that managers have access to current information on global sea level projections, uncertainties, regional impacts, and planning tools that are available for risk assessment and mitigation. This review supports the needs of the CRMC by summarizing recent scientific findings on global sea level change and by providing an inventory of geospatial datasets that are available for sea level rise planning in Rhode Island. The state's lidar holdings provide an extremely accurate and cost-effective way to monitor coastal response to sea level rise, but their use in Rhode Island first requires an independent assessment to quantify absolute vertical accuracy of the datasets. Two-dimensional shoreline data that are more highly resolved in the temporal domain can be used in conjunction with lidar to quantify rapid changes in coastal morphology. We include in this review recommendations for a sustained monitoring program that utilizes high-resolution elevation models to establish a baseline, and assimilates multiple variables into the decision-making framework when forecasting coastal response to sea level rise.

3.20 Introduction

Rhode Island's barrier-lagoon system is a vital natural resource that provides critical habitat and protects the state's coastal communities against storm damage. The response of this system to changes in global climate is therefore of great interest to those who live along and manage this coastline. Sea level rise (SLR) is expected to be one of the largest and most sustained climate change impacts to coastal environments and populations during the next century (Nicholls et al., 2007). Rising sea levels have the potential to drown coastal wetlands, intensify erosion and flooding in low-lying areas, threaten coastal infrastructure and drinking water, and ultimately displace human populations. Regardless of efforts to stabilize atmospheric greenhouse gas concentrations, SLR is expected to continue for centuries due to the feedbacks associated with global climate processes (Meehl et al., 2007).

The rate of SLR has nearly tripled during the course of the 20th century (Church and White, 2011; Cazenave and Nerem, 2004) and a growing number of semi-empirical studies are predicting sea level changes up to and exceeding one meter by 2100 (Rahmstorf, 2010, and references therein). Whether the increased rate reflects decadal variability or acceleration in the longer-term trend is unclear, however, contributions due to loss of ice in Greenland and Antarctica suggest the latter (Rignot et al., 2011). As a result, local mitigation strategies that incorporate accelerated rates of SLR into coastal planning, design, and habitat restoration are increasing.

In Rhode Island, for example, the Coastal Resources Management Council (CRMC) recently approved some of the nation's first regulations that address SLR. Section 145 - *Climate Change and Sea Level Rise* - of the RI Coastal Resources

Management Program (RICRMP) directs the Council to proactively plan for and adapt to climate change through the integration of SLR scenarios into its operations and decision-making framework (CRMC, 2010). In addition, the Rhode Island Legislature has passed a law to amend the state building code (R.I.G.L. § 23-27.3-100.1.5.5), explicitly addressing sea level rise, and has authorized the CRMC to collaborate with the state building commissioner to adopt freeboard calculations for the purpose of flood plain management.

Both municipal and private interests share the need for accurate SLR assessments to enhance local mitigation actions. However, the ability to forecast coastal evolution in response to SLR is limited in large part by the accuracy of shoreline datasets and the frequency with which they are updated. This review supports coastal management decision-making by: (i) summarizing the current science related to sea level rise predictions and potential impacts to Rhode Island's coastal zone; (ii) reviewing the geospatial datasets that are available for hazard mitigation on the RI south shore; and (iii) providing technical considerations for improved SLR planning and risk assessment. Because future trends will require a baseline from which to compare observed changes, we include recommendations for enhanced coastal monitoring in southern Rhode Island.

3.30 Sea level rise by 2100

The Fourth Assessment Report (AR4) from the Intergovernmental Panel on Climate Change (IPCC) estimated that global sea level is likely to rise between 18 to 59 cm by 2100 (IPCC, 2007). Yet a major criticism of the AR4 projections was that they excluded any contribution to SLR from increased rates of ice sheet flow because

present understanding of the process was too limited for reliable model estimates. Since the publication of the AR4, global sea levels have been rising more rapidly than IPCC model predictions (Rahmstorf et al., 2007) and acceleration in ice flow has been observed around the edges of Greenland and Antarctica from both radar (Rignot et al., 2008) and gravity measurements (Velicogna, 2009). Using surface and bed topography, and measured ice velocities, Pfeffer et al. (2008) provided the first projections of sea level change to include ice flow dynamics on Greenland. Accounting for these processes, the authors estimated between 0.8 to 2 meters of eustatic sea level rise during the next century. Other studies (Rahmstorf, 2007; Horton et al., 2008 Vermeer and Rahmstorf, 2009; Jevrejeva et al., 2010) have utilized a semi-empirical relationship to correlate global sea level changes to global mean surface temperature (a good approximation for 20th century observations). When this relationship is applied to the range of 21st century warming scenarios presented in the AR4, sea levels between 75 and 190 cm above 1990 levels are predicted (Vermeer and Rahmstorf, 2009). The distinction between IPCC (2007) estimates, semi-empirical methods, and models that account for ice sheet dynamics can be seen in the range of global SLR predictions shown in Figure 3.1.

Future increase in sea level must be considered within the context of patterns in extreme weather or climate events, particularly the extent and frequency of severe coastal storms (IPCC, 2012). The consequences of SLR become acute during storm events, as waves gain access to increasingly higher coastal elevations over time. This phenomenon can be observed locally in tide gauge measurements from Newport, RI, which show a long-term increase in the absolute number of hours that the coast has

been subjected to significant storm surges during the past 80 years (Figure 3.2). While there remains little consensus regarding how tropical cyclone frequency may change as the climate warms, an increasing number of studies now predict that the incidence of rare, high-intensity hurricanes will increase during the 21st century (Emanuel et al. 2008; Knutson et al., 2010; Bender et al., 2010; IPCC, 2012), emphasizing the need for accurate studies that assess coastal vulnerability.

3.31 Impacts to the southern Rhode Island coastal environment

Both the magnitude and effects of future sea level change will not be globally uniform. Relative sea level (measured by a tide gauge with respect to the land upon which the gauge is situated) is the result of both absolute changes in water levels and movements of the continental crust. In Newport, RI for example, tide gauge measurements since 1930 show a long-term SLR rate of 2.58 ± 0.19 mm yr^{-1}, which is the cumulative result of these factors. The local impacts of future sea level change will therefore depend on the relative contribution of:

(i) eustatic sea level - global changes in the amount of water in the ocean (meltwater from continental ice); and specific volume (diabatic heating);

(ii) isostacy - changes in land surface elevations that are related to the lithospheric response to ice or sediment loading and land subsidence due to extraction of water or oil;

(iii) dynamic sea level – variability due to changing ocean currents and redistribution of mass in the ocean.

Projections of eustatic sea level rise are summarized above, but the latter two factors vary regionally and are less well understood. Isostacy has historically been estimated using the difference between relative sea level trends (determined from local tide gauge observations) and eustatic rates of SLR (e.g. USACE, 2011; Douglas, 1991), although with this approach, the isostatic contribution varies with the period of observation. Model projections of dynamic sea level changes indicate 15-50 cm of SLR (in addition to eustatic SLR) during the 21st century due to weaker rates of deep water formation in the U.S. northeast (Yin et al, 2009; Hu et al., 2009). Other studies examining melting of the West Antarctic Ice Sheet (e.g. Bamber et al. 2009) predict peak rates of SLR at approximately 40° N latitude due to changes in Earth's gravity and rotation as water mass is redistributed between land and ocean. Although estimates vary, dynamic and isostatic factors are crucial to consider as they have the potential to raise sea level projections by approximately 25-100% in the northeast U.S.

While coastal erosion in Rhode Island is not uniquely tied to sea level, it is nonetheless an important factor when evaluating future coastal vulnerability (Figure 3.2). Recent work has determined that 84% of the coastline between Westerly, RI and South Dartmouth, MA is already experiencing chronic erosion at an average long-term rate of -0.3 m yr^{-1} (Hapke et al., 2010). Geologic studies have also shown that the south shore barrier spits are highly sensitive to changing sea levels and overwash processes due to their narrow, low profile, and generally respond by migrating landward (Dillon, 1970). Yet the response of this and other barrier coastlines to very rapid rates of SLR (such as those projected for the next century) is not well understood. Break-up or in place drowning of barriers attributed to accelerated SLR

has been observed in recent decades in eastern Canada (Carter et al., 1987), the Mississippi Delta (Penland et al., 1985), and northern Alaska (Ruz et al., 1992).

Likewise, the inundation of tidal wetlands is an additional concern for coastal managers in Rhode Island. Like barrier islands, salt marshes have evolved during the late Holocene transgression and have kept pace with sea level through the process of sediment trapping, accretion, and peat development. For marshes to persist, surface elevations must increase at rates equal to or greater than projected SLR. When a natural marsh system cannot keep pace with rising waters or encounters a barrier to landward migration, it will eventually be converted to an intertidal mudflat or subtidal open water (Cahoon et al. 2009). Using the sea level affecting marshes model (SLAMM) along the RI south coast, Hancock (2009) estimated an overall 44% reduction in salt marsh habitat by 2100 with a sea level rise of 1 meter per century. The simulation assumed salt marshes were able to migrate to areas that are currently freshwater wetland or dry land, since almost all salt marsh habitat currently in existence would be inundated by 2075 under this scenario.

Global climate change is presenting many challenges that may ultimately require a change in the basic philosophy of coastal zone management that the larger planning and scientific community will need to address. As local management priorities shift from preservation to adaptation, a sincere effort will be required to learn from and to share with others facing similar challenges, both nationally and internationally. Given the uncertainties in predicting SLR, future land use and management strategies in Rhode Island will depend greatly on the extent, accuracy, and collection frequency of new coastal elevation data and other monitoring tools.

3.40 Geospatial data

While there are many factors that determine the degree to which coastal areas will be susceptible to SLR (including geomorphology, alongshore sediment gradients, tidal range, and storm frequency), ground elevations and inundation levels are generally considered the most critical datasets when assessing coastal vulnerability (Cahoon et al., 2009; Gesch, 2009). The organization, format, and resolution of coastal elevation data are fundamental to understanding their suitability to SLR mitigation. A single repository of metadata for southern Rhode Island will therefore be a useful reference for users of geospatial data statewide, and supports the CRMC's current initiatives by identifying tools and techniques that facilitate comprehensive and coordinated long-range planning for SLR. Included here is a brief discussion of the advantages and limitations of these datasets as applied to hazard assessments and SLR planning in southern Rhode Island.

3.41 Digital elevation models

Gridded digital elevation models (DEMs) are widely used for mapping and quantifying SLR impacts as they can rapidly assess areas at risk for coastal flooding with a simple cell-by-cell analysis of model elevations. SLR risk assessments (i.e. "topographic vulnerability" or "bathtub" models) commonly follow a straightforward mapping protocol that combines models with imagery and flood data to create inundation surfaces and identify resources at risk (e.g. Culver et al., 2010; NOAA, 2009). Additional geospatial data layers can provide estimates of impacts to land area, critical habitats, coastal infrastructure, and real estate (e.g. Rowley et al., 2007).

For coastal Rhode Island, elevation data are available from a variety of sources, including topographic maps, photogrammetry, light detection and ranging (lidar), and radar. Ground elevations from these sources have been compiled in digital format as multipoint data, raster grids, or triangulated irregular networks. A descriptive inventory of each of the digital terrain datasets for Rhode Island's south shore can be found in Vinhateiro (2008), and Table 3.1 lists the published accuracy and point density values for the various elevation models as well as the extent of coverage. For reference, Table 3.2 compares common reporting metrics for spatial data accuracy (Maune et al., 2007; Gesch et al., 2009).

The suitability of a given DEM for sea level rise assessment depends on important technical considerations, especially point density (Figure 3.3) and elevation uncertainties (Figure 3.4 –from Gesch, 2009). The USGS National Elevation Dataset (NED), for example, contains the most accurate seamless elevation data for the conterminous United States and is commonly used to estimate coastal inundation (Najjar et al., 2000; Titus and Richmond, 2001; Weiss et al, 2011). In Rhode Island, NED coverage consists of raster grids with 1 and 1/3 arc-second (~30 m and ~10 m) post spacing, which have been assessed for vertical accuracy with a root mean square error (RMSE) of ± 2.44 m (Gesch, 2007). By contrast, lidar-derived DEMs for coastal Rhode Island have post spacings of 2-meters or less, and reported RMSE values between 5.5 and 30 cm (Table 3.1). These differences are essential to understand when mapping inundation surfaces with respect to land (Figure 3.4). The minimum relative sea level rise increment that can accurately be mapped with a ± 2.44 m RMSE is

approximately 9.5 meters, whereas lidar elevations with 5.5 cm vertical accuracy can assess sea level changes as small as 22 cm (Table 3.2).

Comparing NED and lidar elevations in this way presumes that published accuracies of each dataset are valid. This assumes that QA/QC reporting metrics are representative of the entire dataset and are consistent between datasets (discussed further in the recommendations to follow). These uncertainties and caveats notwithstanding, the vertical accuracy and increased spatial detail of Rhode Island's lidar data far surpass the quality of DEMs derived from other techniques, such as photogrammetry, radar interferometry, and contour interpolation (Table 3.1). Lidar has also been found to be the most cost-effective means of mapping coastal flood zones within FEMA accuracy standards (National Research Council, 2007).

3.42 Digital vector shorelines

Photogrammetric- and map-derived shorelines are an additional source of data that have historically been used for assessing the impacts of SLR on regional scales (Galgano et al., 1998; Leatherman, 2003). Currently, 10 U.S. states, including Rhode Island, use vector shoreline data to determine coastal construction setbacks (NOAA, 2012a). The process involves digitizing visual shoreline indicators such as the high water line (HWL) (Pajak and Leatherman, 2002), foredune (Stafford and Langfelder, 1971), or the beach toe (Norcross et al., 2002) from a sequence of historic maps, charts, and aerial photography. Vector shorelines can also be extracted from elevation datasets such as lidar (Stockdon et al., 2002) or by using stereo photogrammetry to derive a datum-based shoreline from aerial photographs. When examined through

time, vector shorelines provide an indication of which sites are undergoing rates of change that are more rapid, and which sites are sensitive to changes in storm activity.

Uncertainty in the position of vector shorelines arises from: (i) mapping methods (accuracy of source maps and photos, georeferencing errors, shoreline digitizing); (ii) identification of the shoreline indicator (interpretation error); and (iii) short-term variability of true shoreline positions (Anders and Byrnes, 1991; Crowell et al., 1991; Moore, 2000). The third term requires site-specific data regarding the periodic behavior of the shoreline at a local scale (Vinhateiro et al., in prep). Based on the assumption that these errors are random and independent of one another, total uncertainty for each shoreline is typically reported as the square root of the sum of squares (Taylor, 1997).

The U.S. Geological Survey (USGS) has recently published a compilation of digitized high water line data, representing the most comprehensive collection of historical shoreline positions from New England and the Mid-Atlantic (Himmelstoss et al., 2010). For southern Rhode Island, the dataset includes shorelines from 16 years ranging from 1872 to 2006. In addition, the National Geodetic Survey (NGS) have compiled 6 years of datum-based shoreline data for the RI south shore as part of the national shoreline archive. For this review, all vector shoreline data (and reported uncertainty/accuracy) available for the Rhode Island south shore are listed in Table 3.3.

3.50 Toward improved shoreline monitoring for southern Rhode Island

As evidenced in this dissertation, the southern Rhode Island shoreline is sensitive to changes in the extent and frequency of coastal storms, and to continuous

processes like sea level rise, on both human and geologic time scales. Moreover, coastal landforms on the south shore are dynamic, and constantly evolve in response to sedimentary processes. Our findings emphasize the need for accurate baseline data and improved monitoring to model and quantify future climate change impacts in Rhode Island. We therefore recommend the following elements toward a program of enhanced and sustained shoreline monitoring in southern Rhode Island.

3.51 Geospatial and temporal analysis of lidar datasets

Monitoring shoreline response to coastal hazards in Rhode Island has historically been a two-dimensional endeavor – shoreline mapping supported by a limited number of cross-shore profile transects. Yet as shown in Figure 3.5, Rhode Island has several high-resolution elevation datasets that can also be used to define a robust coastal baseline; and when examined in sequence, can reveal information about the spatial extent of dynamic terrain features and the long-term response of coastal landforms to SLR and other climate forcings.

On a national scale, elevation datasets have been used for SLR assessments and other risk studies during the last two decades (e.g. Titus et al., 1991; Titus and Richmond, 2001; Najjar et al., 2000; Gornitz et al., 2002; Gesch, 2009), although the use of DEMs for coastal change analysis in Rhode Island has been far more limited (e.g. Thompson, 2008; Hancock, 2009; Vinhateiro, 2008). Yet with more than a decade since the first lidar surveys in Rhode Island, a time-series of high-resolution elevation data are now available for considerable portions of the south coast (Figure 3.5). In sequence, these data provide an opportunity to more precisely characterize evolution of the beach-dune system and identify areas vulnerable to coastal erosion.

They also may be used to quantify many outstanding research questions that require spatio-temporal analysis at high resolution, including estimates of the instantaneous beach/berm volume on the RI south shore, the primary direction and rate of longshore sediment transport, and the flux of sediment into the coastal lagoons.

A straightforward, GIS-based methodology for analysis of multi-temporal coastal lidar has been developed and refined over recent years (e.g. Overton et al., 2006; Mitasova et al., 2009). The workflow takes into account the diversity in point density, scanning patterns, and accuracies that have resulted from the rapid development of lidar technology during the past decade, in order to generate a consistent series of elevation surfaces that may be compared across the time domain. Map algebra, and other standard GIS tools can then be used to quantify changes in beach volume / topography and to objectively classify eroding areas. Mitasova et al., (2010) also describe new metrics for quantifying coastal change from multi-temporal DEMs, which can be communicated in functional and easy-to-understand maps. Minimum and maximum elevation surfaces (representing the envelope of change), rate-of-change, standard deviation, and other aspects of coastal terrain dynamics can be computed on a per-cell basis, across the time domain and allow for assessment of coastal hazard risk in a way that can help inform planning and management decisions.

3.52 High-accuracy geodetic control

The addition of coastal topography to shoreline monitoring efforts will represent a major advance for coastal management and climate change mitigation in Rhode Island. As noted above, however, the variability in published QA/QC reporting metrics for the state's elevation models calls for further review (Table 3.1). To

compare DEMs more objectively and evaluate their use for coastal change studies, a single assessment tool is needed to quantify absolute vertical accuracy for all elevation data in Rhode Island. This analysis would apply the same methodology and reference information to each DEM, and would provide the same reporting statistics for each dataset.

NOAA/NGS and the Rhode Island Department of Transportation (RIDOT) have already collected a dense network of elevation data that can be used as ground control for such an assessment. These include elevation benchmarks and other surveyed coordinates archived by the Rhode Island Geographic Information System (RIGIS) that can be used to independently compare the published accuracy of coastal elevation models and verify that interpolation or other geoprocessing steps have not introduced additional error. A subset of these data (n=467 points state-wide) has high-accuracy in both the horizontal and vertical dimension and can be easily used for an initial comparison with coastal DEMs (Figure 3.6). Systematic errors that arise from differences between monumented survey points and elevation models may also be used to apply corrections to the entire DEM, assuming errors are uniformly distributed (e.g. Mitasova et al., 2009).

A more comprehensive methodology for constructing a geodetic control network is in development for the coastal National Parks in the northeastern United States (Murdukhayeva et al., 2011). The approach uses stable geodetic benchmark locations as "backbone monuments," spaced at ~10-km intervals. These locations are surveyed using geodetic-grade GPS systems which provide elevation accuracies on the order of 1-2 cm. Backbone monuments also serve as base station locations for

additional elevation data collected using a real-time-kinematic (RTK) GPS rover. The 10-km spacing between backbone monuments is necessary to provide ample coverage between the GPS rover and base station. Collectively, backbone sites and additional RTK elevations make up a database of high-accuracy elevation control that can verify published metadata for coastal DEMs and independently quantify elevation uncertainties.

With little effort, a similar approach can be applied to the Rhode Island south shore using the inventory of existing monuments. Figure 3.6 also shows the location of NGS survey monuments in Washington County, RI with stability rating A (monuments least likely to experience vertical displacement over time) that would be excellent candidates for field reconnaissance. Once located and established, a subset of these points can be used as backbone monuments for a comprehensive local network.

For sea level assessment, an advantage of using high-stability points is that they also provide a time invariant baseline that can be periodically monitored for vertical displacement due to tectonism, isostasy and other forces driving subsidence in coastal Rhode Island (Shinkle and Dokka, 2004). The current practice of establishing isostatic land movement as the difference between the local sea level trend and eustatic mean sea level trend (USACE, 2011) may be overly simplistic. Implicit in this practice is the assumption that the eustatic component is constant globally, and that the difference is entirely due to land surface changes. At the Newport, RI tide gauge, this method results in a subsidence rate of 0.88 mm yr^{-1} ($\pm$ 0.6 mm yr^{-1}), which is roughly half the magnitude predicted by postglacial isostatic rebound models (Tushingham and Peltier, 1991; Douglas, 1991), and is inconsistent with observations from continuous

GPS measurements (Sella et al., 2007). Thus, with long-term monitoring, an added benefit of a local geodetic network is the ability to more accurately quantify relative SLR at coastal locations away from tide gauges.

3.53 High-resolution mapping with terrestrial-based lidar

High frequency beach profiling on the south shore has demonstrated that both volume and shoreline position fluctuate appreciably on seasonal/annual scales and in response to episodic storm events (Vinhateiro et al., in prep; Lacey and Peck, 1998). The ability to monitor these trends is important when trying to predict dynamic changes in beach volume that may result from future storm waves, or when trying to quantify the impacts of beach replenishment projects. While the extent and detail of coastal change that can be obtained from aerial lidar is a vast improvement over 2-D shoreline measures, lidar surveys in Rhode Island remain infrequent, and therefore cannot be used to quantify short-term coastal processes.

Terrestrial-based lidar offers a high-accuracy alternative to airborne lidar that has proven effective for repeat monitoring of rapidly changing natural environments (Collins and Kayen, 2006). This relatively new technology produces detailed elevation point clouds within the ~1 km range of the scanning instrument, and can be deployed rapidly to evaluate topographic changes related to storm activity (Brodie and McNinch, 2011) and beach nourishment (Pietro et al., 2008; Theuerkauf and Rodriguez, 2012). Surveys of larger areas (10s of kilometers) can be created by combing data from adjacent surveying stations, or by continuously scanning from a moving platform (e.g. Brodie and McNinch, 2011). Terrestrial lidar point cloud data

can eventually be manipulated to produce DEMs for integration with previous and future aerial lidar datasets.

The high density of lidar data allow for the detailed three-dimensional characterization of site topography that is necessary to support coastal process studies, although underlying sediment-transport processes cannot be entirely understood without concurrent nearshore measurements. Thus, an additional advantage of terrestrial-based lidar systems is the ability to simultaneously measure coastal topography and bathymetry from a survey vessel equipped with both interferometric sonar and a scanning lidar system (Flocks and Clark, 2011). The two systems can be integrated through an onboard differential Global Positioning System (GPS) receiver and motion sensor (POS MV), which provides the necessary positional measurements to compensate for the vessel's motion. Recent experiments in Biloxi, MS and along the Chandeleur Islands have demonstrated that the two systems can be successfully integrated and rapidly deployed to provide high-resolution imaging of sub-aerial and shallow-water environments simultaneously (Flocks and Clark, 2011).

High-resolution mapping of the Rhode Island shoreface in conjunction with terrestrial lidar data will provide a critical baseline for future research; particularly for quantifying sediment volumes lost to the transport system and for identifying potential borrow sites for beach nourishment. Sediment transported offshore during storm events remains poorly quantified on the RI south shore and when transported beyond the depth of closure (~12 m), sediment can become lost to the shoreline (Klinger, 1996; Goff et al., 2010). This process represents a critical gap in Rhode Island's sediment budget, which cross-shore profiles, shoreline maps, and sub-aerial lidar have

been unable to fully capture. The integration of nearshore bathymetry and lidar topography offers an opportunity to properly address this longstanding issue.

3.54 Tidal datums and relative sea level

The impacts of SLR are inherently tied to variability in tide levels. Thus, site-specific SLR assessments require that topography (measured relative to an orthometric datum) be adjusted in order to express surge or inundation levels relative to a local tidal reference. Because tidal elevations are not constant, this transformation can introduce additional uncertainty, particularly when applying a single tidal correction to a large area like the Rhode Island south shore. For example, at the Newport, RI tide gauge, mean higher high water (MHHW, observed over the 19-year National Tidal Datum Epoch) is 0.55 m above NAVD88 (the official orthometric vertical datum for the U.S.), while at Weekapaug, RI the difference is only 0.34 m (NOAA, 2012b). Additional differences at locations between the two stations are influenced by factors such as shoreline orientation and water depths. These differences are significant, considering that the range of variability (~30 cm) is roughly equal in magnitude to the upper bounds of projected SLR for the U.S. Northeast by 2050 (UCS, 2006).

VDatum is a (free) tool developed by NOAA/NGS, which can help compensate for these discrepancies by providing higher accuracy tidal elevations at specific coastal locations. The VDatum software package provides estimates of the elevation differences between tidal and orthometric datums using hydrodynamic models that are fitted to match observations at local tide gauges (Milbert, 2002; Parker, et al., 2003). The VDatum tool was initially developed to integrate bathymetry (measured relative to a sea level datum) and land topography datasets, by transforming

all coastal elevations to a common vertical reference. However, the sea surface transformation grids used by VDatum can also be used to simply calculate an alongshore residual - representing variations between local sea level and the NAVD88 geopotential surface at individual locations.

As applied to sea level monitoring, the alongshore variability in tidal datums has straightforward implications when assessing areas at risk for inundation – that is, areas with relatively elevated high water datums are more susceptible to SLR (Figure 3.7). Furthermore, alongshore variability in tidal range is important for any predictive modeling of shoreline change. Morton (2003) note that regions with low tidal range can experience higher potential for inundation and greater risk of dune breaching from storm surges than areas with a higher tidal range.

3.55 Integrating SLR and data uncertainties into coastal decision-making

Given the projections of global warming, predictive capabilities of shoreline change and other coastal response to SLR are needed for Rhode Island. A number of communities along the south shore have experienced chronic erosion during the last several decades and that number is likely to grow. Effective coastal zone management will therefore require accurate data, and a decision-making framework that takes into account historical observations of coastal change, as well as modern forcings, and future predictions, and communicates uncertainties as well as risk. The enhanced sea level monitoring and risk assessment activities recommended here should therefore be accompanied by a management tool that accurately characterizes coastal vulnerability to SLR and utilizes the best available data for decision-making.

As described in this review, efforts to quantify the impact of SLR on coastal erosion have traditionally used (i) inundation ("bathtub") models, which fail to address dynamic coastal processes and are limited by the accuracies in both the coastal elevation datasets and SLR projections, and (ii) the extrapolation of historic shoreline trends. Both of these approaches rely on broad assumptions in the coastal response to SLR that may be problematic for future coastal zone management. As an example, the coastal setback designations in the RICRMP are based on end-point rate erosion statistics using 1939 and 2004 shorelines (Boothroyd and Hehre, 2007). Setbacks that are based on historical erosion rates assume that: (i) vector shoreline positions represent an annual mean; (ii) historic rates of shoreline change are a good approximation for future rates under accelerated SLR; and (iii) uncertainties in the position of historic shorelines are fully accounted for in the calculation of the setback. An alternative approach to predicting coastal SLR impacts relies on coastal vulnerability indices (CVI), which integrate both geologic and physical parameters into a risk index to yield relative measures of a coastline's vulnerability to SLR (Thieler and Hammar-Klose, 1999; Pendleton et al., 2010). Using gridded shoreline data, a CVI can broadly characterize sections of coast with simple baseline criteria that are ranked based on both qualitative and quantitative measures (geomorphology, shoreline change rate, coastal slope, wave height, tidal range, and relative sea level rise). For each section of coastline, a CVI provides in a numerical score that, while not directly linked to a single physical forcing, does indicate where the physical changes from sea level rise are likely to be the greatest. For coastal management, the use of a CVI tool over traditional shoreline change metrics is attractive because they

incorporate multiple datasets that describe a coastline's natural susceptibility to change (geologic data) as well as its response to past changes in environmental conditions (historic shoreline observations). This provides a simple framework to rank and prioritize mitigation efforts or to consider adaptation measures within a study region.

Another innovative approach to modeling coastal vulnerability that has grown out of CVI research uses Bayesian networks (BN) to establish causal relationships between driving forces (SLR rates, hydrologic data), geologic factors (slope, geomorphology), and coastal response (erosion rates, volume change) (Gutierrez et al., 2011a). Like the CVI, a BN utilizes multiple datasets to more accurately characterize coastal change at a particular location; a primary difference is that a BN also allows the user to define ways in which these factors influence each other. For this reason, Bayesian networks are often represented with a schematic diagram to illustrate the interplay between forcing parameters, geologic boundary conditions, and predicted outcomes. The result of a BN is a series of probability density functions (probabilistic predictions) for shoreline change at a specific location based on the various inputs and defined relationships; the predictions being relevant to the same spatial scale as the input datasets. A BN method for SLR vulnerability was evaluated using historical data for the U.S. Atlantic coast and correctly reproduced 71% of shoreline change observations (Gutierrez et al., 2011b). In addition to the integration of multiple coastal variables, the BN approach calculates the probability of a specific outcome (shoreline change) and can therefore be used to communicate the level of likelihood or

uncertainty for a given scenario – again, an important consideration for coastal management decisions.

To evaluate the BN approach, Gutierrez et al. (2011b) used relatively coarse data resolved in 5 km blocks, but the method can easily be scaled to regions like the RI south shore where more high-resolution data are available. The approach is also flexible in that it can incorporate additional (local) variables that may improve the predictive capacity of the model. For example, Lentz and Hapke (2011) included storm wave data and descriptive beach metrics derived from lidar topography to hindcast post-storm beach change with accuracies ranging from 70-82% at Fire Island, NY. In Rhode Island, variables that describe coastal evolution (see section 3.51 above), and local modifications to the shoreline are additional parameters that could be included to evaluate BN model accuracy on a local scale using observed changes.

3.60 Conclusions

Current rates of sea level change will have wide-ranging effects on Rhode Island's coastal wetland and barrier spit ecosystems, and will threaten the state's coastal infrastructure and human populations. Furthermore, sea level trends are likely to intensify, providing a compelling case for focused research to monitor climate changes and impacts in Rhode Island. As coastal managers consider adaptation and mitigation strategies, they will require accurate and descriptive baseline data and projections of change from which to base decisions. This review supports science-based decision-making and strongly recommends a comprehensive program to monitor coastal evolution on the state's south shore barriers, including:

(i) Incorporation of lidar datasets into local shoreline change analysis.

(ii) Establishment of a high-accuracy geodetic control network for independent assessment of elevation data models and long term monitoring of coastal subsidence.

(iii) Terrestrial-based lidar to quantify short-term topographic changes and relate them to underlying sand transport mechanisms.

(iv) Inclusion of tidal variability in SLR assessment using VDatum transformation grids.

(v) Management tools that integrate multiple coastal datasets to predict coastal vulnerability to sea level rise.

3.70 References

Anders, F.J., and Byrnes, M.R., 1991. Accuracy of shoreline change rates as determined from maps and aerial photographs. *Shore and Beach*, 59, 17-26.

Bamber, J.L.; Riva, R.E.M.; Vermeersen, B.L.A., and Lebrocq, A.M., 2009. Reassessment of the potential sea-level rise from a collapse of the West Antarctic ice sheet. *Science*, 324(5929), 901-903.

Bender, M.A.; Knutson, T.R.; Tuleya, R.E.; Sirutis, J.J.; Vecchi, G.A.; Garner, S.T., and Held, I.M., 2010. Modeled impact of anthropogenic warming on the frequency of intense Atlantic hurricanes. *Science*, 327, 454-458.

Boothroyd, J.C., and Hehre, R.E. (Cartographer). (2007). *Shoreline change maps for the south shore of Rhode Island: Rhode Island Geological Survey Map Folio 2007-2, for RI Coastal Resources Management Council, 150 maps (scale: 1:2,000).*

Brodie, K.L., and McNinch, J.E., 2011. Beach change during a nor'easter: relationships to wave steepness and inner surf zone dissipation. *In: Proceedings, Coastal Sediments '11*. Miami, FL: pp. 1360-1374.

Cahoon, D.R.; Reed, D.J.; Kolker, A.S.; Brinson, M.M.; Stevenson, J.C.; Riggs, S.; Christian, R.; Reyes, E.; Voss, C., and Kunz, D., 2009. Coastal wetland sustainability. *In:* Titus, J.G.; Anderson, K.E.; Cahoon, D.R.; Gesch, D.B.; Gill, S.K.; Gutierrez, B.T.; Thieler, E.R., and Williams, S.J. (eds.), *Coastal Sensitivity to Sea-Level Rise: A Focus on the Mid-Atlantic Region. A report by the U.S. Climate Change Science Program and the Subcommittee on Global Change Research.* Washington DC: U.S. Environmental Protection Agency, pp. 57-72.

Carter, R.W.G.; Orford, J.D.; Forbes, D.L., and Taylor, R.B., 1987. Gravel barriers, headland and lagoons: an evolutionary model. *In: Proceedings, Coastal Sediments '87*. New Orleans, LA: American Society of Civil Engineering Waterways Division, pp. 1776-1792.

Cazenave, A., and Nerem, R.S., 2004. Present-day sea level change: observations and causes. *Reviews of Geophysics*, 42, RG3001.

Church, J.A., and White, N.J., 2006. A 20th century acceleration in global sea-level rise. *Geophysical Research Letters*, 33, L01602-L01604.

Collins, B.D., and Kayen, R., 2006. Land-based lidar mapping-a new surveying technique to shed light on rapid topographic change. Menlo Park, CA: US Geological Survey *(USGS Fact Sheet 2006-3111)*. 4p.

CRMC (Coastal Resources Management Council). 2010. The State of Rhode Island

Coastal Resources Management Program CRMC, 222pp.

Crowell, M.; Leatherman, S.P., and Buckley, M.K., 1991. Historical shoreline change: error analysis and mapping accuracy. *Journal of Coastal Research*, 7(3), 839-852.

Culver, M.E.; Schubel, J.R.; Davidson, M.A.; Haines, J., and Texeira, K.C., 2010. Proceedings from the Sea Level Rise and Inundation Community Workshop. Lansdowne, MD: National Oceanic and Atmospheric Administration and U.S. Geological Survey.

Dillon, W.P., 1970. Submergence effects on a Rhode Island barrier and lagoon and inferences on migration of barriers. *Journal of Geology*, 78, 94-106.

Dolan, R.; Fenster, M.S., and Holme, S.J., 1991. Temporal analysis of shoreline recession and accretion. *Journal of Coastal Research*, 7(3), 723-744.

Douglas, B.C., 1991. Global sea level rise. *Journal of Geophysical Research*, 96(C4), 6981-6992.

Emanuel, K.A.; Sundararajan, R., and Williams, J., 2008. Hurricanes and global warming: Results from downscaling IPCC AR4 simulations. *Bulletin of the American Meteorological Society*, 89, 347-367.

Flocks, J., and Clark, A., 2011. USGS scientists develop system for simultaneous measurements of topography and bathymetry in coastal environments. *Sound Waves*, Sept/Oct. 2011.

Galgano, F.A.; Douglas, B.C., and Leatherman, S.P., 1998. Trends and variability of shoreline position. *Journal of Coastal Research*, SI 26, 282-291.

Gesch, D.B., 2007. Chapter 4 - The National Elevation Dataset. *In:* Maune, D. (ed.), *Digital elevation model technologies and applications: The DEM users manual*. Bethesda, MD: American Society for Photogrammetry and Remote Sensing, pp. 99-118.

Gesch, D.B., 2009. Analysis of lidar elevation data for improved identification and delineation of lands vulnerable to sea-level rise. *Journal of Coastal Research*, SI 53, 49-58.

Gesch, D.B.; Gutierrez, B.T., and Gill, S.K., 2009. Coastal elevations. *In:* Titus, J.G.; Anderson, K.E.; Cahoon, D.R.; Gesch, D.B.; Gill, S.K.; Gutierrez, B.T.; Thieler, E.R., and Williams, S.J. (eds.), *Coastal Sensitivity to Sea-Level Rise: A Focus on the Mid-Atlantic Region. A report by the U.S. Climate Change Science Program and the Subcommittee on Global Change Research.* Washington, DC: U.S. Environmental Protection Agency, pp. 25-42.

Goff, J.A.; Allison, M.A., and Gulick, S.P.S., 2010. Offshore transport of sediment

during cyclonic storms: Hurricane Ike (2008), Texas Gulf Coast, USA. *Geology*, 38, 351-354.

Gornitz, V.; Couch, S., and Hartig, E.K., 2002. Impacts of sea level rise in the New York City metropolitan area. *Global and Planetary Change*, 32(1), 61-88.

Grinsted, A.; Moore, J., and Jevrejeva, S., 2009. Reconstructing sea level from paleo and projected temperatures 200 to 2100 AD. *Climate Dynamics*, 34(4), 461-472.

Gutierrez, B.T.; Plant, N.G., and Thieler, E.R., 2011a. A Bayesian network to predict vulnerability to sea-level rise: data report. Reston, VA: U.S. Geological Survey *(USGS Data Series 601)*. 15p.

Gutierrez, B.T.; Plant, N.G., and Thieler, E.R., 2011b. A Bayesian network to predict coastal vulnerability to sea level rise. *Journal of Geophysical Research*, 116, F02009.

Hancock, R., 2009. Using GIS and simulation modeling to assess the impact of sea level rise on coastal salt marshes. Kingston, RI: University of Rhode Island *(Masters of Environmental Science and Management Major Paper)*. 47p.

Hapke, C.J.; Himmelstoss, E.A.; Kratzmann, M.G.; List, J.H., and Thieler, E.R., 2010. National assessment of shoreline change: Historical shoreline change along the New England and Mid-Atlantic coasts. US Geological Survey *(USGS Open File Report No. 2010-1118)*. 57p.

Himmelstoss, E.A.; Kratzmann, M.; Hapke, C.J.; Thieler, E.R., and List, J., 2010. The national assessment of shoreline change - A GIS compilation of vector shorelines and associated shoreline change data for the New England and Mid-Atlantic coasts. USGS *(U.S. Geological Survey Open-File Report No. 2010-1119)*.

Horton, R.; Herweijer, C.; Rosenzweig, C.; Liu, J.; Gornitz, V., and Ruane, A., 2008. Sea level rise projections for current generation CGCMs based on the semi-empirical method. *Geophysical Research Letters*, 35, L02715.

Hu, A.; Meehl, G.A.; Han, W., and Yin, J., 2009. Transient response of the MOC and climate to potential melting of the Greenland ice sheet in the 21st century. *Geophysical Research Letters*, 36(L10707).

IPCC (Intergovernmental Panel on Climate Change), 2007. Summary for Policymakers. *In:* Solomon, S.; Qin, D.; Manning, M.; Chen, Z.; Marquis, M.; Averyt, K.B.; Tignor, M., and Miller, H.L. (eds.), *Climate Change 2007: The Physical Science Basis. Contribution of Working Group I to the Fourth Assessment Report of the Intergovernmental Panel on Climate Change*. Geneva, Switzerland: UNEP, pp. 1-18.

IPCC (Intergovernmental Panel on Climate Change), 2012. Summary for Policymakers. *In:* Field, C.B.; Barros, V.; Stocker, T.F.; Qin, D.; Dokken, D.J.; Ebi, K.L.; Mastrandrea, M.D.; Mach, K.J.; Plattner, G.-K.; Allen, S.K.; Tignor, M., and Midgley, P.M. (eds.), *Managing the Risks of Extreme Events and Disasters to Advance Climate Change Adaptation* Cambridge, UK: Cambridge University Press,, pp. 1-19.

Jevrejeva, S.; Moore, J., and Grinsted, A., 2010. How will sea level respond to changes in natural and anthropogenic forcings by 2100? *Geophysical Research Letters*, 37, L07703.

Klinger, J.P. (1996). *Sedimentary environments and processes on the Charlestown-Green Hill barrier/headland shoreface and Misquamicut barrier/headland shoreface, south coast of Rhode Island.* M.S. thesis, University of Rhode Island, Kingston, RI.

Knutson, T.R.; McBride, J.L.; Chan, J.; Emanuel, K.; Holland, G.; Landsea, C.; Held, I.; Kossin, J.P.; Srivastava, A.K., and Sugi, M., 2010. Tropical cyclones and climate change. *Nature Geosciences*, 3, 157-163.

Lacey, E.M., and Peck, J.A., 1998. Long-term beach profile variations along the south shore of Rhode Island, USA. *Journal of Coastal Research*, 14(4), 1255-1264.

Leatherman, S., 2003. Shoreline change mapping and management along the US east coast. *Journal of Coastal Research*, SI 38, 5-13.

Lentz, E.E., and Hapke, C.J., 2011. The development of a probabilistic approach to forecast coastal change. *In: Proceedings, Coastal Sediments '11*. Miami, FL: pp. 1853-1866.

Maune, D.F.; Maitra, J.B., and McKay, E.J., 2007. Accuracy standards & guidelines. *In:* Maune, D. (ed.), *Digital Elevation Model Technologies and Applications: The DEM Users Manual*. Bethesda, MD: American Society for Photogrammetry and Remote Sensing, pp. 65-97.

Meehl, G.A.; Stocker, T.F.; Collins, W.D.; Friedlingstein, P.; Gaye, A.T.; Gregory, J.M.; Kitoh, A.; Knutti, R.; Murphy, J.M.; Noda, A.; Raper, S.C.B.; Watterson, I.G.; Weaver, A.J., and Zhao, Z.-C., 2007. Global climate projections. *In:* Solomon, S.; Qin, D.; Manning, M.; Chen, Z.; Marquis, M.; Averyt, K.B.; Tignor, M., and Miller, H.L. (eds.), *Climate Change 2007: The Physical Science Basis. Contribution of Working Group I to the Fourth Assessment Report of the Intergovernmental Panel on Climate Change*. Cambridge, United Kingdom and New York, NY, USA: Cambridge University Press.

Milbert, D., 2002. VDatum transformation tool (new version 1.05). *The GeoCommunity Spatial News*, http://spatialnews.geocomm.com/features/vdatum/.

Mitasova, H.; Overton, M.; Recalde, J.; Bernstein, D.J., and Freeman, C.W., 2009. Raster-based analysis of coastal terrain dynamics from multitemporal lidar data. *Journal of Coastal Research*, 25(2), 507-514.

Mitasova, H.; Hardin, E.; Overton, M., and Kurum, M., 2010. Geospatial analysis of vulnerable beach-foredune systems from decadal time series of lidar data. *Journal of Coastal Conservation*, 14, 161-172.

Moore, L.J., 2000. Shoreline mapping techniques. *Journal of Coastal Research*, 16(1), 111-124.

Murdukhayeva, A.; Bradley, M.; Shaw, N.; Labash, C.; Grybas, H.; Davis, T.; August, P.; Smith, T., and Duhaime, R., 2011. Using high accuracy geodesy to assess risk from climate change in coastal national parks. *The Proceedings of the George Wright Society*, U.S. National Park Service.

Najjar, R.G.; Walker, H.A.; Anderson, P.J.; Barron, E.J.; Bord, R.; Gibson, J.; Kennedy, V.S.; Knight, C.G.; Megonigal, P.; O'Connor, R.; Polsky, C.D.; Psuty, N.P.; Richards, B.; Sorenson, L.G.; Steele, E., and Swanson, R.S., 2000. The potential impacts of climate change on the Mid-Atlantic coastal region. *Climate Research*, 14, 219-233.

National Research Council, 2007. *Elevation Data for Floodplain Mapping*. Washington, DC: The National Academies Press, 168p.

Nicholls, R.J.; Wong, P.P.; Burkett, V.R.; Codignotto, J.O.; Hay, J.E.; Mclean, R.F.; Ragoonaden, S., and Woodroffe, C.D., 2007. Coastal systems and low-lying areas. *In:* Parry, M.L.; Canziani, O.F.; Palutikof, J.P.; van der Linden, P.J., and Hanson, C.E. (eds.), *Climate Change 2007: Impacts, Adaptation and Vulnerability. Contribution of Working Group II to the Fourth Assessment Report of the Intergovernmental Panel on Climate Change,*. Cambridge, UK: Cambridge University Press, pp. 315-356.

NOAA (National Oceanic and Atmospheric Administration), 2009. Coastal inundation mapping guidebook. Charleston, SC: NOAA Coastal Services Center.

NOAA (National Oceanic and Atmospheric Administration), 2010. Mapping inundation uncertainty. Charleston, SC: NOAA Coastal Services Center. 10p.

NOAA (National Oceanic and Atmospheric Administration), 2012a. Protecting the public interest through the National Coastal Zone Management Program: how coastal states use no-build areas along ocean and great lake shorefronts - Draft Report. Silver Spring, MD: NOAA Office of Ocean and Coastal Resource Management. 59p.

NOAA (National Oceanic and Atmospheric Administration), 2012b. Rhode Island tide gauges. http://tidesandcurrents.noaa.gov/station_retrieve.shtml?type=Datums&state=R

hode+Island&id1=845: accessed on February 28, 2012.

Norcross, Z.M.; Fletcher, C.H., and Merrifield, M., 2002. Annual and interannual changes on a reef-fringed pocket beach: Kailua Bay, Hawaii. *Marine Geology*, 190(3-4), 553-580.

Overton, M.; Mitasova, H.; Recalde, J., and Vanderbeke, N., 2006. Morphological evolution of a shoreline on decadal time scale. *In:* McKee Smith, J. (ed.), *Proceedings of the 30th International Conference on Coastal Engineering*. San Diego: pp. 3851-3862.

Pajack, M.J., and Leatherman, S.P., 2002. The high water line as shoreline indicator. *Journal of Coastal Research*, 18(2), 329-337.

Parker, B.; Hess, K.; Milbert, D., and Gill, S., 2003. A national vertical datum transformation tool. *Sea Technology*, 44(9), 1-15.

Pendleton, E.A.; Thieler, E.R., and Williams, S.J., 2010. Importance of coastal change variables in determining vulnerability to sea- and lake-level changes. *Journal of Coastal Research*, 26(1), 176-183.

Penland, S.; Suter, J.R., and Boyd, R., 1985. Barrier island arcs along abandoned Mississippi River deltas. *Marine Geology*, 63, 197-234.

Pfeffer, W.; Harper, J., and O'Neel, S., 2008. Kinematic constraints on glacier contributions to 21st-century sea-level rise. *Science*, 321, 1340-1343.

Pietro, L.S.; O'Neal, M.A., and Puleo, J.A., 2008. Developing terrestrial-lidar-based digital elevation models for monitoring beach nourishment performance. *Journal of Coastal Research*, 24(6), 1555 - 1564.

Rahmstorf, S., 2007. A semi-empirical approach to projecting future sea-level rise. *Science*, 315, 368-370.

Rahmstorf, S.; Cazenave, A.; Church, J.A.; Hansen, J.E.; Keeling, R.F.; Parker, D.E., and Somerville, R.C.J., 2007. Recent climate observations compared to projections. *Science*, 316(5825), 709.

Rahmstorf, S., 2010. A new view on sea level rise. *Nature Reports Climate Change*, 4, 44-45.

Rignot, E.; Bamber, J.L.; Van Den Broeke, M.R.; Davis, C.; Li, Y.; Van De Berg, W.J., and Van Meijgaard, E., 2008. Recent Antarctic ice mass loss from radar interferometry and regional climate modelling. *Nature Geosciences*, 1, 106-110.

Rignot, E.; Velicogna, I.; Van Den Broeke, M.R.; Monaghan, A., and Lenaerts, J., 2011. Acceleration of the contribution of the Greenland and Antarctic ice

sheets to sea level rise. *Geophysical Research Letters*, 38, L05503.

Rowley, R.J.; Kostelnick, J.C.; Braaten, D.; Li, X., and Meisel, J., 2007. Risk of rising sea level to population and land area. *Eos Transactions, American Geophysical Union*, 88(9), 105.

Ruz, A.H.; Hequette, A., and Hill, P.R., 1992. A model of coastal evolution in a transgressed thermokarst topography, Canadian Beaufort Sea. *Marine Geology*, 106, 251-278.

Sella, G.F.; Stein, S.; Dixon, T.H.; Craymer, M.; James, T.S.; Mazzotti, S., and Dokka, R.K., 2007. Observation of glacial isostatic adjustment in "stable" North America with GPS. *Geophysical Research Letters*, 34, L02306.

Shinkle, K.D., and Dokka, R.K., 2004. Rates of vertical displacement at benchmarks in the lower Mississippi Valley and the Northern Gulf Coast. NOAA *(NOAA Technical Report NOS/NGS 50)*. 135p.

Stafford, D.B., and Langfelder, J., 1971. Air photo survey of coastal erosion. *Photogrammetric Engineering*, 37(6), 565-575.

Stockdon, H.F.; Sallenger, A.H., Jr.; List, J.H., and Holman, R.A., 2002. Estimation of shoreline position and change using airborne topographic lidar data. *Journal of Coastal Research*, 18(3), 502-513.

Taylor, J.R., 1997. *An introduction to error analysis: The study of uncertainties in physical measurement*. Sausalito, CA: University Science Books, 327p.

Theuerkauf, E.J., and Rodriguez, A.B., 2012. Impacts of transect location and variations in along-beach morphology on measuring volume change. *Journal of Coastal Research*, In Press, doi: http://dx.doi.org/10.2112/JCOASTRES-D-2111-00112.00111.

Thompson, M., 2008. Global climate change induced inundation modeling of South Kingstown, RI. Kingston, RI: University of Rhode Island *(Masters of Environmental Science and Management Major Paper)*.

Titus, J.G., and Richman, C., 2001. Maps of lands vulnerable to sea level rise: modeled elevations along the US Atlantic and Gulf coasts. *Climate Research*, 18(3), 205-228.

Titus, J.G.; Park, R.A.; Leatherman, S.P.; Weggel, J.R.; Greene, M.S.; Mausel, P.W.; Brown, S.; Gaunt, G.; Threhan, M., and Yohe, G., 1991. Greenhouse effect and sea level rise: the cost of holding back the sea. *Coastal Management*, 19(2), 171-204.

Thieler, E.R., and Hammar-Klose, E., 1999. National assessment of coastal vulnerability to future sea-level rise: preliminary results for the U.S. Atlantic

Coast. US Geological Survey *(USGS Open File Report 99-593)*

Tushingham, A.M., and Peltier, W.R., 1991. ICE 3-G: A new global model of late Pleistocene deglaciation based on geophysical predictions of post glacial relative sea level change. *Journal of Geophysical Research*, 96, 4497-4523.

UCS (Union of Concerned Scientists), 2006. Climate Change in the U.S. Northeast: A report of the Northeast climate impacts assessment. Cambridge, MA: UCS Publications. 35p.

USACE (U.S. Army Corps of Engineers), 2011. Sea-level change considerations for civil works programs. Washington, D.C.: Department of the Army *(Report EC 1165-2-212)*. 32p.

Velicogna, I., 2009. Increasing rates of ice mass loss from the Greenland and Antarctic ice sheets revealed by GRACE. *Geophysical Research Letters*, 36, L19503.

Vermeer, M., and Rahmstorf, S., 2009. Global sea level linked to global temperature. *Proceedings of the National Academy of Sciences*, 106(51), 21527-21532.

Vinhateiro, N., 2008. Sea level rise and the current status of digital terrain data for the south shore of Rhode Island: A white paper in integrated coastal science. Wakefield, RI: Rhode Island Coastal Resources Management Council. 45p.

Weiss, J.L.; Overpeck, J.T., and Strauss, B., 2011. Implications of recent sea level rise science for low-elevation areas in coastal cities of the conterminous U.S.A. *Climatic Change*, 105, 635-645.

Yin, J.; Schlesinger, M.E., and Stouffer, R.J., 2009. Model projections of rapid sea-level rise on the northeast coast of the United States. *Nature Geoscience*, 2(4), 262-266.

Zhang, K.; Douglas, B.C., and Leatherman, S.P., 2001. Beach erosion potential for severe nor'easters. *Journal of Coastal Research*, 17(2), 309-321.

Table 3.1 Characteristics of southern Rhode Island elevation models based on the available metadata.

Elevation model	Survey Date	Data Source (Contractor)	Description	Extent	Horizontal Accuracy	Vertical Accuracy	Average Point Ground Spacing
National Elevation Dataset (NED)	Derived from existing cartographic sources. Published 1999; Updated bi-weekly	USGS	Mosaic of 50,000 individual USGS DEM data files. DEMs were produced in 7.5- by 7.5-minute blocks for the conterminous US, either from digitized cartographic map contour overlays or from scanned NAPP photographs.	Nation-wide	Not tested (assumed equal to grid spacing)	2.44 m RMSE	30 m (1 arc second) 10 m (1/3 arc second)
Shuttle Radar Topography Mission (SRTM)	February 11-22, 2000	NASA, DOD, and USGS	A cooperative project between NASA, the NGA and German and Italian space agencies to generate the most complete high-resolution digital topographic database of the Earth. Data are first return mass points generated from radar interferometry.	60 degrees north latitude and 54 degrees south latitude (approximately 80% of all the land on the Earth)	12.6 m (at 90% confidence)	9 m RMSE	30 m (1 arc second) 90 m (3 arc second)
1:5000 scale Digital Terrain Model of Rhode Island (5KDTM)	April 27-29, 1997	RIDOT	Mass points and breaklines compiled in 2001 RIDOT digital orthophotos (2' pixels); developed by photogrammetry at a sufficient density to support generation of 3 meter contours.	State-wide	3-5 meters	3 meters	12 m
Airborne LIDAR Assessment of Coastal Erosion (ALACE)	September 26, 2000	NOAA/NASA/USGS (NASA)	A collaborative mapping project between NOAA, NASA, and USGS to collect remotely sensed, baseline coastal topographic data for the conterminous U.S.	Shoreline swath from the low water line to the landward base of the dune	80 cm RMSE	15cm RMSE (for bare ground)	2 meters
South Kingstown and Charlestown, RI Digital Terrain Models (Photogrammetry)	April 9, 2006	Town of South Kingstown, RI; Town of Charlestown, RI (EarthData International)	6" GSD elevations, photogrammetrically derived (rectified) from orthophotos for the towns of Charlestown and South Kingstown, RI.	Entire towns of South Kingstown and Charlestown, RI.	30 cm RMSE	20 cm RMSE	31 feet
FEMA Rhode Island Coastline LIDAR Survey	December 16-18, 2006	FEMA (Dewberry)	Remotely sensed, high-resolution elevation points collected by airborne platform for the purpose of coastal flood mapping.	FEMA flood zones in New Shoreham, North Kingstown, Westerly, Charlestown.	91 cm RMSE	5.5 cm RMSE	1.25 m
LIDAR Terrain Data from Rhode Island Formerly Used Defense Sites (FUDS)	April 6-8, 2007	USACE (Sky Res.)	LIDAR mass points and hydro-enforced breaklines integrated to create accurate, high-resolution, bare-earth DEM's and two foot contours for USACE FUDS.	195 square kilometers from six USACE study areas in Rhode Island.	33 cm RMSE	15 cm RMSE	0.35 m
USACE New England Topo/Bathy Lidar	Topography: 11/11/2005-12/02/2005 Bathymetry: 05/27/2007-06/01/2007	USACE (Fugro)	Topo-bathy lidar collected using Compact Hydrographic Airborne Rapid Total Survey (CHARTS) system.	~750 meters inland and up to 1500 meters over the water (depending on water depth and clarity).	Compiled to meet 3 m horizontal accuracy at 2-sigma accuracy specification	30 cm RMSE	2 meters
LIDAR for the Northeast	10/24/2010-12/09/2010	USGS (Photo Science)	~8200 square miles of New England and New York coastal areas	State-wide	Accuracy assessment underway	Preliminary assessment of open terrain - 15 cm RMSE	<1 meter

Table 3.2 Common reporting metrics for spatial data accuracy. National Map Accuracy Standards (NMAS) are compared with National Standard for Spatial Data Accuracy (NSSDA) reporting values and sea level rise scenarios supported by the elevations with these accuracies (after Maune et al., 2007; Gesch et al., 2009).

NMAS contour interval in ft (m)	*NMAS 90% confidence level (m)*	*NSSDA RMSE (m)*	*NSSDA 95% confidence level (m)*	*Minimum SLR increment for inundation modeling (m)*
1 (0.30)	0.15	0.09	0.18	0.36
2 (0.61)	0.30	0.19	0.36	0.73
5 (1.52)	0.76	0.46	0.91	1.82
10 (3.05)	1.52	0.93	1.82	3.64
20 (6.10)	3.05	1.85	3.63	7.62

Table 3.3 Vector shoreline data and uncertainties for southern Rhode Island based on available metadata. *accuracy assessed by Crowell et al (1991) for shorelines between 1882-1954 and reported as RMSE. NGS shorelines in 2003 and 2006 compiled to meet 1.8 meters horizontal accuracy at 95% confidence.

USGS National Assessment of Shoreline Change compilation

Date	*Shoreline type*	*Shoreline source*	*Uncertainty (m)*	*Extent*
1872	HWL	T-Sheet	10.8	Pt Judith - Charlestown Breachway
1873	HWL	T-Sheet	10.8	Charlestown Breachway - Misquamicut barrier
1883	HWL	T-Sheet	10.8	Napatree Point - Maschaug barrier
1886	HWL	T-Sheet	10.8	Maschaug barrier - Winapaug inlet
1939	HWL	Air Photo	10.8	Entire south shore
1948	HWL	T-Sheet	10.8	Napatree Point - Maschaug barrier; Pt. Judith - Matunuck headland
1951	HWL	Air Photo	10.8	Pt. Judith to Misquamicut headland; Napatree barrier
1952	HWL	Air Photo	10.8	Napatree Point - Misquamicut barrier
1954	HWL	T-Sheet	10.8	Matunuck headland - Watch Hill
1963	HWL	Air Photo	5.1	discrete segments of entire south shore
1975	HWL	Air Photo	3.2	Entire south shore
1985	HWL	Air Photo	3.2	Entire south shore
1992	HWL	Air Photo	3.2	Napatree Point - Misquamicut headland
2000	MHW	Lidar	2.3	Entire south shore
2004	HWL	Air Photo	3.2	Entire south shore
2006	HWL	Air Photo	3.2	Harbor of Refuge - Quonochontaug barrier

NGS digital shoreline holdings

Date	*Shoreline type*	*Shoreline source*	*Accuracy (m)**	*Extent*
1882	MHW	T-Sheet	8.4	Napatree Point - Weekapaug headland
1913	MHW	T-Sheet	8.4	Pt Judith -Matunuck headland
1948	MHW	Air Photo	7.7	Pt Judith -Matunuck headland
1948	MHW	Air Photo	7.7	Napatree Point - Misquamicut headland
1948	MHW	Air Photo	7.7	Pt Judith -Matunuck headland
1954	MHW	Air Photo	7.7	Pt Judith -Weekapaug headland
1954	MHW	Air Photo	7.7	Napatree Point - Weekapaug headland
2003	MHW	Digital photo	1.0	Pt Judith - Harbor of Refuge
2006	MHW	Digital photo	1.8	Napatree Point - Harbor of Refuge

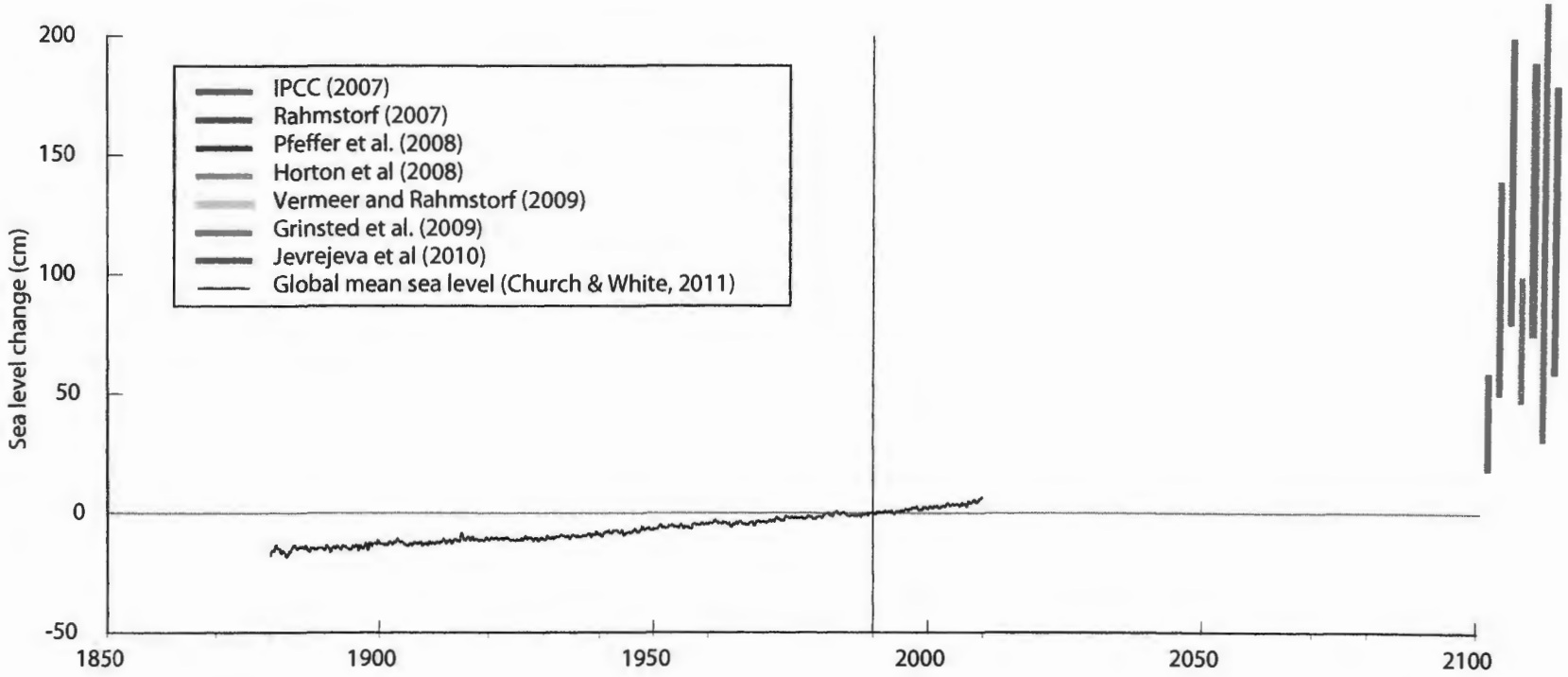

Figure 3.1 Projections of 21st century eustatic sea level rise from recent peer-reviewed literature compared to tide-gauge reconstructions from 1880 to 2009. Note the relatively low range of IPCC (2007) projections, which did not account for increases in ice sheet flow.

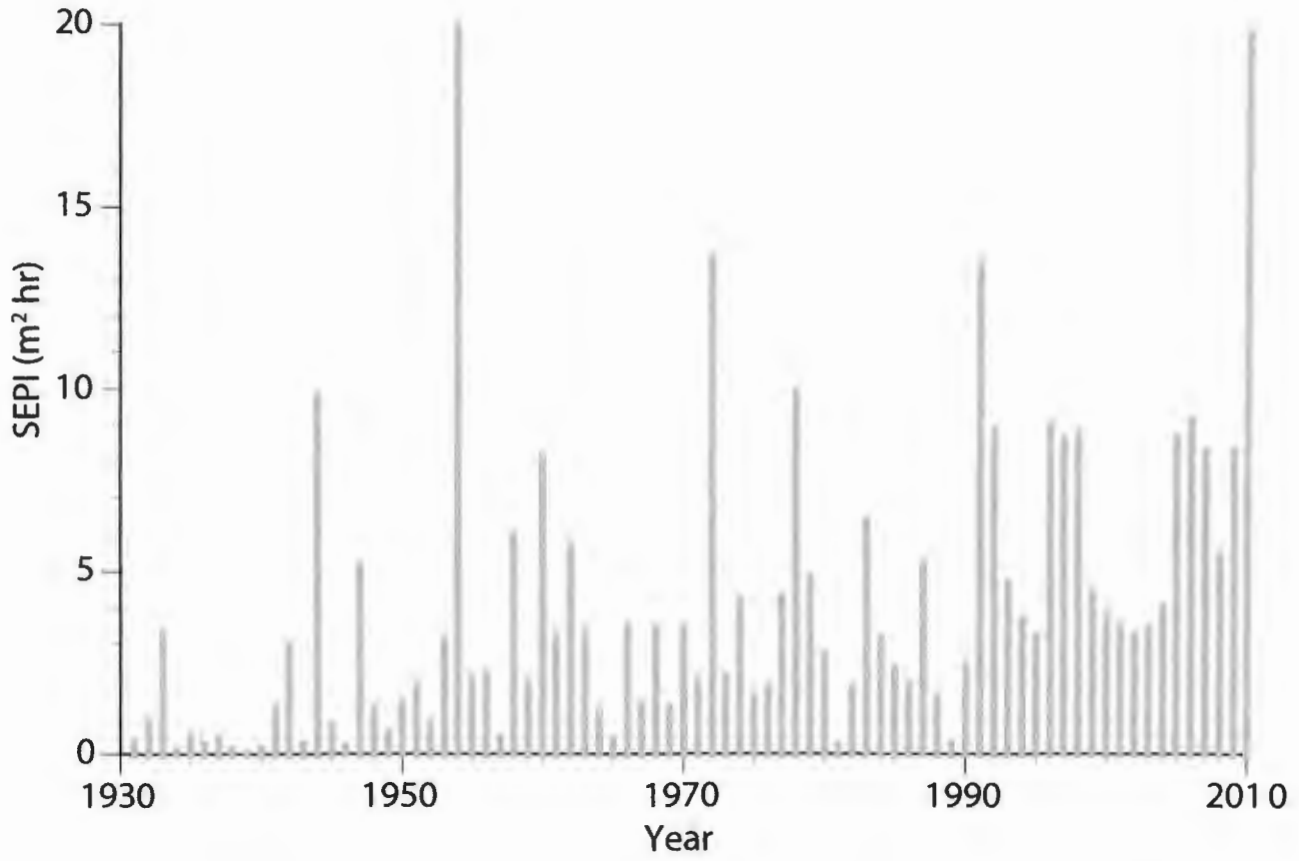

Figure 3.2 Annualized storm erosion potential index (SEPI) between 1930 and 2010 at Newport, RI. SEPI is defined as the sum of the products of hourly storm surge above 2 standard deviations and water levels greater than MHHW, and is a measure of the erosion potential of a storm (Zhang et al., 2001), The overall increase during the 20th century indicates the potential for sea level rise to exacerbate storm impact.

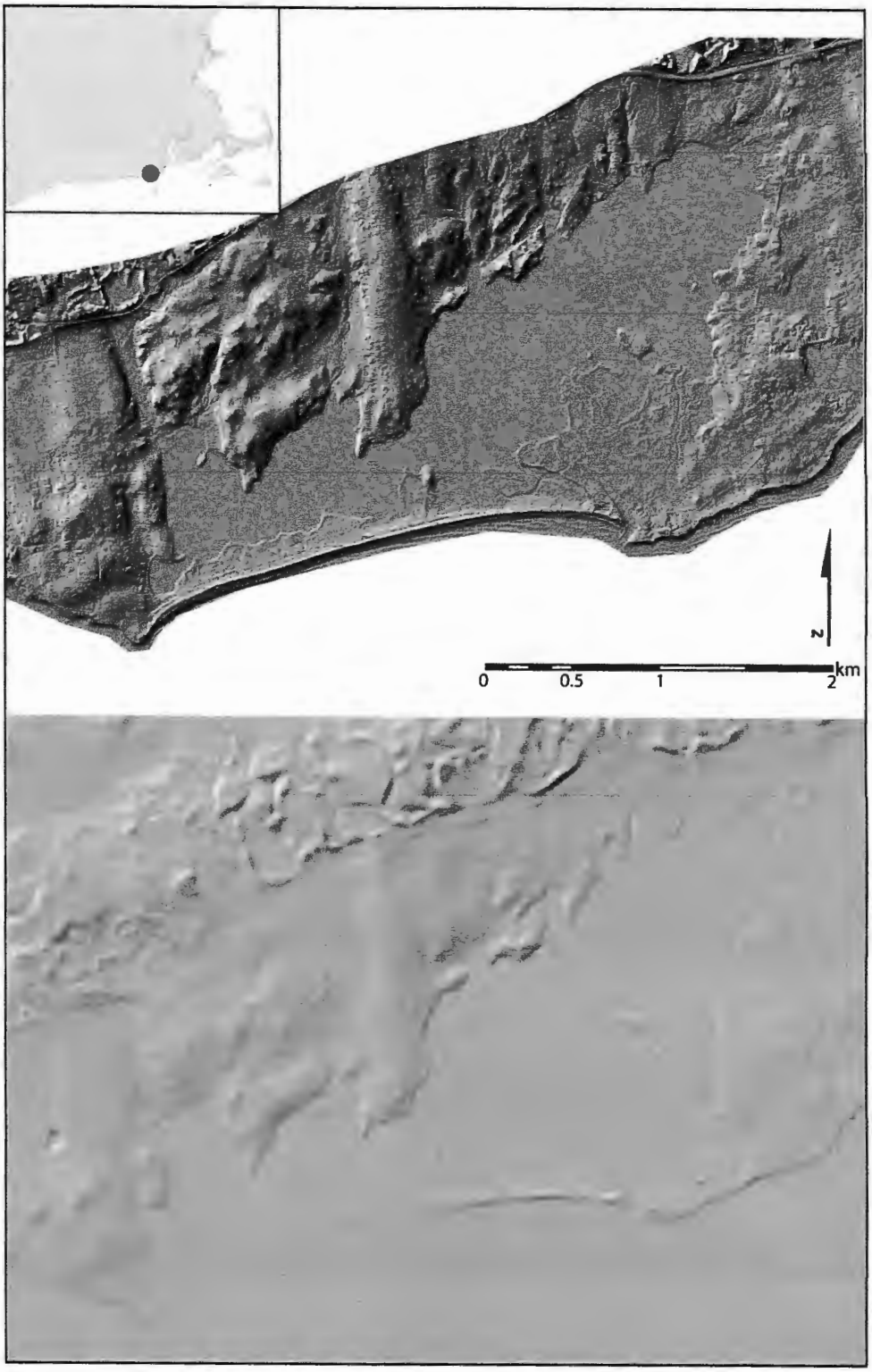

Figure 3.3 Comparison of the spatial resolution of (a) 1.25-meter (lidar) and (b) 10-meter (1/3 arc-second NED) elevation models at Quonochontaug Pond, RI.

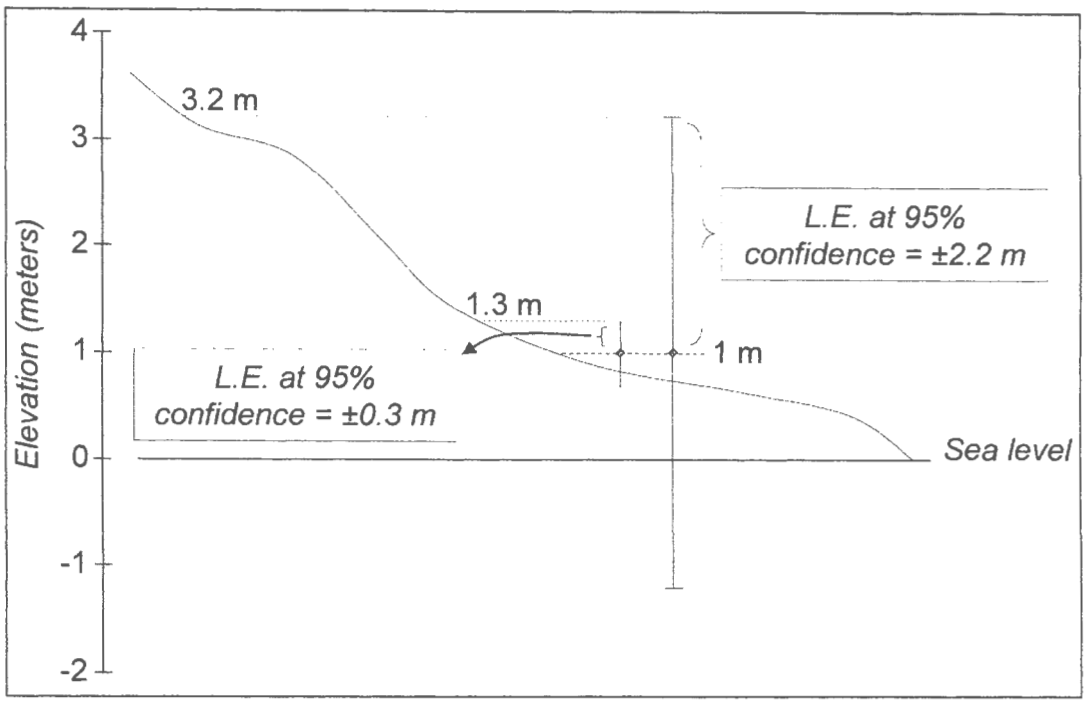

Figure 3.4 Example of how linear error (L.E.) associated with different elevation data sources is projected onto the land surface given a 1-meter inundation level (from Gesch, 2009).

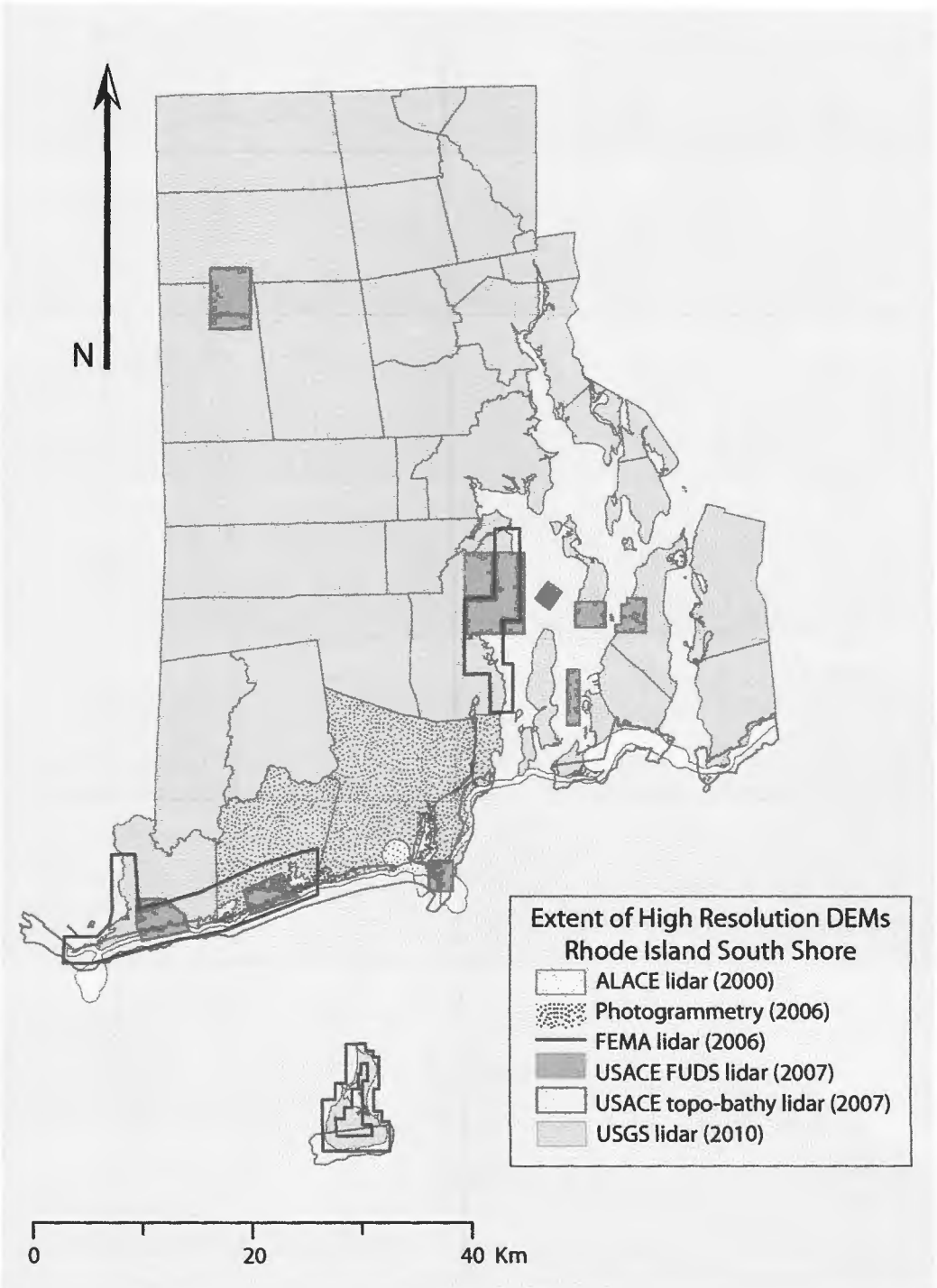

Figure 3.5 Extent of high-resolution lidar and photogrammetrically-derived elevation models available for southern Rhode Island.

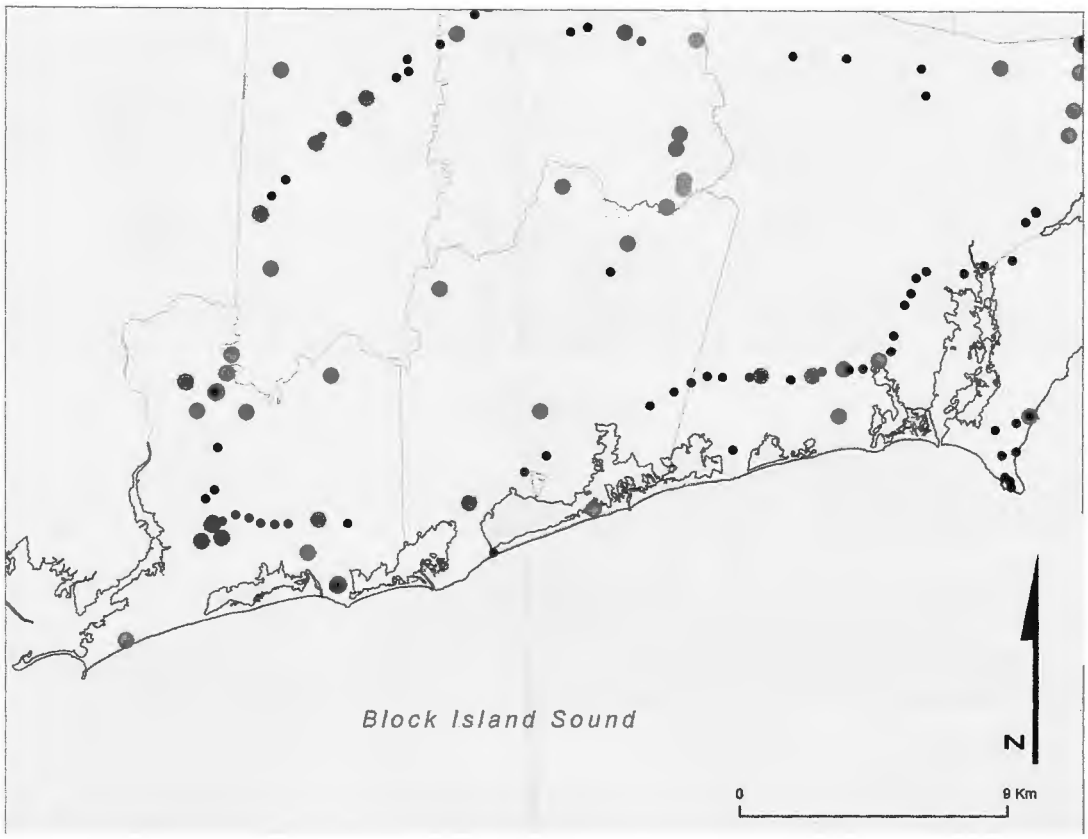

Figure 3.6 Geodetic survey monuments in Washington County, RI. Black points are locations of RIDOT and NGS monuments classified as first, second, or third order horizontal control (accuracy of 5 cm or less) and first second or third order vertical control (accuracy of 1.2 cm or less) (data source: RIGIS). Green circles are monuments classified by NGS as stability rating A.

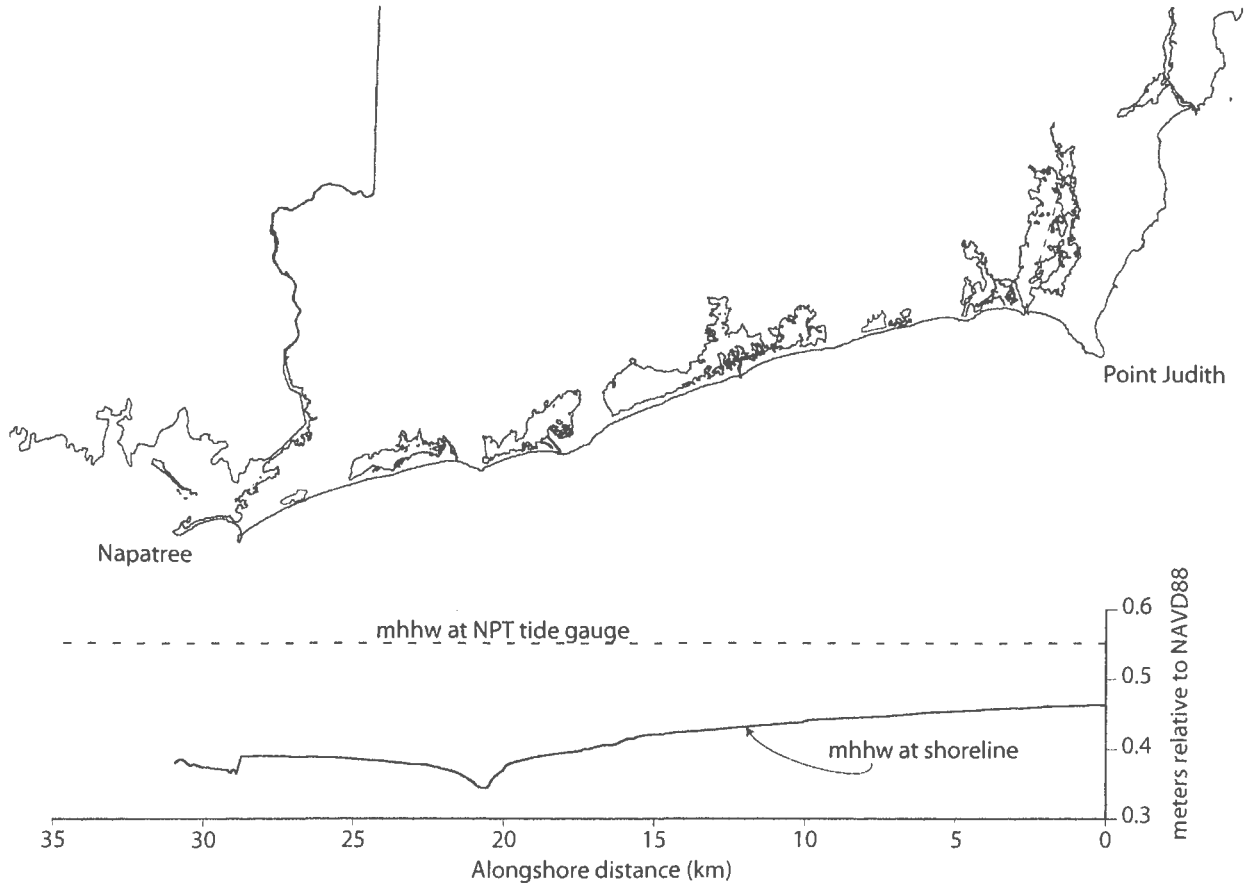

Figure 3.7 Variation in the mean higher high water (MHHW) tidal surface along the RI south shore. The lower curve shows alongshore changes in MHHW as measured relative to the North American Vertical Datum of 1988 (NAVD88). The dashed line indicates the elevation of MHHW at the Newport, RI tide gauge. Alongshore MHHW was calculated with VDatum, using a dense lidar point dataset (n=13,900) to represent the 0m NAVD88 contour between Point Judith and Napatree point RI.

Appendix A. Reconstruction of relative storm intensities

Advective-settling

A recent advancement in the study of paleo-event deposits has been the development of inverse sediment transport modeling techniques to provide estimates of inundation magnitude (primarily flow depths and flow velocities) from sedimentary deposits. These models have primarily been applied to tsunami deposits (Jaffe & Gelfenbaum 2007; Soulsby et al., 2007; Moore et al., 2007), but as recent studies have shown, similar approaches can be applied with equal success to hurricane deposits if the underlying assumptions of the model are met. Woodruff et al. (2008) validated the use of an inverse advective-settling model for sedimentary deposits from the 1928 San Felipe hurricane in Laguna Grande, Puerto Rico. Wallace and Anderson (2010) used this method to classify paleo-hurricanes in the western Gulf of Mexico as intense using the predicted storm surge value from Hurricane Allen (1980) as a baseline.

The advective-settling model proposed by Woodruff et al. (2008) relies on the physics of sediment transport in order to estimate local flow conditions. The approach builds on work by Moore et al. (2007) who quantified tsunami inundation based on grain size distributions from laterally sorted deposits. For an onshore, unidirectional flow, Moore et al. (2007) used the "law of the wall" (the vertical velocity profile derived from the Prandtl mixing theory) to equate the time it takes a particle to settle from the top of a turbulent flow to the bed with the time needed to advect the suspended particle a horizontal distance into the lagoon at an average flow velocity. Flow depth – flow velocity combinations derived from this method can be scaled assuming a critical flow rate at the barrier (Froude number = 1), where the eroded

dune acts as a hydraulic control. This additional constraint was introduced by Woodruff et al. (2008) to obtain a solution that is calibrated to the flow depth over the barrier:

Equation (A1)

$$<h_b>=\left(\frac{x_L{}^2 w_s{}^2}{g}\right)^{1/3}$$

The Woodruff et al. (2008) model is relevant for laterally sorted deposits that are assumed to have travelled primarily in suspension from their source (the barrier) to the deposit. With several simplifying assumptions, this method uses particle settling velocity of the coarsest fraction of the deposit (w_s) and sediment transport distance (x_L) to calculate a flow depth (h_b) at the barrier necessary to form the observed deposit.

For many reasons, Quonochontaug Pond is an ideal site to utilize this approach. To begin with, Rhode Island's barrier spits receive sediment from the erosion of poorly-sorted glaciofluvial sand and gravel found in the headland bluffs and on the shoreface. Because the source for the coarse fraction is heterogeneous with respect to grain size, a wide range of particle sizes is available for transport, which allows for relative comparison of storm deposits. The landward fining trend for individual deposits correlated between cores also indicates that particles were spatially sorted during transport across the lagoon (Figure 1.5). In addition, the presence of a relatively deep channel that separates the surge platform from the low-energy lagoon

basin supports the assumption that coarse grains transported from the barrier likely traveled in suspension and incipient suspension.

Modern analogue

We assessed the validity of the advective-settling model using the 1938 hurricane deposit as a modern analogue for predicted $<h_b>$ values. At Newport, RI, the measured surges associated with this storm were 3.5 m (Figure 1.2), although observations of combined wave heights between 4.1 and 5.2 m above msl were documented along the RI south shore (Tannehill, 1938; Paulsen et al., 1940). To calculate $<h_b>$ we used the siliciclastic D_{95} size class to represent maximum grain size from the deposit (Figure A1a). The model predicts a maximum instantaneous water level above the barrier during breaching, thus it is equal to the cumulative effects of storm surge and maximum wave runup (minus the elevation of the barrier). Estimates for $<h_b>$ from the 1938 deposit range from 2.15 to 2.89 m above the barrier (Figure A1b). To adjust these values to a local tidal datum we used the methods of Newcomer (1991) to first lower the foredune to a 100-year storm event erosional profile, and added the calculated $<h_b>$ to the elevation of the post-storm barrier. The maximum water levels predicted by advective-settling therefore range between 4.1 and 4.5 m relative to contemporary msl. Quantitative modeling of storm surge, wave height, and sediment transport during the 1938 hurricane (e.g. Canizares and Irish, 2008) has not been done for southern Rhode Island, yet our estimates of $<h_b>$ are in general agreement with the best available historical data regarding flood magnitudes from the 1938 event, particularly at cores located a suitable distance from the barrier.

Additional sediment transport due to barrier migration.

At present, the advective-settling technique is one of the only quantitative means for examining relative differences in storm intensity at a given location. Inundation magnitudes predicted using this approach are sensitive to changes in the distance of sediment transport over time and thus a relative comparison assumes the barrier has maintained its current configuration. The cumulative effects of sea level rise and storms (major factors in the development of barrier islands) can increase the sensitivity of backbarrier sites to overwash processes by translating the shoreline farther inland and narrowing the barrier beach through time. These effects are notable in the sediment record from Quonochontaug Pond, where the scale of overwash deposits from modern storms stands out prominently in the record. On millennial scales, the calculated values of $<h_b>$ show a spurious trend, increasing over time as a result of this apparent change in overwash threshold (Figure A2).

To account for some of this error we used aerial photographs and geodetic survey charts to estimate historical rates of shoreline change at the Quonochontaug barrier. A compilation of shoreline indicators collected between 1873 and 2004 indicates that this shoreline has eroded at a relatively uniform rate during the last ~140 years (Himmelstoss, 2010). Regression of shoreline positions at 15 transects spaced at 50 m alongshore in front of the barrier yields an average rate of shoreline retreat equal to -0.12 m yr^{-1}. We used this rate to translate the position of the barrier with time (and thereby the distance term (x_L) in the advective settling equation). The overall effect of this additional term is negligible in the modern period, and increases estimates of $<h_b>$ by approximately 50% for the oldest deposits. Similar rates of barrier migration (between -0.09 and -0.11m yr^{-1}) are found using the methods of Bruun (1962) and

Dean and Maurmeyer (1983), combined with published estimates of regional sea level change (Donnelly et al., 2004; Engelhart et al., 2009) and assuming a depth of closure at 12 m. Although the assumption of an equilibrium profile that keeps pace with sea level rise is a simplification of the natural processes, we find it suitable for estimating changes in x_L on millennial time scales.

References

Bruun, P., 1962. Sea-level rise as a cause of shore erosion. *Journal of Waterways and Harbors Division*, 88, 117-130.

Canizares, R., and Irish, J.L., 2008. Simulation of storm-induced barrier island morphodynamics and flooding. *Coastal Engineering*, 55, 10889-11101.

Dean, R.G., and Maurmeyer, E.M., 1983. Models for beach profile response. *In:* Komar, P.D. (ed.), *Handbook of Coastal Processes and Erosion.* Boca Raton, FL: CRC Press, pp. 151-166.

Donnelly, J.P.; Cleary, P.; Newby, P., and Ettinger, R., 2004. Coupling instrumental and geologic records of sea-level change: Evidence from southern New England of an increase in the rate of sea-level rise in the late 19th century. *Geophysical Research Letters*, 31, L05203-L05206.

Engelhart, S.E.; Horton, B.P.; Douglas, B.C.; Peltier, W.R., and Tornqvist, T.E., 2009. Spatial variability of late Holocene and 20th century sea-level rise along the Atlantic coast of the United States. *Geology*, 37(12), 1115-1118.

Ferguson, R.I., and Church, M., 2004. A simple universal equation for grain settling velocity. *Journal of Sedimentary Research*, 74(6), 933-937.

Himmelstoss, E.A.; Kratzmann, M.; Hapke, C.J.; Thieler, E.R., and List, J., 2010. The national assessment of shoreline change - A GIS compilation of vector shorelines and associated shoreline change data for the New England and Mid-Atlantic coasts. USGS *(U.S. Geological Survey Open-File Report No. 2010-1119).*

Jaffe, B.E., and Gelfenbaum, G., 2002. Using tsunami deposits to improve assessment of tsunami risk. *Solutions to Coastal Disasters '02 Conference Proc.*, 836-847.

Moore, A.L.; Mcadoo, B.G., and Ruffman, A., 2007. Landward fining from multiple sources in a sand sheet deposited by the 1929 Grand Banks tsunami, Newfoundland. *Sedimentary Geology*, 200(3-4), 336-346.

Paulsen, C.G.; Bigwood, B.L.; Harrington, A.W.; Hartwell, O.W., and Kinnison, H.B., 1940. Hurricane floods of September 1938. Washington, DC: U.S. Department of the Interior, Geologic Survey *(No. Water-Supply Paper 867).*

Soulsby, R.L.; Smith, D.E., and Ruffman, A., 2007. Reconstructing tsunami run-up from sedimentary characteristics - a simple mathematical model. *In: Coastal Sediments '07.* ASCE, pp. 1075-1088.

Tannehill, I.R., 1938. Hurricane of September 16 to 22, 1938. *Monthly Weather Review*, 66, 286-288.

Wallace, D.J., and Anderson, J.B., 2010. Evidence of similar probability of intense

hurricane strikes for the Gulf of Mexico over the late Holocene. *Geology*, 38(6), 511-514.

Woodruff, J.D.; Donnelly, J.P.; Mohrig, D., and Geyer, W.R., 2008. Reconstructing relative flooding intensities responsible for hurricane-induced deposits from Laguna Playa Grande, Vieques, Puerto Rico. *Geology*, 36(5), 391-394.

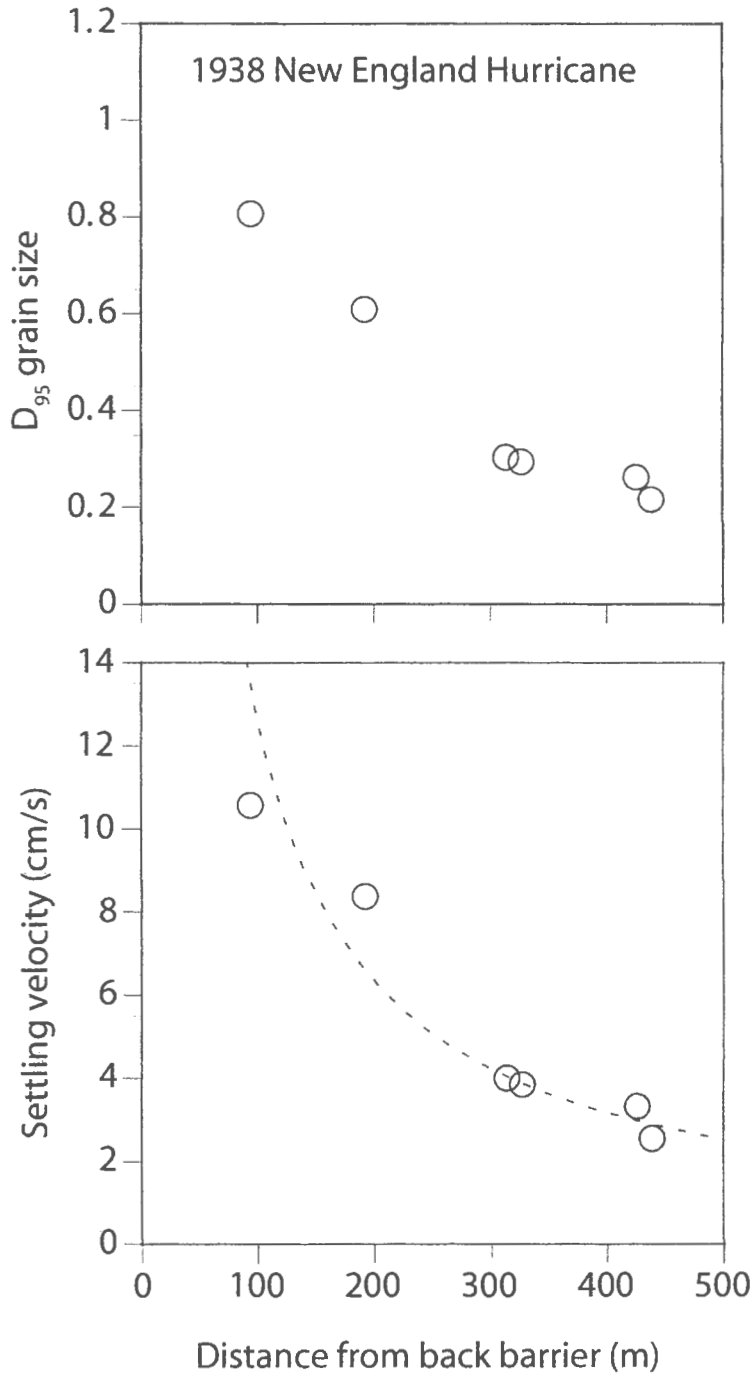

Figure A1. Assessment of advective-settling model using the 1938 New England hurricane deposit. a) D_{95} grain-size of A.D. 1938 deposit in each core. b) Particle settling velocities for grain sizes shown in (a) using the relationship developed by Ferguson and Church (2004). Dashed line shows average $\langle h_b \rangle$ of 2.54 m. Grey shading indicates model distribution for range of wave heights noted on the south shore during the 1938 hurricane (4.1-5.2 meters). Figure after Woodruff et al. (2008).